CHALMERS
UNIVERSITY OF TECHNOLOGY

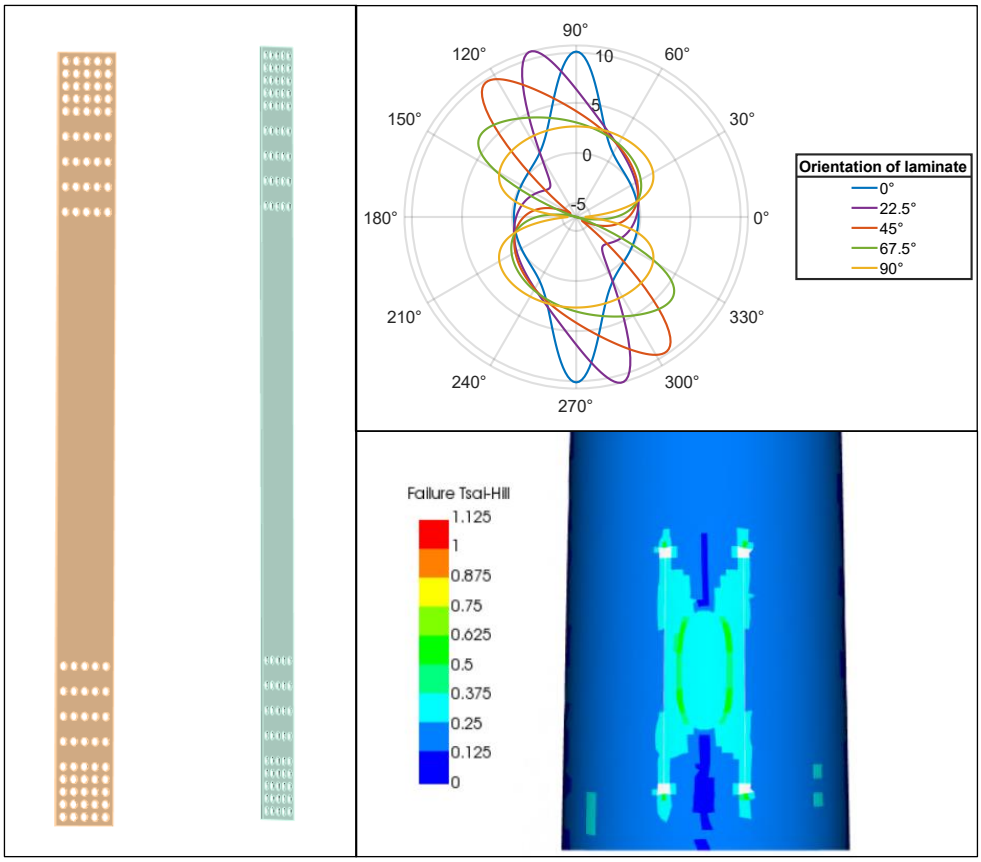

FINDING SOLUTIONS FOR OPENINGS IN LAMINATED WOOD WIND TURBINE TOWERS

Master's thesis in Structural Engineering and Building Technology

TIM SCHÜLER

Department of Architecture and Civil Engineering
Division of Structural Engineering
Research Group Lightweight Structures
CHALMERS UNIVERSITY OF TECHNOLOGY
Master's Thesis ACEX30
Gothenburg, Sweden 2024

MASTER'S THESIS ACEX30

Finding solutions for openings in laminated wood wind turbine towers

Master's Thesis in the Master's Programme Structural Engineering and Building Technology

TIM SCHÜLER

Department of Architecture and Civil Engineering
Division of Structural Engineering
Lightweight Structures
CHALMERS UNIVERSITY OF TECHNOLOGY
Göteborg, Sweden 2024

Finding solutions for openings in laminated wood wind turbine towers
Master's Thesis in the Master's Programme Structural Engineering and Building Technology

TIM SCHÜLER

Examensarbete ACEX30
Institutionen för arkitektur och samhällsbyggnadsteknik
Chalmers tekniska högskola, 2024

Department of Architecture and Civil Engineering
Division of Structural Engineering
Lightweight Structures
Chalmers University of Technology
SE-412 96 Göteborg
Sweden
Telephone: + 46 (0)31-772 1000

Cover:
Left: Holed stiffeners; Right top: Stress distribution around an opening in a Kerto-S laminate with different orientations; Right bottom: Inverse reserve factors for stiffeners in wind turbine tower wall

Department of Architecture and Civil Engineering
Göteborg, Sweden, 2024

Finding solutions for openings in laminated wood wind turbine towers

Master's thesis in the Master's Programme Structural Engineering and Building Technology

TIM SCHÜLER

Department of Architecture and Civil Engineering
Division of Structural Engineering
Lightweight Structures
Chalmers University of Technology

ABSTRACT

Construction with laminated veneer lumber (LVL) still is an emerging field within timber engineering. Introducing openings in timber laminates creates challenges caused by the material's orthotropic properties. Analytical investigations about stress concentrations forming around these openings have been conducted, showing that both layup of the laminate and orientation of fibres greatly impact resulting stresses. Fluctuation of stresses over rotation angle is significantly higher in a unidirectional laminate than in a plywood laminate. Classical laminate theory was applied to investigate possibilities of computing material properties for timber laminates with arbitrary layup. A relation predicting material properties both for LVL and plywood was found. Theoretical values indicate standard values may underestimate material properties significantly due to different layups given the same properties. Two methods were investigated to reduce stresses around openings: adding reinforcing structures and modifying laminate layup. Reinforcing structures showed that redistributing stresses within a timber laminate wall is especially challenging when reinforcement is not integrated into the wall. Stiffeners with varying stiffness placed in the wall yield best results, reducing stress concentrations in both normal in-plane material directions and in-plane shear. Maximum stress and Tsai-Hill failure criteria were applied to evaluate material utilization in the laminate. Modifying layup showed introducing higher strength material around the opening has a more substantial impact on performance than creating layups with different lamina orientations. Reinforcing structures were observed to have a smaller impact on material utilization than modifying the laminate material. Combination of the two methods revealed that reinforcing a laminate with a non-unidirectional layup is not beneficial and counteracts laminate mechanics.

Key words: Laminated veneer lumber, orthotropic laminate, classical laminate theory, stress concentrations in LVL, Tsai-Hill, laminate timber wall

Analys av koncept för förstärkning av öppningar i vindkraftverk gjorda av laminerat fanerträ

Examensarbete inom mastersprogrammet Konstruktionsteknik och Byggnadsteknologi

TIM SCHÜLER

Institutionen för arkitektur och samhällsbyggnadsteknik
Avdelningen för Konstruktionsteknik
Lättviktskonstruktioner
Chalmers tekniska högskola

SAMMANFATTNING

Konstruktioner med laminerat fanerträ (LVL) utgör fortfarande en liten del av träkonstruktioner och är ett växande område inom träteknik. Att skapa öppningar i trälaminat leder till utmaningar på grund av materialets ortotropiska egenskaper. Analytiska undersökningar om spänningskoncentrationer som bildas runt en öppning har gjorts. Resultaten visar att både laminatets uppbyggnad och fibrernas orientering har stor inverkan på de resulterande spänningarna. Variation av spänningar över rotationsvinkel är avsevärt högre i ett enkelriktat laminat än i ett plywoodlaminat. Klassisk laminatteori tillämpades för att undersöka möjligheterna att beräkna materialegenskaper hos trälaminat med godtycklig uppbyggnad. Ett samband som förutspår materialegenskaper för både LVL och plywood hittades. Teoretiska värden indikerar att standardvärden kan underskatta materialegenskaperna avsevärt då olika uppbyggnader ges samma materialegenskaper. Minskning av spänningar runt en öppning undersöktes med två metoder: implementering av förstärkande strukturer och modifiering av laminatets uppbyggnad. Förstärkande strukturer visade att omfördelning av spänningar i en trälaminatvägg är särskilt utmanande när förstärkningen inte är integrerad i väggen. Styvplåtar med varierande styvhet placerade i väggen ger bäst resultat och minskar spänningskoncentrationer både i normala planmaterialriktningar och i planskjuvning. Maximal spänning och Tsai-Hill-brottkriteriet tillämpades för att bestämma materialutnyttjandet i laminatet. Det har visats att applicering av material med högre brottgränser runt öppningen har större inverkan på kapaciteten än att skapa uppbyggnader med olika lagerorienteringar. Förstärkande strukturer har mindre inverkan på materialutnyttjandet än att modifiera laminatmaterialet. Kombination av de två metoderna visade att förstärkande strukturer i ett laminat med icke-enkelriktad uppbyggnad inte är fördelaktiga och motverkar laminatets inneboende mekanik.

Nyckelord: Laminerat fanerträ, ortotropiskt laminat, klassisk laminatteori, spänningskoncentrationer i LVL, Tsai-Hill, laminatvägg

Contents

List of Figures

List of Tables

Acknowledgments

The work for this master's thesis was carried out between January and June of 2024. The project is a corporation between the Department of Structural Engineering, Lightweight Structures, at Chalmers University of Technology, Uniso Technologies and Modvion, Sweden.

I would like to express my gratitude towards my supervisors Torkel Davidsson, Uniso, and Stefan Ågren, Modvion. Your continuous support throughout the work together with your impressive knowledge in computational engineering has enabled me to get insights in the field I could not have imagined. Thank you for always having an open ear and consulting me in whatever doubts I had!

Further, I want to thank my examiner Robert Jockwer at Chalmers for all constructive discussions. Your knowledge in timber engineering has been of great value and an impactful resource for this work. Your guidance but also challenging me to investigate new things has led to many interesting results in this project.

Additionally, also based at Chalmers, I want to express my gratitude towards Leif Asp. With your competence in composite mechanics and being the (self-announced) "wise old man on the side", you have contributed to applying composite mechanics in timber engineering. Your open ear and professionalism have made working with you a great experience.

Having faced several challenges, I want to thank Mattis Dahl Eriksson, Uniso, and David Engerberg, Modvion, but also the colleagues at Uniso's inhouse office for helping me with all issues I have had. Your help and guidance in technical questions has been as valuable as all our coffee-chats to take my mind off work for a while.

Lastly, I want to raise a glass to my classmates and friends at Chalmers. In the period of the work, we have had both constructive and nonsense discussions enrichening and sometimes enlightening me. Clara, Rauan, Alice, Elsa, Saffa and Cecilia, I thank you for all our lunches where minds could soar freely and me gaining insights in topics I didn't know I needed. Alex, having a chat over lunch or an afterwork drink has more than often calmed my nerves and gotten me out of my work-bubble. Thank you for being a likewise consoling and cheering friend!

Göteborg June 2024

Tim Schüler

Notations

Roman upper-case letters

A	Extensional stiffness matrix
ACP	Ansys Composite PrepPost
B	Coupling stiffness matrix
C	Elastic constant matrix
CF	Carbon fibre
CL-theory	Classical laminate theory
D	Bending stiffness matrix
E_L, E_1	Young's modulus parallel to the (main) fibre direction
E_T, E_2	Young's modulus perpendicular to the (main) fibre direction
EWP	Engineered wood product
E_x	Longitudinal laminate stiffness
E_y	Transversal laminate stiffness
E_θ	Tangential Young's modulus
G	Shear modulus
GF	Glass fibre
Glulam	Glued laminated timber
IRF	Inverse reserve factor
LVL	Laminated veneer lumber
M	Moment vector
MPa	Megapascals
N	Force vector
P	Uniaxial load
Q	Stiffness matrix
SCF	Stress concentration factor
T	Biaxial load
T1	Stress transformation matrix
T2	Strain transformation matrix
UD	Unidirectional

Roman lower-case letters

a	Ellipse major radius
b	Ellipse minor radius
h	Height
kNm	Kilonewton meter
r	Radius
w	Opening width

Greek lower-case letters

α	Offset angle between lamina and laminate coordinate system
γ	Engineering strain
δ	Midpoint between maximum and minimum stress
ε	Strain
ε^0	Strain vector
θ	Polar angle to opening contour
κ	Curvature vector
σ	Stress
σ_{Lu}	Ultimate longitudinal tensile strength
$\sigma_{Lu'}$	Ultimate longitudinal compressive strength
σ_{Tu}	Ultimate transversal tensile strength
$\sigma_{Tu'}$	Ultimate transversal compressive strength
σ_θ	Tangential stress
τ	Shear stress
τ_{LTu}	Ultimate shear strength
υ	Poisson's ratio
φ	Angle of laminate orientation

1 Introduction

1.1 Background

The transition to renewable energy sources plays a major role in reaching the climate goals set by the UN. Construction of windmills is one key strategy for producing more environmentally friendly energy. To reach higher capacities, wind turbine towers must be constructed taller, bringing conventional steel-solutions to its limits. Modvion is researching and building prototypes of wind turbine towers in laminated veneer lumber (LVL). This offers the possibility of constructing wind turbine towers in modules, facilitating transport to construction sites and at the same time reducing carbon emissions during production. The access to the towers is today integrated in a raised concrete foundation (see Figure 1.1). In the next step to decrease the carbon footprint of the wooden towers, it is aimed at reducing the foundation height, thus creating a need for an opening in the LVL itself. The topic will be investigated by analysing stresses and stress concentrations around the opening at the foot of the tower. Impact of choice of material or dimensions of the cross section at a distance from the opening not directly affecting the stress concentrations is not scope of this work. Concepts will be evaluated using finite element analysis in Ansys Multiphysics.

Figure 1.1. Modvion's tower "Wind of Change".

1.2 Aim and objectives

The thesis investigates the cracking and failure of orthotropic laminates in general and LVL in particular. The intention is to understand stress concentrations and failure in the material around an opening in a tubular construction made from LVL. A finite-element analysis is conducted, where different approaches for reinforcing an opening in a tower module are investigated and compared.

Several topics will be investigated in the thesis:

- Is it possible to obtain properties for veneers in a LVL panel given the panel moduli and ratios? Can material properties for LVL panels with arbitrary layup be computed with these veneer properties?
- Which parameters are essential for stress concentrations around holes and openings in orthotropic laminates and how do they impact failure?
- How should the opening be formed to minimize stress concentrations?
- How can an opening be reinforced as material efficient as possible?

1.3 Basic assumptions and limitations

1.3.1 Geometry

The wind turbine tower is built by stacking modules of curved plates on top of each other. Modvion's latest tower *Wind of Change* will be taken as a reference. At the foundation the timber tower is clamped to the concrete, creating a vertical cantilever. Due to the difference in diameter at the top and at the foundation, the tower gets a conical shape over height as shown in Figure 1.2. The height and diameters are fixed, the cross section of the wall can however be changed locally to enable the reinforcement to be integrated in the wall. Being an orthotropic material, element orientations must be assigned. Tower longitudinal, vertical, direction is assigned material x, tangential direction material y and through-thickness material z direction.

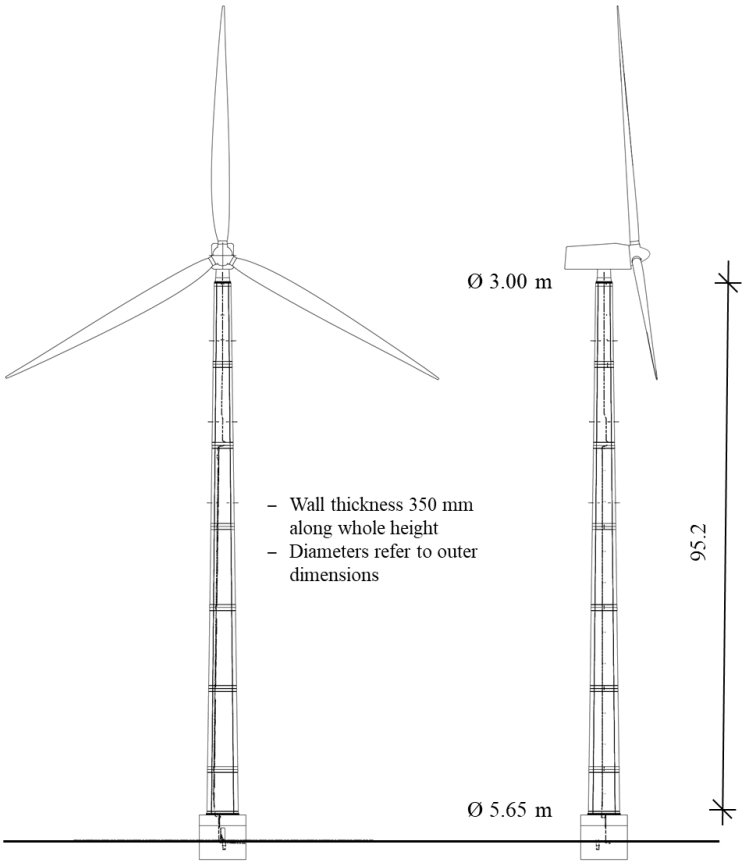

Figure 1.2 Dimensions of investigated wind turbine tower.

1.3.2 Loads

Given loads are used based on dimensioning from Modvion and Uniso. For the analysis, loads are considered to act at the top of the wooden tower, at a height of 95.2 m. Governing moments come from the wind turbine and are bending (6420 kNm) and torsion (5200 kNm). Loads from wind will be considered as a horizontal force acting on the blades of the turbine with a magnitude of 770 kN. Additional wind loads along the tower will not be considered. The turbine itself contributes with a vertical load of 1560 kN. Dynamic loads and fire and hygrothermal phenomena will not be investigated. Fatigue assessment is not scope of the work.

1.4 Outline of thesis

Chapter 2, Theory – material, introduces laminated veneer lumber and showcases concepts used for reinforcing similar constructions.

In Chapter 3, Theory – mechanics, analytic theories are described and applied to compute how stress concentrations around openings in laminates vary.

Chapter 4, Reducing stress concentrations around openings, addresses methods on how to modify an opening and its surrounding to minimize the need for additional reinforcement.

Chapter 5, Finite element modelling, describes investigated reinforcement concepts and shows first results from finite element analysis.

In Chapter 6, Evaluation of concepts, investigated concepts are evaluated regarding feasibility and amongst each other. Best performing concepts are combined to obtain an improved performance.

Chapter 7, Conclusion and outlook, concludes the thesis, summarizing findings and giving an outlook on possible future work.

2 Theory – material

Reinforcing timber structures comes with challenges not arising for other construction materials. To understand the challenge of creating openings in wooden wind turbine towers, this chapter will give an overview of the material and show how openings are reinforced in similar constructions.

2.1 Laminated veneer lumber

2.1.1 Production

Laminated veneer lumber (LVL) is an engineered wood product (EWP). Veneers are created by peeling timber logs, leading to a distinct orientation of fibres. These veneers are graded and cut, big imperfections are removed and stacking is done such that remaining imperfections are spread out (Hakkarainen, 2019). Sheets are made by stacking veneers either in uniform fibre direction or with multiple veneers oriented perpendicular to the main fibre direction. While timber is a heterogenous material, LVL sheets can be considered to have homogenous properties due to the spreading out of imperfections and homogenization of material. Sheets with veneers in uniform direction are labelled LVL P, LVL S or Kerto-S, while plates with cross layers are labelled LVL C, LVL X, or Kerto-Q, depending on producer nomenclature. When layering veneers with alternating, perpendicular orientation, the product is called *plywood*. The direction of the panel in which majority of the veneer fibres are running is called *main fibre direction*. After gluing and pressing, various cutouts can be made from the LVL sheets. This allows for forming shapes reaching from standard dimensions to beams with specific geometries. These structural elements can thus have dimensions not possible to manufacture with structural timber. Optional sanding can be performed with the aim of controlling the thickness of sheets or achieve a higher optical finish. Spruce and pine are majorly used for standard products in the European market, birch and beech is used for high strength LVL. In following investigations, species in references is not specified further than "spruce" and "beech". Considering the most common species in Europe, spruce LVL is most likely made of *Picea abies* and beech LVL consists of *Fagus sylvatica*.

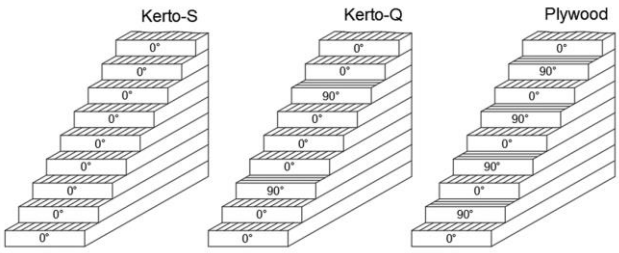

Figure 2.1. Layup of a 9-layered Kerto-S, Kerto-Q and plywood sheet.

To create tubular sections, Modvion bends multiple 9-layerd LVL sheets, each with a nominal thickness of 25 mm, and glues them together. Subsequently cutting off excess material along the edges leaves 14.6 m tall modules that can be stacked on top of each other on site to build the wind turbine towers, as shown in Figure 1.2.

2.1.2 Properties

Wood is an orthotropic material with unique material properties in three main directions. In an uncut log these are defined as longitudinal, tangential, and radial. LVL conserves wood properties in longitudinal and tangential directions in the veneer plane, radial properties act out of the veneer plane. Figure 2.2 illustrates main axes in the uncut timber log and in the resulting veneer sheet. Young's moduli are denoted E_L or E_1 parallel to (main) fibre direction and E_T or E_2 perpendicular to (main) fibre direction. Strength and stiffness of timber is dependent on

several factors such as species, growth rate, external influences on the tree and imperfections and irregularities such as knots in the wood. Being orthotropic, properties also depend on material direction. Strength and stiffness in longitudinal direction is multiple times higher than in tangential and radial direction. This is true for both structural timber and EWPs, although stiffness and strength of EWPs are higher than in structural timber. The reason for this is the homogenization mentioned above. Both the spreading out and the capacity of glue lines to transfer stresses between veneers reduces the impact of irregularities on the structural performance of the final product significantly. In addition, monitoring and modifying veneers lead to a high quality and low variation in material properties, allowing for lower reduction factors when dimensioning with EWPs. Due to the reasons listed, LVL sheets are in this study considered to be homogenous orthotropic.

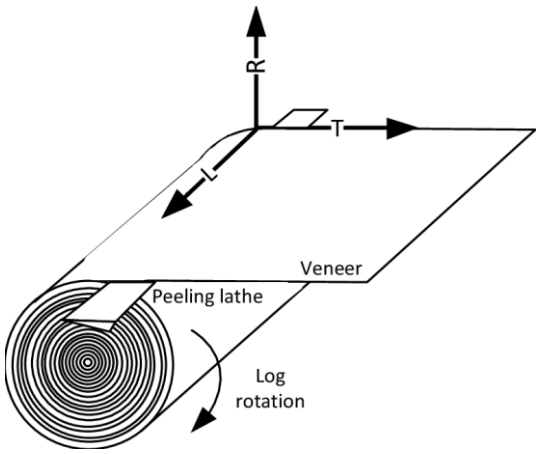

Figure 2.2. Material directions in a timber log and veneer. (Tomppo, 2013)

LVL panels offer good in plane strength and stiffness, radial or out-of-plane properties are very low. Kerto-S is superior when loading in-plane parallel to main fibre direction due to the uniform layup and same orientation of veneers. In this case, all veneers contribute to the strength of the sheet along the axis of loading. Kerto-Q possesses increased stiffness and strength in-plane perpendicular to the main fibre direction due to rotation of several veneers. Depending on thickness and amount of layers, two or more veneers are stacked perpendicular to the main fibre direction of the sheet, which provides strength and stiffness in this direction. Shear modulus, *G*, and out of plane properties are not affected by layup according to standard strength and stiffness classes. Plywood is one form of LVL with properties in plane being similar in longitudinal and transversal material direction. Investigating standard LVL products, material properties can be found in the *LVL Handbook* (Hakkarainen, 2019). Only few studies have been conducted to find engineering properties, such as Poisson's ratio, for LVL products. Given a product data sheet from Metsä Wood Oy for finite element calculations, Poisson's ratios for Kerto-S and Kerto-Q panels are specified. Wang et al. (2022) investigated material properties for birch plywood (*Betula pendula*). Poisson's ratio was in this case found to be $\upsilon = 0.034$. Elastic moduli for the used plywood were $E_1 = 9400\,MPa$ and $E_2 = 6700\,MPa$, resulting in a ratio of $E_1/E_2 = 1.40$. Since standard products in the European market are built with softer spruce instead of stronger birch veneers, moduli must be chosen from values for spruce plywood. Poisson's ratio is dependent on the elastic moduli in direction parallel and perpendicular to the main fibre direction, therefore a ratio between moduli of standard products close to that of the investigated birch plywood must be found. Spruce plywood resembling the ratio the closest is 15 mm plywood with a ratio $E_1/E_2 = 1.37$, thus material properties from this layup in combination with the researched Poisson's ratio will be used in this study. Material parameters for investigated standard products are summarized in Table 2.1 below. Properties in the fields left blank are not needed for investigations in this study.

Table 2.1. Material properties for standard LVL products.

	Parameter	Kerto-S	Kerto-Q, spruce	Kerto-Q, beech	Plywood (15 mm)
Stiffnesses [MPa]	E_1 E_2 G	13800 450 600	10500 2000 600	13200 2500 820	5780 4216 600
Poisson's ratio	υ	0.6	0.1	0.1	0.034
Compression strength [MPa]	Parallel to grain Perpendicular to grain		26 9	50 20	
Tension strength [MPa]	Parallel to grain Perpendicular to grain		26 6	50 10	
Shear strength [MPa]	Edgewise		4.5	7.8	

2.2 Reinforcements in laminates and tubular constructions

Introducing an opening weakens a structure and creates stress concentrations increasing the risk of failure. There are several similar constructions to wooden wind turbine towers that can be looked at to gain inspiration and understand how stress concentrations are delt with in existing structures. LVL beams and aircraft fuselages are both constructed with orthotropic laminates, steel wind turbine towers exhibit a similar geometry and loads and in nature natural growth visualizes an optimal solution for coping with disturbances in a material.

2.2.1 Holes in LVL beams

Studies on openings in LVL have been conducted for LVL beams and concepts for reinforcing these have been investigated. Similar studies on LVL walls subjected to tension or compression and shear have not been done. Especially M. Ardalany has published several studies on openings in LVL beams in bending. In the work of Ardalany et al. (2013) multiple methods for reinforcing circular openings are presented, shown in Figure 2.3. These can be summarized into two groups: local reinforcement with screws or rods and reinforcement around the whole hole with sheets made of plywood or nailed steel plates. For local reinforcement fully threaded screws or epoxied-in rods were used and placed at the location with the highest stresses. Screws were drilled either perpendicular or with an angle to the main fibre direction. Both screws and rods could either penetrate partially or fully through the height of the beam. For reinforcement with sheets, plywood was glued to the beam or nailed steel plates were fastened around the opening.

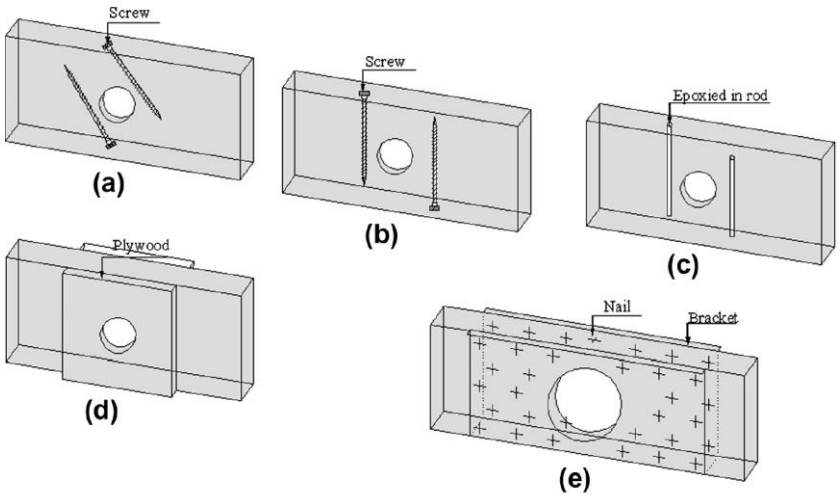

Figure 2.3. Concepts for reinforcing LVL beams. (Ardalany et al., 2013)

It was shown that local reinforcement did not prevent cracks to form but crack growth was stopped from propagating over the reinforcement. Critical aspect to consider when using rods is that the drilled hole for the rod must not impact the cross section such that it weakens it and decreases its capacity. Covering sheets made from plywood efficiently prevented cracks to form and the beams failed in mid span, rather than around the opening. Compared to nailed steel plates, the glue line between beam and cover sheets creates a continuous stress transfer. In addition to the drawback of local transfer of stresses through the nails, steel plates also showed a risk of buckling in areas with compressive stresses. Crack formation and growth around the opening in the LVL beam was dependent on relative hole size. For small holes the nailed steel plate offered sufficient reinforcement, for holes larger than 0.5 times the beam height cracks could not be prevented to form and grow around the hole.

Other studies have assessed reinforcement in glued laminated timber (Glulam) beams with carbon fibre (CF) or glass fibre (GF) (e.g. Kliger *et al.*, 2007). Since Glulam beams are formed by gluing structural timber together, rather than using veneers, resulting stresses are not comparable to those in a laminate. However, the idea of using different materials such as CF or GF to reinforce openings can be translated to LVL products. CF and GF can be engineered to exhibit required stiffnesses and strengths in a desired direction and provide solutions in a wider range than plywood.

2.2.2 Aircraft fuselages

Modern aircraft are being built in CF composite materials due to their high relative strength and the possibility to be designed and produced to fit a range of specific requirements. Aircraft fuselages are loaded in in-plane compressive loads being multiple times higher than the shear loads (Shroff, Acar and Kassapoglou, 2017). Introducing an opening leads to a weakening of the global structure. Fibres in the composite are cut and stresses concentrate at opening contours. In contrast to turbine towers, aircraft fuselages must fulfil high safety standards concerning stability in case of crashes. In addition, opening reinforcements must both stabilize the global structure while at the same time being able to transfer loads from doors into the fuselage. Best-practice is to reinforce openings such as cabin or cargo doors by inserting stiffeners around the opening. These are made of isotropic materials and provide a reinforcement that is orientation-independent and provide possibilities of redirecting stresses both coming from distinct loading points and the overall fuselage. Illustrated in Figure 2.4 is a *standard monolithic integral door surround structure*. For cargo doors, laminate thickness in some cases is increased around the opening to increase fatigue resistance. One major difference between CF composite aircraft fuselages and the wooden wind turbine towers is that although

investing huge resources in development to optimize structures, aircraft fuselages are still bolted instead of glued. Bolting orthotropic laminates induces local stresses and weakens the material, here the wooden turbine towers might be more progressive than the aircraft industry.

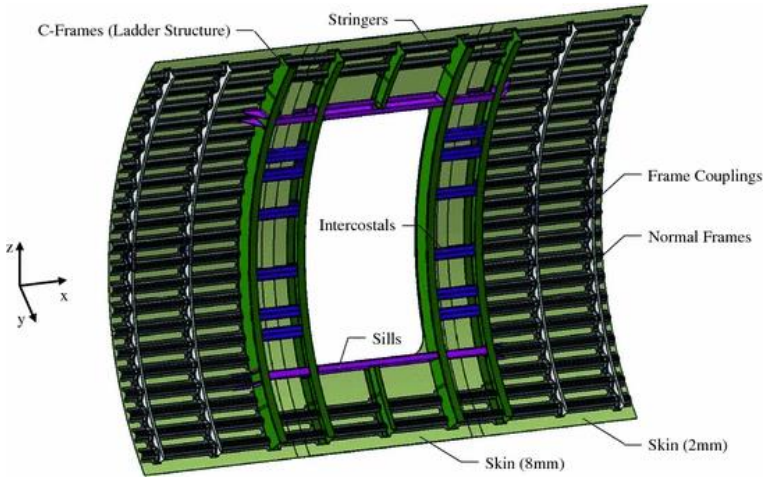

Figure 2.4. Standard monolithic integral door surround structure in an aircraft fuselage. (Schmidt et al., 2016)

2.2.3 Steel wind turbine towers

A wide range of solutions can be engineered to reinforce openings in steel wind turbine towers due to the isotropic properties of steel and the possibility to rigidly attach segments to the original structure. On behalf of the European Commission, Veljkovic et al. (2012) investigated the optimization and use of high strength steel in wind turbine towers. Creating a slenderer shell caused the need to review the door opening stability. Rather than stress redistribution, buckling resistance becomes the governing challenge in finding working concepts. Seven configurations for stiffening the opening were suggested and analysed (see Figure 2.5). All concepts included a reinforcing ring around the opening. In concept a, c and g the ring was dimensioned to be rigid. In four configurations (b – e) local vertical and horizontal stiffeners were attached to the ring. Two concepts (d and e) included circumferential horizontal stiffeners above and below the opening, while three concepts (e – g) suggest vertical stiffeners at the left and right side of the opening. It was found that a rigid ring around the opening provided the best reinforcement while local vertical and horizontal stiffeners attached to the opening ring were comparatively less effective. Vertical stiffeners were superior to circumferential horizontal stiffeners since they provide a better reinforcement for axial stresses in the tower.

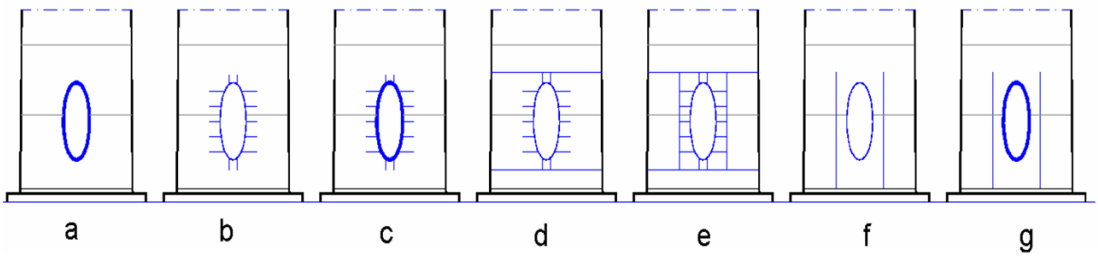

Figure 2.5. Reinforcement concepts for high strength steel wind turbine towers. (Veljkovic et al., 2012)

2.2.4 Biomimicry of natural reinforcement

Although not being an opening, knots and imperfections in trees lead to stress concentrations in the wood. Vertical loads in trees are carried by continuous lignin fibres oriented in direction of growth. Knots are formed when branches grow out of the tree trunk. Fibres in these areas are therefore oriented in direction of growth of the branches and do not contribute to the global stability of the tree. As a result, weak spots are formed and adjacent fibres must compensate for loss of strength. The only way of achieving this without widening the tree trunk is by condensing fibres around the knot. As shown in Figure 2.6 fibres curve around the imperfection and reduce the spacing between each other without intersecting. This results in an optimal load transfer around knots without having to introduce other materials for reinforcement. This concept is also applicable in fluid dynamics and can be shown by trajectories formed when a fluid with directional flow interferes with an object. Adapting the concept of stiffeners following optimal stress flow around an arbitrary opening has been investigated by Alhajahmad and Mittelstedt (2022) for evaluation and improvement of buckling performance of aircraft windows. Leaning on nomenclature from fluid dynamics, these curved stiffeners are called *streamline stiffeners*. The study showed buckling load can be increased by up to 52 % for uniaxial and up to 54 % for biaxial load for a circular opening in a laminate sheet subjected to in-plane compressive loads. This is for the case when a hybrid reinforcement structure is used where reinforcement consists of a mix of streamline stiffeners in the load direction and straight stiffeners in the direction perpendicular to the load. The similarity between engineered stiffeners and nature becomes clear in Figure 2.6. Here a stiffened panel with streamline stiffeners both in load and perpendicular to load direction is illustrated.

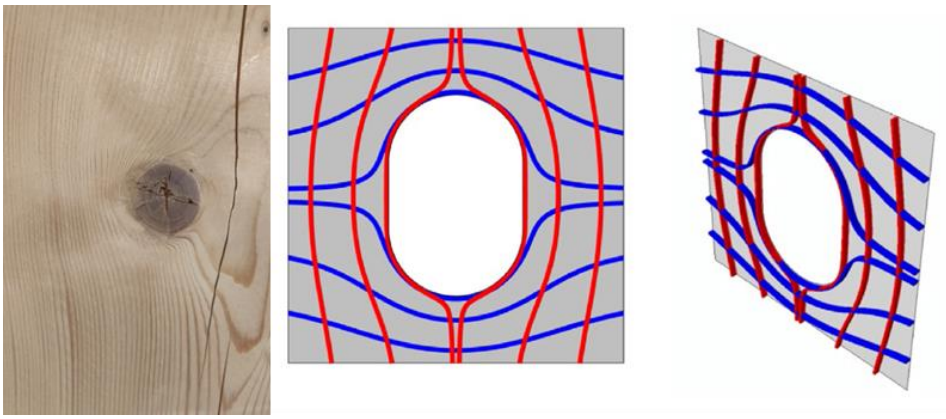

Figure 2.6. Left: Lignin fibres curving around a knot. Right: Streamline stiffeners investigated by Alhajahmad and Mittelstedt (2022).

3 Theory – mechanics

To understand stress concentration, one must understand the underlaying mechanics of an orthotropic laminate. A short introduction to classical laminate theory will be given, describing a method for computing mechanical properties of laminates. Subsequently, stress concentrations and failure around openings in orthotropic materials and laminates will be reviewed.

3.1 Classical laminate theory

Classical laminate theory (here denoted *CL-theory* to avoid confusion with cross laminated timber, denoted CLT in civil engineering) is used to obtain material parameters for a laminate and predict its behaviour and failure. The methodology and denomination in this chapter is oriented by the work of Agarwal, Broutman and Chandrashekhara (2017). Here, only those parts of CL-theory needed for understanding following calculations will be presented and explained.

A laminate is formed by bonding several laminae together. One lamina can consist of different constituents, e.g. carbon fibre and epoxy resin. Orientation and axes of the laminate is denoted with subscript x and y, forming a global coordinate system. Laminae are characterized using local coordinates oriented by the fibres, thus each lamina has an own coordinate system which can differ from the global. The local notation is made with subscript L (longitudinal) and T (transversal). In this report symmetric laminates are investigated. These are constructed with an equal and symmetric number of laminae, with respect to orientation and properties, around the laminate mid plane. The aim of CL-theory is to analyse and predict behaviour and failure in laminates and its laminae. For the model to hold a few assumptions must yield:

- the laminate is sufficiently thin to assume plane stress
- material properties are constant through the thickness of each lamina
- glue lines between laminae are infinitesimal thin
- glue lines are not deformable by shear

In an arbitrary body, the general state of stress and strain at any given point is described by nine stress and nine strain components. According to Hooke's law, stresses and strains are related through the stiffness of a material. Since each stress must be related to nine strains and each strain be related to nine stresses, 81 independent elastic constants must be defined. In an anisotropic material, due to symmetry of stress and strain tensors and thermodynamic considerations, the independent elastic constants can be reduced to 21. Further, for each introduced plane of symmetry, elastic constants can be reduced. An orthotropic material exhibits symmetry around three orthogonal planes. This results in six stress and strain components and nine independent elastic constants. Stress-strain relation for an orthotropic material can be written in matrix form with engineering strains and elastic constants denoted *C* as:

$$\begin{Bmatrix} \sigma_1 \\ \sigma_2 \\ \sigma_3 \\ \tau_{23} \\ \tau_{13} \\ \tau_{12} \end{Bmatrix} = \begin{bmatrix} C_{11} & C_{12} & C_{13} & 0 & 0 & 0 \\ C_{12} & C_{22} & C_{23} & 0 & 0 & 0 \\ C_{13} & C_{23} & C_{33} & 0 & 0 & 0 \\ 0 & 0 & 0 & C_{44} & 0 & 0 \\ 0 & 0 & 0 & 0 & C_{55} & 0 \\ 0 & 0 & 0 & 0 & 0 & C_{66} \end{bmatrix} \begin{Bmatrix} \varepsilon_1 \\ \varepsilon_2 \\ \varepsilon_3 \\ \gamma_{23} \\ \gamma_{13} \\ \gamma_{12} \end{Bmatrix} \tag{3.1}$$

Composite laminates show superior strength in plane. Out of plane properties are often significantly weaker or neglectable, resulting in a plane-stress state. This sets components out-of-plane (σ_3, τ_{23} and τ_{13}) to zero, reducing the element constitutive equation further. For an

orthotropic material oriented along material axes, stiffness coefficients, Q, can be defined from the elastic constants and stress-strain relation be written as:

$$\begin{Bmatrix} \sigma_1 \\ \sigma_2 \\ \tau_{12} \end{Bmatrix} = \begin{bmatrix} Q_{11} & Q_{12} & 0 \\ Q_{12} & Q_{22} & 0 \\ 0 & 0 & Q_{66} \end{bmatrix} \begin{Bmatrix} \varepsilon_1 \\ \varepsilon_2 \\ \gamma_{12} \end{Bmatrix} \tag{3.2}$$

Stiffness matrix for each lamina can be obtained with engineering constants as follows:

$$Q = \begin{bmatrix} \frac{E_L}{1 - \upsilon_{LT}\upsilon_{TL}} & \frac{\upsilon_{LT}E_T}{1 - \upsilon_{LT}\upsilon_{TL}} & 0 \\ \frac{\upsilon_{LT}E_T}{1 - \upsilon_{LT}\upsilon_{TL}} & \frac{E_T}{1 - \upsilon_{LT}\upsilon_{TL}} & 0 \\ 0 & 0 & G_{LT} \end{bmatrix} \tag{3.3}$$

This leaves five independent material parameters needed for applying CL-theory. Required in-plane properties for assembling each lamina's stiffness matrix are:

- E_L: Young's modulus parallel to the grain
- E_T: Young's modulus perpendicular to the grain
- υ_{LT}: major Poisson's ratio
- υ_{TL}: minor Poisson's ratio
- G_{LT}: shear modulus

For future computation, a correlation between moduli of elasticity and Poisson's ratios is formulated:

$$\frac{\upsilon_{LT}}{E_L} = \frac{\upsilon_{TL}}{E_T} \tag{3.4}$$

To describe laminate properties, all lamina stiffness matrices must be joined. Since the stiffnesses are defined in local coordinates, matrices must be converted to describe local stiffnesses in global coordinates. Dictating the conversion is the angle describing the offset between global and local coordinate systems, α. For conversion, transformation matrices, denoted *T1* (stress transformation matrix) and *T2* (strain transformation matrix), must be defined. Expressed in trigonometric functions, *T1* and *T2* are:

$$T1 = \begin{bmatrix} cos(\alpha)^2 & sin(\alpha)^2 & 2\,sin(\alpha)\,cos(\alpha) \\ sin(\alpha)^2 & cos(\alpha)^2 & -2\,sin(\alpha)\,cos(\alpha) \\ -sin(\alpha)\,cos(\alpha) & sin(\alpha)\,cos(\alpha) & cos(\alpha)^2 - sin(\alpha)^2 \end{bmatrix} \tag{3.5}$$

$$T2 = \begin{bmatrix} cos(\alpha)^2 & sin(\alpha)^2 & sin(\alpha)\,cos(\alpha) \\ sin(\alpha)^2 & cos(\alpha)^2 & -sin(\alpha)\,cos(\alpha) \\ -2\,sin(\alpha)\,cos(\alpha) & 2\,sin(\alpha)\,cos(\alpha) & cos(\alpha)^2 - sin(\alpha)^2 \end{bmatrix} \tag{3.6}$$

With these matrices defined, local stiffness matrices in global coordinates, $\bar{Q}$, can be computed:

$$\bar{Q} = [T1]^{-1} \cdot [Q] \cdot [T2] \tag{3.7}$$

In a laminate, applied forces and moments result in strains and curvatures. Constitutive relations for the laminate can be written in symbolic, general form as:

$$\begin{pmatrix} N \\ M \end{pmatrix} = \begin{bmatrix} A & B \\ B & D \end{bmatrix} \begin{pmatrix} \varepsilon^0 \\ \kappa \end{pmatrix} \tag{3.8}$$

Here *N* and *M* are vectors describing forces and moments in laminate x, y, and xy direction respectively. ε^0 and κ are resulting strains and curvatures in x, y, and xy direction respectively. Matrix *A* is called extensional stiffness matrix and relates forces to strains. Matrix *D* is called bending stiffness matrix and equivalently relates moments to curvature. *B*, the coupling stiffness matrix, relates forces to curvature and moments to strains. Solving equation (3.8), the constitutive relations can be written as:

$$N = A\varepsilon^0 + B\kappa = \begin{bmatrix} A_{11} & A_{12} & A_{16} \\ A_{12} & A_{22} & A_{26} \\ A_{16} & A_{26} & A_{66} \end{bmatrix} \begin{pmatrix} {\varepsilon_x}^0 \\ {\varepsilon_y}^0 \\ {\gamma_{xy}}^0 \end{pmatrix} + \begin{bmatrix} B_{11} & B_{12} & B_{16} \\ B_{12} & B_{22} & B_{26} \\ B_{16} & B_{26} & B_{66} \end{bmatrix} \begin{pmatrix} \kappa_x \\ \kappa_y \\ \kappa_{xy} \end{pmatrix} = \begin{pmatrix} N_x \\ N_y \\ N_{xy} \end{pmatrix} \tag{3.9}$$

$$M = B\varepsilon^0 + D\kappa = \begin{bmatrix} B_{11} & B_{12} & B_{16} \\ B_{12} & B_{22} & B_{26} \\ B_{16} & B_{26} & B_{66} \end{bmatrix} \begin{pmatrix} {\varepsilon_x}^0 \\ {\varepsilon_y}^0 \\ {\gamma_{xy}}^0 \end{pmatrix} + \begin{bmatrix} D_{11} & D_{12} & D_{16} \\ D_{12} & D_{22} & D_{26} \\ D_{16} & D_{26} & D_{66} \end{bmatrix} \begin{pmatrix} \kappa_x \\ \kappa_y \\ \kappa_{xy} \end{pmatrix} = \begin{pmatrix} M_x \\ M_y \\ M_{xy} \end{pmatrix} \tag{3.10}$$

In a symmetric laminate, forces only lead to strains and moments only lead to curvatures, thus the coupling stiffness matrix is zero. Furthermore, in this study only forces and strains will be used for computations, making thorough description of the bending stiffness matrix redundant. The extensional stiffness matrix is obtained by summarizing *i* local $\bar{Q}$ matrices over laminate height:

$$A = \sum_{k=1}^{i} \bar{Q}_k \cdot (h_k - h_{k-1}) \tag{3.11}$$

Here *h* describes the through-thickness coordinate of the lamina border measured from the laminate mid-plane. In other words, the extensional stiffness matrix is a summation of local stiffness matrices multiplied with their respective lamina height.

Olsson (2006) suggests engineering properties of the laminate can be obtained from *A* matrix constituents in a symmetric balanced layup through equations (3.12) – (3.16). Here h_{tot} denotes total laminate height:

$$E_x = \left(1 - \frac{{A_{12}}^2}{A_{22}A_{11}}\right) \cdot \frac{A_{11}}{h_{tot}} \tag{3.12}$$

$$E_y = \left(1 - \frac{{A_{12}}^2}{A_{22}A_{11}}\right) \cdot \frac{A_{22}}{h_{tot}} \tag{3.13}$$

$$\upsilon_{xy} = \frac{A_{12}}{A_{22}} \tag{3.14}$$

$$\upsilon_{yx} = \frac{A_{12}}{A_{11}} \tag{3.15}$$

$$G_{xy} = \frac{A_{66}}{h_{tot}} \tag{3.16}$$

Laminates with a layup such that laminate x and y direction have similar properties are called *quasi-isotropic* laminates. For such laminates, layup must be symmetrical and balanced around the laminate mid-plane, resulting in orientation-independent strength and stiffness. Denotation of laminate layups is made with square brackets and separating lamina with a slash. An 8-layered laminate could be described as [0/0/45/-45/-45/45/0/0], indicating middle laminae are rotated 45°. For a symmetric laminate as above, a shorter denotation can be used, where symmetry is indicated with subscript "s". The same 8-layered laminate can therefore be denoted as $[0/0/45/-45]_s$. Layups which are not symmetric but show a regularity in layer rotation are in

this study called *quasi-symmetric*. Instead of subscript "s", subscript "(s)" is used to indicate quasi-symmetry. The short notation for the arbitrary layup [0/0/25/-25/25/-25/25/-25/0/0] becomes $[0/0/25/-25/25]_{(s)}$.

Applying CL-theory, change in engineering properties of a Kerto-Q panel over rotation angle are plotted in Figure 3.1. Here the homogenization of panel properties into lamina properties has been done to show the impact of rotation angle on stiffness and contraction.

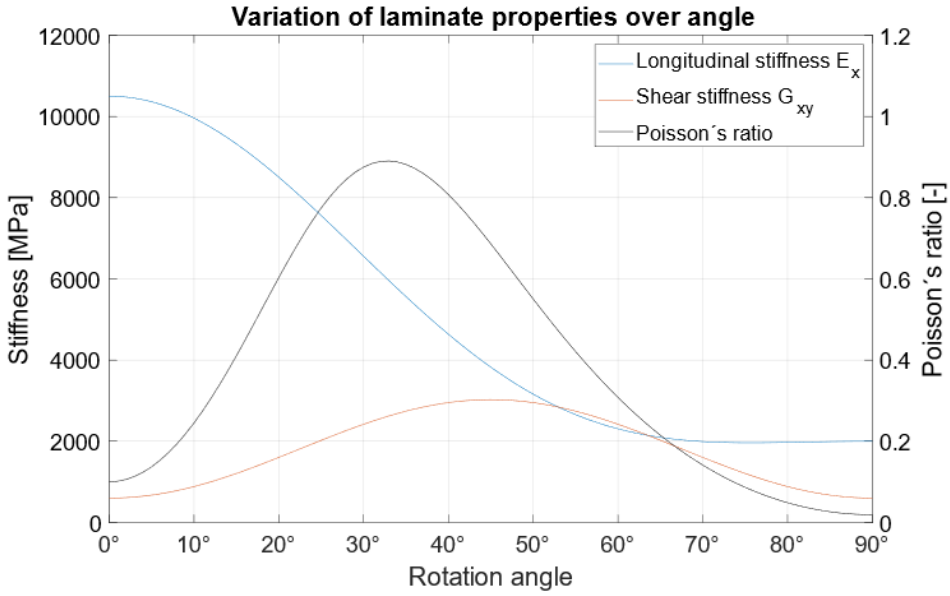

Figure 3.1. Variation of engineering properties in a laminate over angle.

Shear stiffness is symmetrical around 45° where it reaches its peak. Longitudinal stiffness declines strongly between 10° and 60° and reaches its transversal, or 90° stiffness, at around 70°. This implies a rotation over 45° is not preferable when aiming at designing for high longitudinal and shear stiffness in the laminate. Small changes in angle between 0° and 10° don't have a big impact neither on longitudinal, nor on shear stiffness.

3.2 Failure criteria

Failure in an orthotropic laminate occurs when the ultimate strength in one or more material directions is reached and the resulting stresses cannot be redistributed to other laminae or material directions. To compute failure in a laminate, failure criteria must be defined. These can reach from simple criteria looking at each material direction separately to criteria with increased complexity of interaction between properties in different material directions. Starting at the end of low complexity and failure criteria predicting rather non-conservative performance, maximum stress theory (Hart-Smith, 1984) can be found. This theory corelates strains and stresses from the laminate to its laminae. Premise for the maximum stress criterion is that the laminate deforms uniformly. Strain is therefore continuous through the laminate. Due to difference in orientation of laminae, the induced strain will lead to varying stress through the laminate. Laminae with fibre orientation resulting in a high stiffness in the global domain will attract higher stresses compared to laminae with fibre orientation resulting in a low stiffness in the global domain. Failure occurs when a lamina reaches its ultimate stress capacity for a given material direction. This results in five independent failure criteria, oriented along the principal material directions in each lamina. Tensile stresses are defined as positive while compressive stresses are defined as negative. Failure occurs if any of the following equations with applied stresses σ_L, σ_T or τ_{LT} is fulfilled:

$$\sigma_L > \sigma_{Lu} \tag{3.17}$$

$$\sigma_L < \sigma_{Lu'} \tag{3.18}$$

$$\sigma_T > \sigma_{Tu} \tag{3.19}$$

$$\sigma_T < \sigma_{Tu'} \tag{3.20}$$

$$\tau_{LT} > \tau_{LTu} \tag{3.21}$$

Here, σ_{Lu} and σ_{Tu} denote ultimate tensile strengths while $\sigma_{Lu'}$ and $\sigma_{Tu'}$ indicate ultimate compressive strengths in longitudinal and transversal direction respectively. τ_{LTu} defines ultimate in plane shear strength. The independency of equations implies that adding stresses in a new material direction will not weaken the lamina when stresses in another direction already exist. In reality, there might be coupling effects between the laminae which decrease the capacity of the laminate. The Tsai-Hill or maximum work theory (Tsai, 1965) considers all failure components to interact and form a uniform failure criterion:

$$\left(\frac{\sigma_L}{\sigma_{Lu}}\right)^2 - \frac{\sigma_L \sigma_T}{{\sigma_{Lu}}^2} + \left(\frac{\sigma_T}{\sigma_{Tu}}\right)^2 + \left(\frac{\tau_{LT}}{\tau_{LTu}}\right)^2 \geq 1 \tag{3.22}$$

In this case σ_{Lu} and σ_{Tu} are ultimate strengths in tension or compression, depending on the nature of applied stresses. Based on von Mises yield criterion, failure occurs when the combination of stresses in different material directions reach a limit value (normalizing stresses with ultimate strengths gives a limit value of 1). This implies the absence or presence of stresses in one direction affects the lamina's capacity in another direction. While maximum stress failure criterion gives a perception of the nature of failure, maximum work failure criterion only estimates at what stresses the lamina will fail, thus not providing information about the failure mode. Both these failure criteria have been shown to give good estimations of failure strength of timber and LVL in previous studies ((Mascia and Simoni, 2013; Merhar, 2021)). Commonly used for CF composites are Tsai-Wu (Tsai and Wu, 1971) and Hashin (Hashin and Rotem, 1973) theories. Tsai-Wu adds more complexity to the Tsai-Hill theory by introducing one additional material-dependent interaction-parameter. This parameter is determined by intensive testing and curve fitting of the results, which is expensive and difficult to perform. While being done for CF composites, no data has yet been established for timber materials. Hashin's failure criterion dives deeper into the nature of failure and is failure mode based. It consists of four independent equations defining capacities in longitudinal and transversal fibre direction for tension and compression. It also correlates shear loading to tensile failure in longitudinal direction and considers out of plane shear capacity for the transversal compressive failure mode. For the contribution of shear loading to tensile failure a material parameter is needed which has not yet been obtained for timber. There are numerous additional failure theories for laminates with increasing complexity which due to lacking material data for LVL are unfeasible for this study and therefore will not be presented further.

3.3 Openings in orthotropic laminates

When subjecting constructions with openings to forces, stresses around the opening will increase. In isotropic materials these increases will be symmetric around the opening with respect to the axis of applied load. Orthotropic materials provide different material properties in different directions and stress concentrations will differ with respect to the different moduli and the ratios between them. Following is an analytical assessment of stress concentration factors and the contribution of the different material direction's stiffnesses on these.

3.3.1 Stress concentrations

Lekhnitskii (1968) describes stress concentrations around openings in orthotropic plates and gives expressions for analytical computations. Given expressions for multiple load cases, in this thesis only tension and shear loads will be applied. For the theory to be applicable, uniform stress must be assumed around the opening in the investigated plate. No variation in thickness of the plate or local change in stiffness occurs and plane stress is assumed. For description of orientation of material and forces around the opening, cartesian coordinates (main axes denoted x and y) will be used, while stress concentrations around the opening contour will be localised in polar coordinates. Four material parameters must be defined. Namely, these are Young's moduli parallel to the principal axes (E_1 and E_2), (major) Poisson's ratio (υ_{12}) and shear modulus (G) in plane. With these, some general notations can be introduced:

$$k = \sqrt{\frac{E_1}{E_2}} \tag{3.23}$$

$$n = \sqrt{2 \cdot \left(\frac{E_1}{E_2} - \upsilon_{12}\right) + \frac{E_1}{G}} \tag{3.24}$$

Furthermore, Young's modulus at the opening contour, E_θ, acting tangential to the edge can be defined. Let θ be the polar angle to the opening contour measured from the x-axis:

$$\frac{1}{E_\theta} = \frac{\sin^4\theta}{E_1} + \left(\frac{1}{G} - \frac{2\upsilon_{12}}{E_1}\right)\sin^2\theta\cos^2\theta + \frac{\cos^4\theta}{E_2} \tag{3.25}$$

Load can be applied in alignment or with an angle φ to the principal material/fibre direction. This is done by rotating the panel with a given angle φ, while load is always applied in the same direction in the global domain. For $\varphi = 0°$, fibres are oriented in x- or 0° direction, while $\varphi = 90°$ implies panels have been rotated such that fibres align with y- or 90° axis. Lastly, denotation of loads is made with capital letters P (uniaxial load) and T (biaxial load). Loads are considered acting along one unit area, resulting in uniform stresses in the laminate. By defining loads as unit loads of 1 N, resulting stress concentration factors (SCF) will be obtained by calculating σ_θ. It should be noted that the calculations hold for both positive and negative loads. Thus, positive SCF suggest stresses in same orientation as applied load, i.e. tensile forces leading to tensile stresses and negative SCF indicate stresses in opposite orientation as applied load, i.e. tensile forces leading to compressive stresses.

3.3.1.1 Uniaxial loading

When loading uniaxially, tension is applied along the x-axis as shown in Figure 3.2. A general expression can be given for tangential stresses at the opening contour for tension (Lekhnitskii, 1968):

$$\begin{aligned}\sigma_\theta = P \cdot \frac{E_\theta}{E_1} \cdot \{&[-cos^2\varphi + (k+n)sin^2\varphi] \cdot k \cdot cos^2\theta \\ &+ [(1+n)cos^2\varphi - k \cdot sin^2\varphi] \cdot sin^2\theta \\ &- n(1+k+n)\sin\varphi\cos\varphi\sin\theta\cos\theta\}\end{aligned} \tag{3.26}$$

By computing stresses for each angle around the opening contour and plotting SCF on polar plots, variation of SCF can be visualized. Following Figure 3.3 shows SCF for varying sheet orientations in a unidirectional (UD) laminate with a ratio of $E_1/E_2 \approx 31$, coinciding with properties of a standard Kerto-S panel.

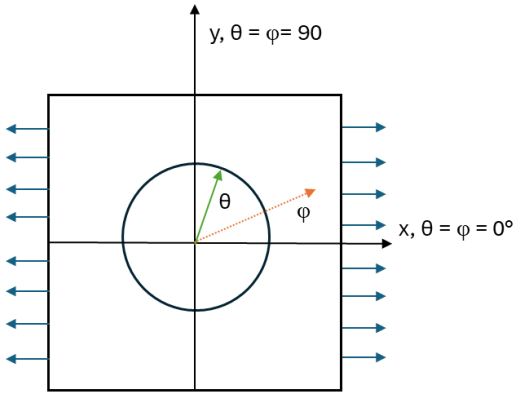

Figure 3.2. Coordinates and stresses in a laminate subjected to tension.

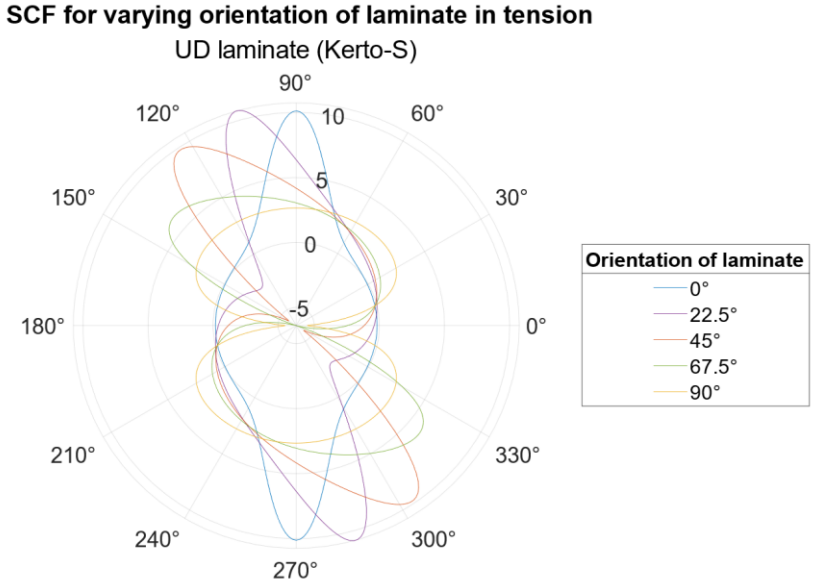

Figure 3.3. Stresses around a hole in laminates with different orientations in tension.

Two observations can be made:

1. For laminates oriented parallel to the principal directions (φ = 0°, 90°, 180°, 270°), stresses are symmetrical with respect to the axis of applied load. For all other cases stresses are symmetrical to the midpoint of the opening.
2. Loading the laminate in direction with its strong axis results in large SCF acting along the weak axis of the laminate. By rotating the laminate, SCF acting with opposite orientation as the applied force are induced, in this case leading to compressive forces along the axis of applied tensile force.

It has been shown in equations (3.23), (3.24) and (3.26) that elastic moduli in principal material directions govern resulting SCF at the opening contour. The above investigated Kerto-S panel resembles a UD-laminate with a highly dominant material direction. In products with other stiffnesses, resulting SCF will differ. Kerto-Q displays a ratio of $E_1/E_2 = 5.25$, decreasing the dominance of the stiff direction in the laminate. Going even further, plywood shows a ratio $E_1/E_2 = 1.37$, making the orthotropic material behave almost quasi-isotropic. Plotting SCF for orienting panels in 0°, 45° and 90° shows that lessening the ratio between moduli evens out SCF (see Figure 3.4). The high and low peaks of stresses in a UD laminate vanish in panels with a less dominant main material direction.

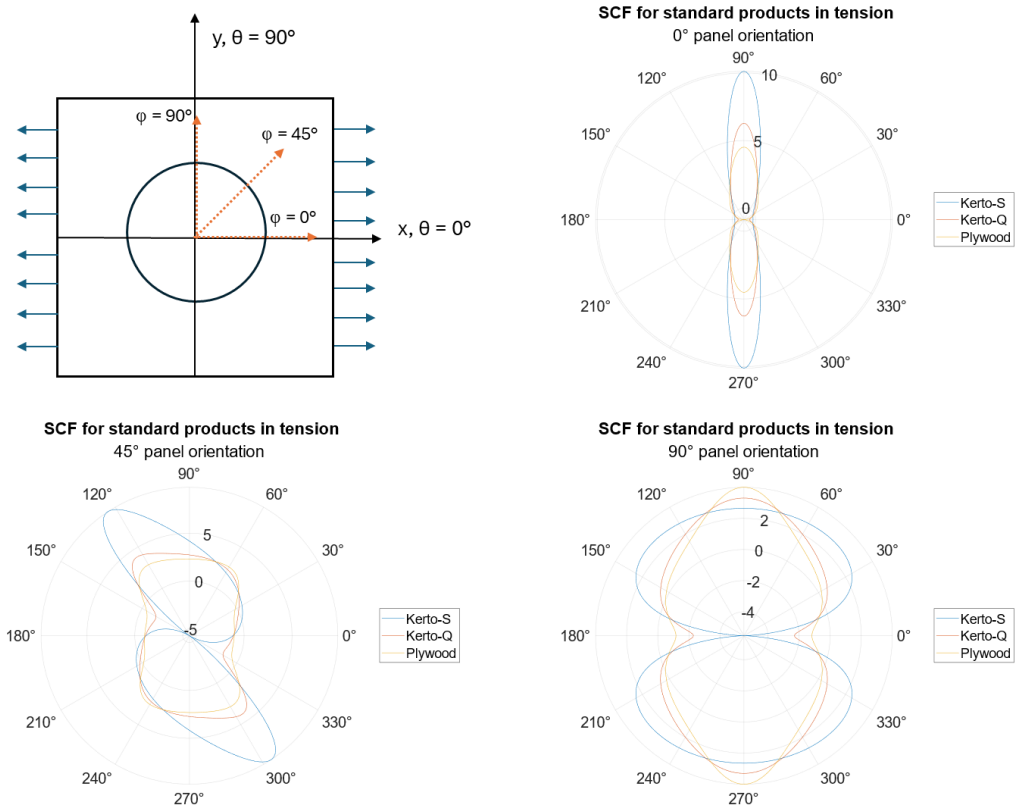

Figure 3.4. Stresses around a hole in standard products in tension for different orientations. Top left: Panel and main fibre orientation. Top right: SCF for 0° panel orientation. Bottom left: SCF for 45° panel orientation. Bottom right: SCF for 90° panel orientation.

The orthotropy of the laminate implies strengths are different for each material axis and resulting stresses differ in the two material directions. To see how the stresses vary, the tangential stresses obtained can be split into stress components in material x- and y-direction. This is done by trigonometric functions and the angle to the opening contour, θ. Along the axes $\theta = 0°$ and $\theta = 180°$, defining material x-direction, tangential opening stresses act in material y-direction and the x-component is zero. In the same way, along the axes $\theta = 90°$ and $\theta = 270°$, defining material y-direction, tangential opening stresses act in material x-direction and the y-component is zero. This correlation results in definition of stress components as follows:

$$\sigma_x = sin(\theta) \cdot \sigma_\theta \tag{3.27}$$

$$\sigma_y = cos(\theta) \cdot \sigma_\theta \tag{3.28}$$

Plotting the distribution of stresses in a Cartesian coordinate system illustrates the distribution of resulting stresses on material directions. In Figure 3.5, stress components of standard products with holes in tension are plotted over contour angle. Remarkable is that although the strong x-direction is around 30 times stiffer than the weaker y-direction in a Kerto-S panel, max SCF for the strong material direction only reaches a factor of around 10 compared to the weak material direction. At the same time, strength in tension parallel to the grain for a Kerto-S plate is more than 30 times higher than the strength perpendicular to the grain. This implies the laminate will always fail in its weak direction in a failure parallel to the fibres. While this is true in a UD laminate, the same cannot be observed in laminates with less dominant strong axes. In a Kerto-Q laminate for instance, SCF in the strong material direction are around 8 times higher than in the weak direction, while strength is only around 4 times higher. A Kerto-Q plate

will therefore fail perpendicular to its main fibre direction. The same reasoning holds for plywood, with nature of failure similar to failure in Kerto-Q plates.

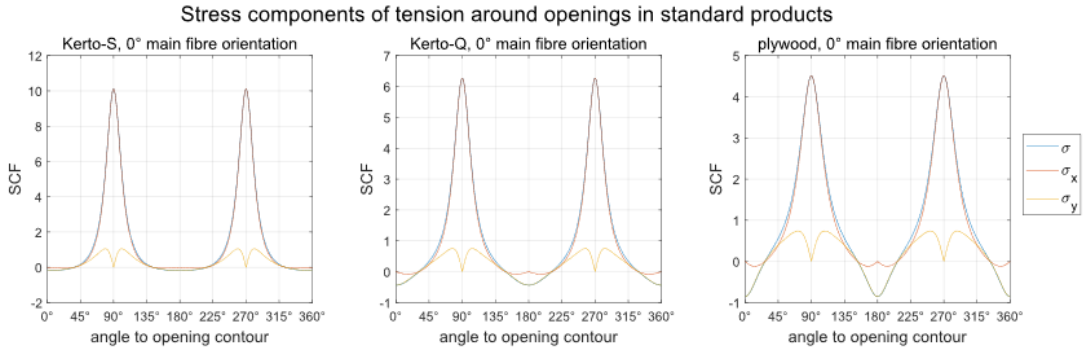

Figure 3.5. Stress components in standard products subjected to tension.

3.3.1.2 Biaxial loading

For biaxial loading, tension is applied along the edges of the plate, distributed evenly parallel to the main axes x and y according to Figure 3.6. The resulting principal stress therefore resembles a uniaxial force applied along the bisector of the x and y axis, i.e. φ = 45°. As for tension, a general expression for tangential stresses at the opening contour with respect to the angle of applied shear load can be formulated (Lekhnitskii, 1968):

$$\sigma_\theta = T \cdot \frac{E_\theta}{2E_1} \cdot (1 + k + n) \cdot \{-n \cdot \cos 2\varphi \sin 2\theta + [(1 + k)\cos 2\theta + k - 1]\sin 2\varphi\} \tag{3.29}$$

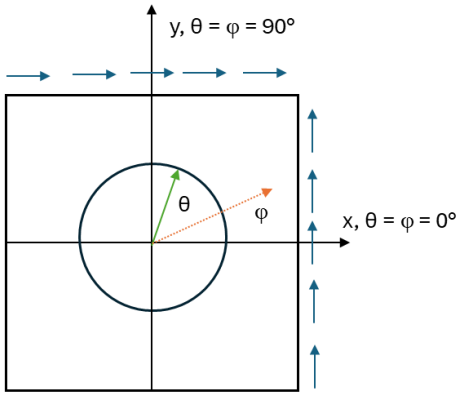

Figure 3.6. Coordinates and stresses in laminate subjected to shear.

The same UD-laminate as in the case for tension is subjected to shear and resulting SCF are plotted in Figure 3.7. Note that resulting SCF at the opening contour for -90° (or 270°) and +90° panel orientation are alike.

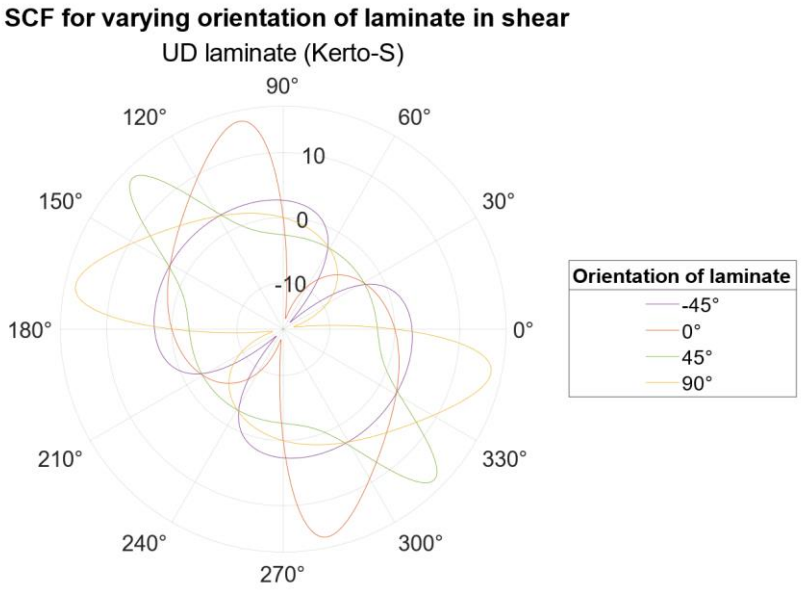

Figure 3.7. Stresses around a hole in laminates with different orientations in shear.

Similar observations as for the case with uniaxial loading can be made:

1. Stresses at the opening contour are symmetrical with respect to the axis of principal load for laminates oriented parallel or perpendicular to the axis of principal load (φ = 45°, 135°, 225°, 315°). For all other orientations stresses are symmetrical to the midpoint of the opening.
2. Loading the laminate with principal stresses in direction with its strong axis results in large SCF acting along the weak axis of the laminate. By rotating the laminate, SCF acting with opposite orientation as the applied principal force are induced, in this case leading to compressive forces along the axis of applied principal force.

Plotting SCF for orienting panels in -45°, 0°, and 45° to its strong direction shows similar tendencies as for the uniaxial loading (see Figure 3.8). Lessening the ratio between moduli evens out SCF and the high and low peaks of stresses in a UD laminate vanish in panels with a less dominant main material direction. In addition, it is noticeable that 0° loading in shear resembles the stress concentration pattern for the 45° loading in tension. The same resemblance can be observed for shear loading in 45° oriented laminates compared to 0° oriented tensioned laminates and -45° oriented laminates compared to 90° oriented tensioned laminates.

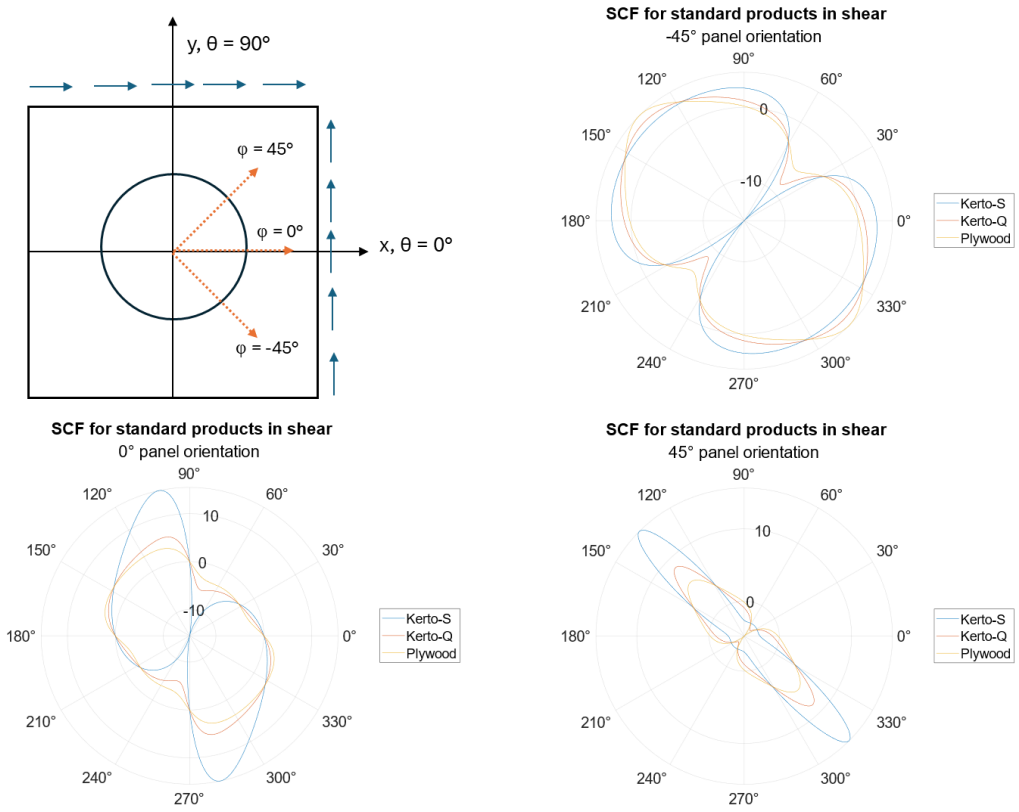

Figure 3.8. Stresses around a hole in standard products in shear for different orientations. Top left: Panel and main fibre orientation. Top right: SCF for -45° panel orientation. Bottom left: SCF for 0° panel orientation. Bottom right: SCF for 45° panel orientation.

As for uniaxial loading, splitting resulting SCF in stress components reveals nature of failure. For shear, results do not depend on how dominant the strong material direction is. Difference in SCF is never bigger than difference in strength, meaning failure will always have the same nature, namely perpendicular to main fibre direction.

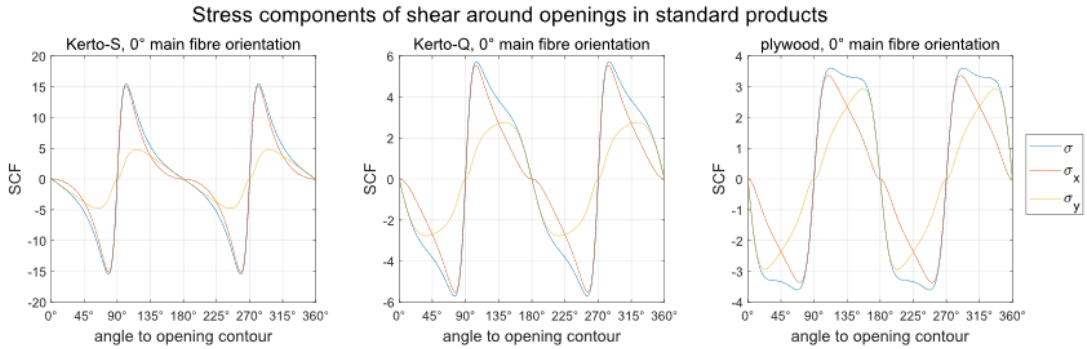

Figure 3.9. Stress components in standard products subjected to shear.

4 Reducing stress concentrations around openings

Stresses occurring at and around an opening origin from two things: change in geometry and change in stiffness. When creating an opening, the geometry of the whole structure changes due to the removed material and creates disturbances in stress flow. In the same way, by removing material, stiffness is decreased and stress concentrations are formed. Therefore, before reinforcing an opening, the opening geometry and surrounding material can be investigated and adjusted to reduce stress concentrations along the opening contour. In the following, geometry of the opening, material properties and panel orientation will be varied to see their respective impacts on stress concentrations. Governing load cases are uniaxial and biaxial loading. Elements are oriented with their strong (x) axis vertically (global y), weak in plane (y) axis horizontally (global -x) and out of plane in global z-direction. For investigation of stresses around the opening, polar coordinates are used with the origin or 0° axis along the global x axis, oriented counterclockwise such that global y-axis equals polar 90°.

4.1 Variation of opening geometry

Standard dimensions for openings in wind turbine towers are not set. Requirements vary for different operators. In this study, boundaries are set for a total height of 200 cm and width of the opening of 75 cm, at least at one vertical and horizontal axis. Chosen geometries are presented in Figure 4.1 and show a variation in corner radius and corner characteristics. In the following, denotation is made as width = *w*, radius = *r*, ellipse major radius = *a* and ellipse minor radius = *b*. A short summation of geometries follows:

a) rectangular opening with semicircles at top and bottom, *r = w/2 = 375 mm*
b) ellipse with radii *a = 1000 mm, b = 375 mm, a/b = 2.7*
c) rectangular opening with semiellipses at top and bottom, *a = 750 mm, b = 375 mm, a/b = 2*
d) rectangular opening with elliptical corners, *a = 750 mm, b = 250 mm, a/b = 3*
e) rectangular opening with semielliptic top, *a = 750 mm, b = 375 mm, a/b = 2*, and elliptical bottom corners, *a = 375 mm, b = 187.5 mm, a/b = 2*
f) rectangular opening with rounded corners, *r = w/4 = 187.5 mm*

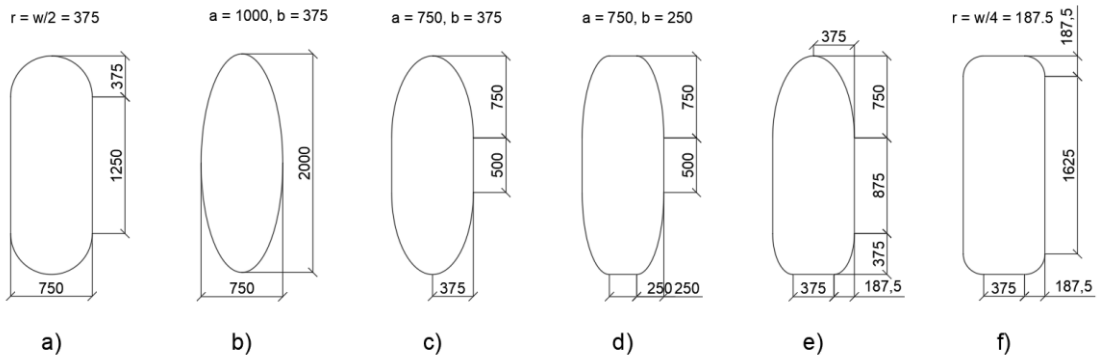

Figure 4.1. Overview of investigated opening geometries.

A wall section for each opening geometry was created in Ansys Multiphysics with dimensions 3.75 m x 6 m, big enough to form uniform stresses around the opening. Thickness of the wall was set to 350 mm with homogenous properties of Kerto-Q LVL through the thickness. Mesh size of 0.1 m and quadratic order shell elements were used. Stresses were retrieved as path results around the opening contour.

4.1.1 Tensile loading

To create a uniform tensile stress in the wall segments, a vertical displacement of 1 mm at the top edges was induced. Stress fields for stresses in material x- and y-direction are illustrated in Figure 4.2 and Figure 4.3. The overall trend of stress distribution presented in Chapter 3.3.1.1 holds for the investigated opening shapes. Tensile stress concentrations occur at the left and right edges of the opening while compressive stress concentrations are formed at the top and bottom.

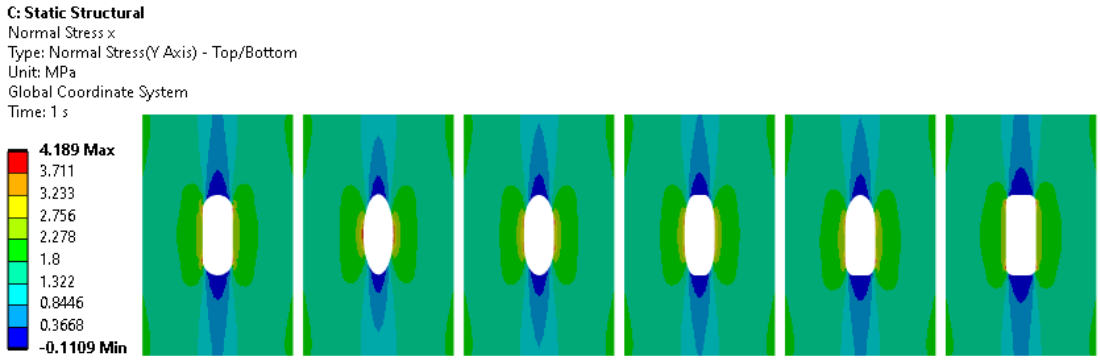

Figure 4.2. Resulting stresses in longitudinal direction for investigated opening geometries.

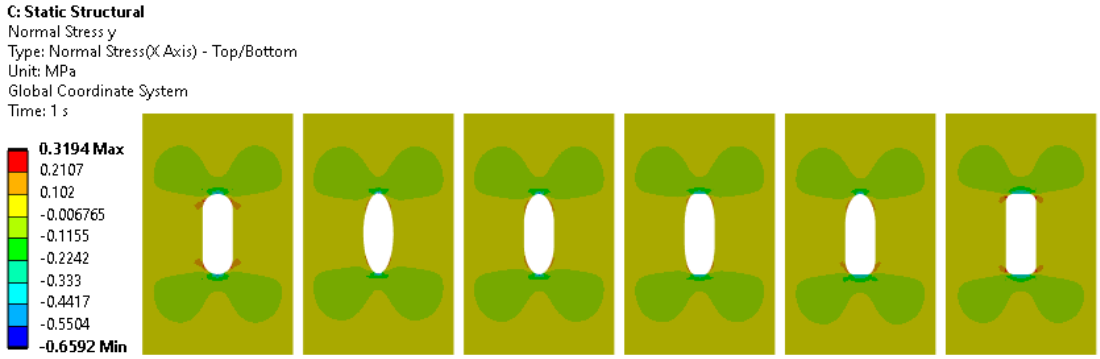

Figure 4.3. Resulting stresses in tangential direction for investigated opening geometries.

4.1.1.1 Stress concentrations in strong material direction

For all shapes, peaks in stresses in the material x-direction form at the change of contour radius. At any point where an elliptical or round corner meets a straight, vertical segment stress concentrations are induced. Since the elliptical opening b) does not exhibit straight segments, stress concentrations are condensed around the horizontal opening tip along the 0° axis. Plotting stress variation over opening contour for all opening shapes in Figure 4.4 allows for a comparison of stresses between opening geometries.

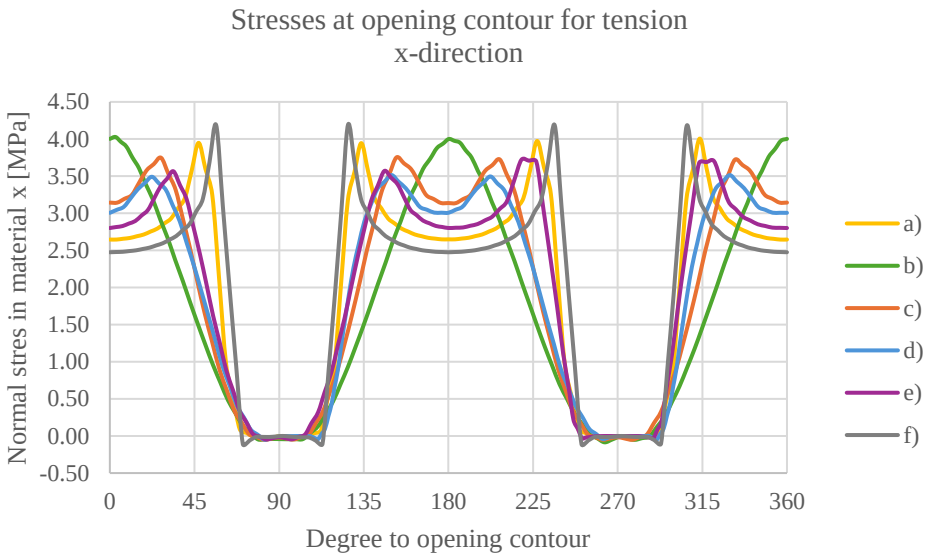

Figure 4.4. Variation of longitudinal stresses around different opening geometries.

Geometries with circular corners show higher and more distinct peaks in stresses than geometries with elliptical corners. Introducing straight edges at the left and right border moves and reduces stress peaks for shapes with elliptical corners. At the same time, a reduction of stresses along the vertical, straight segment can be observed. This is true regardless of corner characteristics. Geometry a) exhibits stress peaks with a magnitude similar to the stresses for an elliptical opening, with the difference that these occur twice as often as in the elliptical shape. Reducing radius in a circular cornered geometry increases stress concentrations at the critical coordinates. Introducing straight horizontal edges at the top and/or bottom of the opening geometry creates plateaus of uniform stresses along these straight edges. For the doubly symmetrical geometries d) and f), these can be observed to form both around 90° and 270°, while the simple symmetrical geometry e) only exhibits uniform stress at the bottom at 270°.

4.1.1.2 Stress concentrations in weak material direction

Peaks in material y-direction occur at the same polar angle, regardless of shape. Again, peaks for shapes with circular corners are higher and more distinct than for shapes with elliptical corners (see Figure 4.5). In contrast to stresses in material x-direction, stresses in the weak material direction form peaks of greater magnitude in compression than in tension. The effect of straight horizontal edges becomes clearer since they limit the maximum compressive stresses and cut the stress peaks. Vertical straight edges have a similar impact as horizontal straight edges have on stress concentrations in the strong material direction. Along the vertical straight edges stresses are 0. The elliptical geometry b) reaches a stress-free state only along the 0° and 180° polar axes, due to not possessing straight edges.

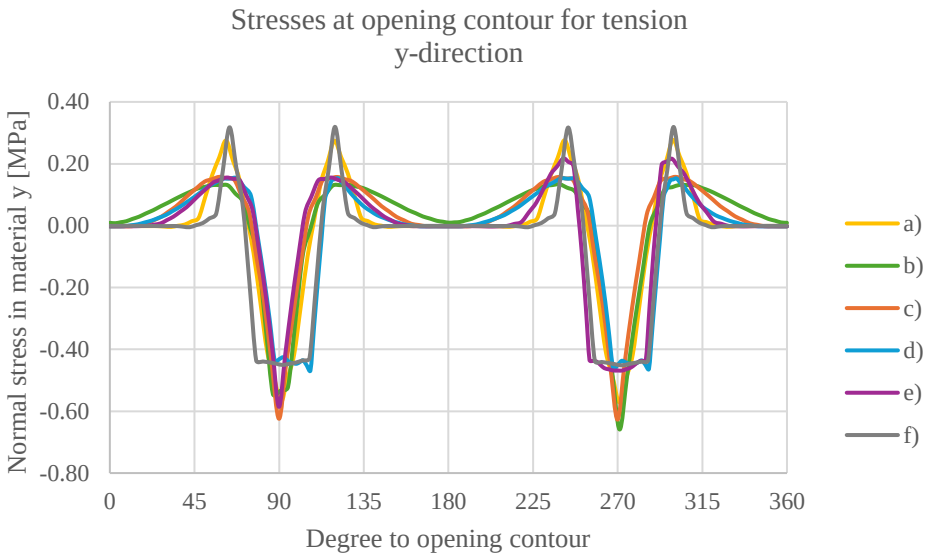

Figure 4.5. Variation of tangential stresses around different opening geometries.

The geometry with lowest stress peaks and smallest range in stresses in both strong and weak direction is geometry d). Cutting off stress peaks with straightened horizontal and vertical edges and having elliptical corners with a ratio $a/b = 3$ makes the geometry superior among the investigated shapes.

4.1.2 Shear loading

To create a uniform shear stress in the wall segments, a horizontal displacement of 1 mm at the top edges was induced. Resulting shear stresses around the opening contour in xy-plane (illustrated in Figure 4.6) were compared. Analogies with Chapter 3.3.1.2 cannot be seen in the same way as for tensile loading.

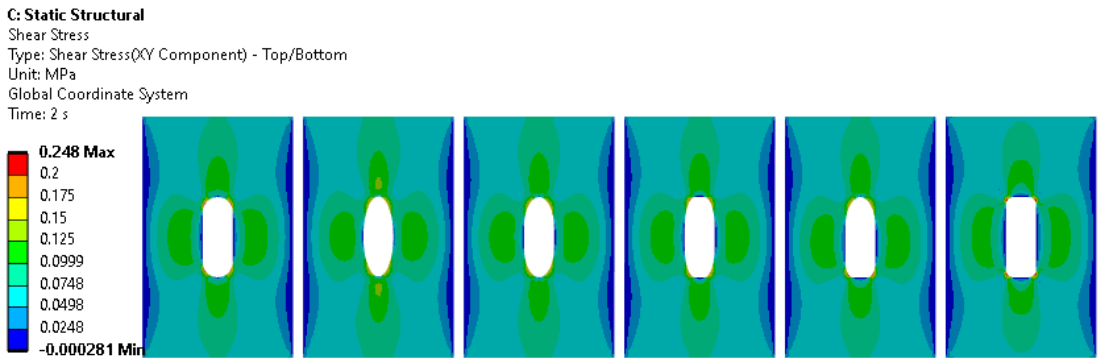

Figure 4.6. Resulting shear stresses for investigated opening geometries.

All opening geometries show the same overall stress distribution. Noticeable is that stress flows naturally around the opening, thus for shapes with straight edges stress flows around the opening in a curvature. Peak stresses appear at the points where the opening geometry interferes with the optimal shape. This phenomenon becomes the clearest in element f), where a distinct ellipse is visualized by colouring areas with low stresses in dark blue. Element b) on the other hand possesses a geometry close to the optimal shape, thus only few areas are stress-free or only exhibit low stresses. Plotting stress variation for all elements (Figure 4.7) confirms this trend. The elliptical opening b) has the lowest fluctuation of stresses around the opening contour while f) shows distinct peaks in the graph where the corners of the opening interfere with the optimal shape. Geometries c) and d) with semielliptical top and bottom or semielliptical corners

outperform both geometries with circular corners. Again, the smaller the radius the higher the peaks, showing especially for geometry e) with lower magnitudes at the top (≈ 60° and ≈ 120°) than at the bottom (≈ 240° and ≈ 300°).

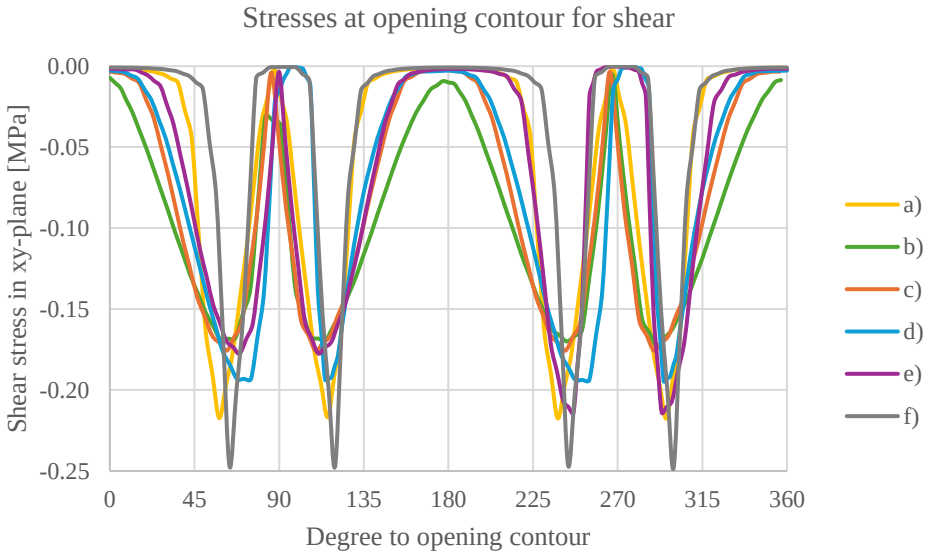

Figure 4.7. Variation of shear stresses around different opening geometries.

4.1.3 Geometry evaluation

An evaluation of results from the separate analyses can be conducted to determine which geometry performs best overall. For this, the maximum and minimum stress and the stress range for every geometry and material direction is obtained and ranked. Best performance results in 1 point, worst in 6 points. Ranking is done with equal weighting between criteria. A mean value for each stress component is formed resulting in an overall performance of each geometry. Table 4.1 displays the ranking of geometries.

Table 4.1. Ranking of opening geometries.

	a)	b)	c)	d)	e)	f)
normal x	3	5	3	2	2	6
max	4	5	3	1	2	6
min	1	5	3	4	2	6
range	4	5	3	1	2	6
normal y	4.7	3.7	3.7	1.7	4.3	3.0
max	5	1	3	2	4	6
min	3	6	5	2	4	1
range	6	4	3	1	5	2
shear	4.3	1.0	2.0	3.3	4.7	5.7
max	3	1	2	4	6	5
min	5	1	2	3	4	6
range	5	1	2	3	4	6
total	4.0	3.2	2.9	2.3	3.7	4.9
max	4.0	2.3	2.7	2.3	4.0	5.7
min	3.0	4.0	3.3	3.0	3.3	4.3
range	5.0	3.3	2.7	1.7	3.7	4.7

As discussed, element d) performs best in stresses resulting from tensile loading. Fluctuation is the lowest for both stresses in material x- and y-direction. In assessment of shear stresses the elliptical opening geometry b) receives a perfect score with best performance in all categories. The total average indicates geometry d) performs best in a combined evaluation. Straight vertical and horizontal edges combined with elliptical corners outperform all other investigated geometries. Especially the average range ranking indicates d) exhibits the smallest fluctuation among the investigated shapes. Worst are the two geometries with circular corners, a) and f). Both show high fluctuations and peaks in stresses.

4.1.4 Optimization iteration

From the previous study, it becomes clear optimization for tension and shear require different geometries. While an ellipse is the optimal shape for handling shear stresses, straight edges with elliptical corners seem to perform well in tension. For improvement, the elliptical corners can be tweaked to improve performance of the opening geometry further. In addition, to minimize disruptions in the opening contour, the corners could be formed parabolic with changing radius. A method formulated by Grodzinski, described in *Peterson's Stress Concentration Factors* (Pilkey and Pilkey, 2008) shows how a changing radius can be modelled. Originally, this shape was created for optimizing stress flow in welds. Illustrated in Figure 4.8 is the shape with boundaries of semiaxes set to match the opening geometry. The idea is to divide each semiaxes into the same number of segments and connect same segment numbers. Resulting is a shape with varying radius used in the optimized opening geometry. Straight edges at the top, bottom and the sides of the opening geometry are kept.

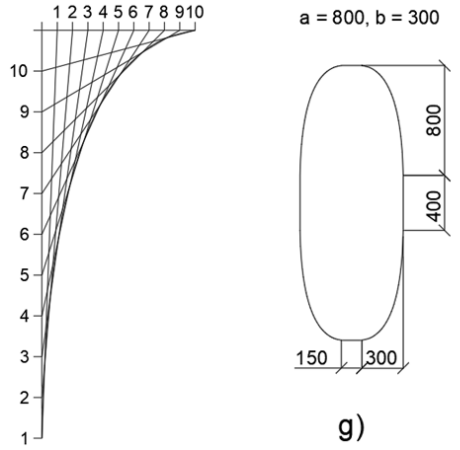

Figure 4.8. Optimized opening geometry.

The optimized structure is evaluated against the two previous best performing geometries in tension and shear, b) and d). Resulting stresses in the three material directions are presented in Figure 4.9. Overall, stress patterns form in the same manner as for the previously investigated geometries. The same characteristic stress peaks can be seen and the location of maximum stresses form according to the observations made in previous chapters. Variation of stress along the opening in material x-direction and shear is plotted in Figure 4.10 and Figure 4.11. For stresses in material x-direction, the optimized geometry outperforms the previous best geometry. Stress peaks form closer together due to the shortened straight edges at the sides. Minimum stresses stay unchanged and form a plateau around a stress-free state. For shear stresses, improvements against geometry d) are only minor. It seems however peaks are more distinct than for geometry d), indicating interference with natural stress flow is reduced slightly.

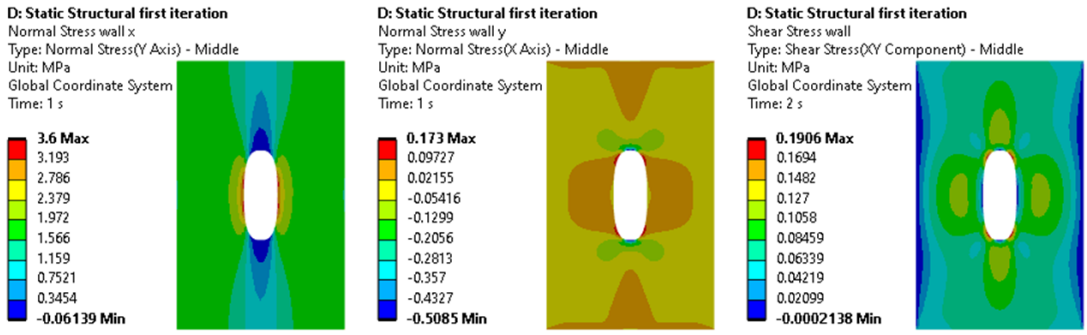

Figure 4.9. Resulting stresses for optimized opening geometry.
Left: Stresses parallel to the fibre. Middle: Stresses perpendicular to the fibre. Right: Shear.

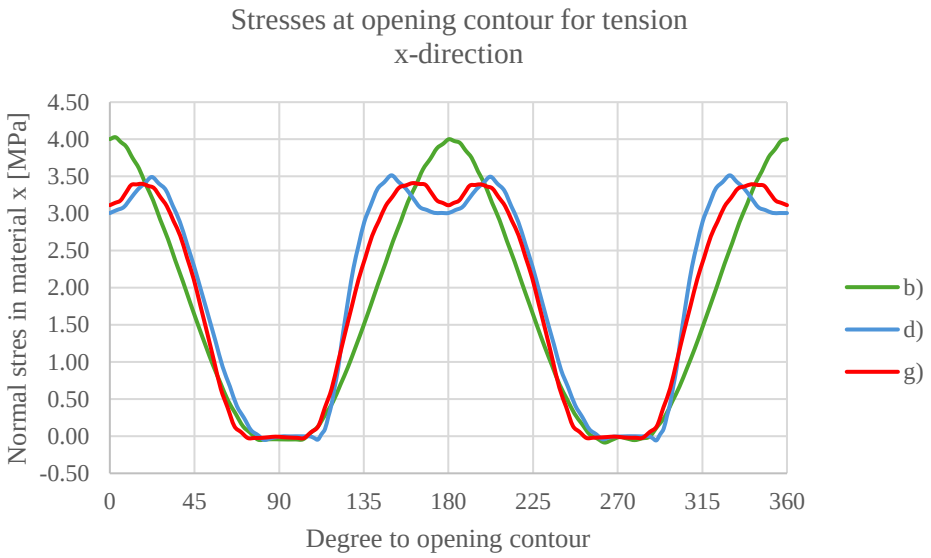

Figure 4.10. Variation of longitudinal stresses around optimized opening geometry.

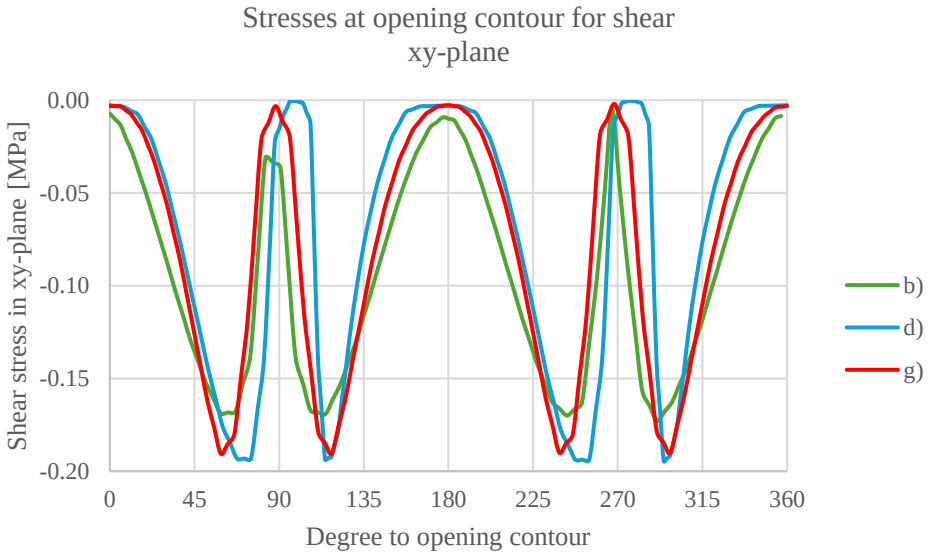

Figure 4.11. Variation of shear stresses around optimized opening geometry.

A comparison and weighting as done for previous concepts reveals the improved geometry indeed performs better compared to the benchmark geometries b) and d). Table 4.2 shows that improvements in max stresses compared to geometry d) and in min and stress ranges compared to geometry b) over the three material directions, are made. This results in the geometry outperforming all previous geometries. Therefore, this opening geometry will be used in subsequent assessments. The complete evaluation table is appended in Appendix 9.1.

Table 4.2. Ranking overview of benchmark and optimized opening geometries.

rank	b)	d)	g)
max	2.0	3.0	2.7
min	3.0	2.3	2.0
range	3.0	2.3	2.3
total	2.7	2.6	2.3

4.2 Variation of panel orientation

Gaining information about how the panel layup and ratio of stiffnesses in different material directions affects the performance of the product can be used in creating concepts for reinforcing an opening in a LVL wall. Most constructions and studies made on LVL include beams loaded in bending. Very little to no empirical data can be found for LVL constructions loaded in tension and compression. No calculation methods for computing properties of LVL veneers have been established. CL-theory on the other hand offers multiple studies and calculation methods for behaviour of orthotropic laminates and its plies. The goal of this section is to find a way of computing properties of a LVL panel with an arbitrary layup. Composite materials are engineered and produced to suit defined applications. Controlling manufacturing on fibre level assures each lamina fulfils set requirements. Timber as a natural grown resource cannot be engineered in the same way. Imperfections in the wood lead to heterogenous properties and CL-theory can only be used as an estimation of performance of EWPs. Although the homogenization of the product on panel-level gives homogenous orthotropic properties, on veneer or lamina level, the material must still be considered heterogenous orthotropic. In continuation, an idealized model of LVL is used when applying CL-theory and obtained results must be considered as theoretical values.

4.2.1 Obtaining veneer properties

To obtain veneer properties, CL-theory will be applied on LVL products. The goal is to compute properties of a Kerto-Q panel starting from various material data. If the method succeeds, engineering properties for panels with arbitrary layup can be determined. The computation consists of three steps:

1. Find sources for material data
2. Compute lamina and laminate stiffness matrices
3. Derive engineering properties and compare obtained values with standard values

Each of the steps offers 2 different computation methods, leaving a total of $2^3 = 8$ possible combinations to investigate. Afterwards, the best match with standard values will be defined and used in the following analysis.

4.2.1.1 Sources for material data

Being a UD-laminate, the laminate properties of the Kerto-S panel can be seen to be the same as each of its laminae. This implies laminate properties of the Kerto-S panel can act as input data for each lamina. In this case, both stiffnesses and major Poisson's ratio are known from

the product data sheet. Missing minor Poisson's ratio is computed using Equation (3.4). Instead of taking panel properties as input, one could also consider taking timber material properties to form stiffness matrices. Strengths and stiffnesses for various wood species are known and collected in different literature. Kohlhauser and Hellmich (2012) have undertaken studies on obtaining Poisson's ratios from timber specimens in a combined mechanical and ultrasonic testing. Giving an overview of ratios from previous studies, their work will be taken as source for timber material properties. As stated as premise for CL-theory, only in-plane (longitudinal and tangential) properties are considered. An overview of the different parameters used is given in the following Table 4.3.

Table 4.3 Data sets for material properties

Material property	Kerto-S	Kohlhauser & Hellmich
E_L	13800	15810
E_T	450	1640
υ_{LT}	0.6	0.466
υ_{TL}	0.02	0.048
G	600	940

4.2.1.2 Lamina stiffness matrix

Given the material properties, stiffness matrices can be formed in different ways. Two approaches for obtaining the lamina stiffness matrix will be investigated:

1. Material properties as engineering constants (E_L, E_T, υ_{LT} and G_{LT}) and use those to compute stiffness matrix constituents.
2. Material properties as constituents of the stiffness matrix.

Due to the influence of Poisson's ratios in computation, the resulting matrices will differ.

According to CL-theory, engineering properties are used to compute elastic constants and the stiffness matrix can be obtained as defined in Equation (3.3). For the case of using laminate properties as input, this results in a stiffness matrix for each lamina or veneer as:

$$Q = \begin{bmatrix} 13\,968 & 273 & 0 \\ 273 & 455 & 0 \\ 0 & 0 & 600 \end{bmatrix} [MPa] \tag{4.1}$$

Note that in this case stiffnesses in the laminate in longitudinal and transversal directions are decreased compared to stiffnesses in the single laminae due to the influence of Poisson's ratio. In a similar manner, the stiffness matrix when using timber material properties is obtained.

When using laminate properties as input, one could argue that engineering properties already form elastic constants, thus creating stiffness matrix constituents. For the unidirectional constituents Q_{11}, Q_{22} and Q_{66}, the material properties from Table 4.3 can be taken as input. Biaxial constituent Q_{12} is influenced by Poisson's ratio and an expression to compute Q_{12} with other matrix constituents and υ_{LT} must be formulated. This is to prevent mixing calculation with engineering constants with calculation with matrix constituents. Taking the definition of Q_{22} in Equation (3.3) and rearranging for E_T gives:

$$E_T = Q_{22}(1 - \upsilon_{LT}\upsilon_{TL}) \tag{4.2}$$

Further, stating the definition of Q_{12} and substituting E_T with Equation (4.2) leaves an expression only dependent on matrix constituents and υ_{LT} as follows:

$$Q_{12} = \frac{\upsilon_{LT} \cdot Q_{22}(1 - \upsilon_{LT}\upsilon_{TL})}{1 - \upsilon_{LT}\upsilon_{TL}} = \upsilon_{LT} \cdot Q_{22} \tag{4.3}$$

Computing lamina stiffness matrix results in stiffnesses differing slightly from the previous computation method. For the case using laminate data as input, the local stiffness matrix with values closer to the material properties of the Kerto-S laminate is obtained.

$$Q = \begin{bmatrix} 13\,800 & 270 & 0 \\ 270 & 450 & 0 \\ 0 & 0 & 600 \end{bmatrix} [MPa] \tag{4.4}$$

Difference in lamina stiffness matrices is at under 2 %. It could be questioned whether this difference influences the final engineering properties. However, since the error might be amplified in following computation steps both alternatives will be kept as computation methods.

4.2.1.3 Forming Kerto-Q stiffness matrices and deriving engineering properties

Having obtained the local, lamina stiffness matrix, laminate stiffness can be computed. As stated in Equation (3.7), local stiffness matrices in global coordinates, $\bar{Q}$, are defined. These can either be used to obtain a laminate stiffness matrix where each lamina is added as a fraction of the total laminate height, or the extensional stiffness matrix (*A*) can be formed according to Equation (3.11). To derive engineering properties one can either use constituents of the laminate stiffness matrix (Q-matrix method) or use the A-matrix method suggested by Olsson (2006). Again, these two methods will give slightly different results. Starting with lamina stiffness matrix Q from Equation (4.4), resulting engineering properties for a 9 – layered panel with two cross layers for the two methods is presented in Table 4.4. Again, the differences are only minor, resulting Poisson's ratios are identical.

Table 4.4 Obtained engineering properties

Engineering property	Q-matrix method	A-matrix method
E_L	10833	10812
E_T	3417	3410
υ_{LT}	0.08	0.08
υ_{TL}	0.025	0.025
G	600	600

4.2.2 Theoretical values compared to standard values

According to standard values, different Kerto-Q panels have the same properties, although differing in layup and thickness. A 9 – layered Kerto-Q laminate has two cross layers, as has a 11 – layered Kerto-Q laminate. This implies the fraction of cross-plies (2/11 vs 2/9) has no impact on the laminate's stiffness properties. In CL-theory, this statement is false. Laminate stiffness for a 11 – layered panel will have a decreased stiffness perpendicular to main fibre direction compared to a 9 – layered laminate due to the fraction of cross-plies being smaller. Therefore, it is essential to compute theoretical engineering properties for different Kerto-Q panels to see which layup matches the standard values the best. For verification of the calculation method, laminate properties for layups of 7, 8, 9, 10, 11 and 13 layers were computed. Note that panels up to 11 layers have two cross-plies while 13 – layered panels are equipped with three cross-plies. Obtained values are compared with standards and relative difference is measured. To determine which layup and theoretical values match the standard values best overall, standard deviation between the different relative errors is computed for each layup.

In general, absolute values between theory and standards do not match. Especially theoretical values obtained when taking material properties from Kohlhauser and Hellmich (2012) as input overestimate performance of the panels. While stiffness in longitudinal direction is roughly 20

% higher than standard values, stiffness in transversal direction is increased with around 100 % in all layups. This can be explained with standardized values being conservative to ensure requirements on performance are met in all products although a majority of products might overperform standard values. Safety factors used when computing are not available, therefore scaling of results to increase comparability is difficult. The only constant engineering property throughout all layups is shear modulus. A reduction of moduli and Poisson's ratios can be made with the relative difference between shear modulus obtained with material properties as input data and shear modulus stated in standards. This means reducing engineering properties to $600/940 = 0.638$ of the calculated value. Doing so does however lead to the longitudinal stiffness being 20 % - 30 % lower, transversal stiffness 33 % - 80 % higher than standard values. Taking Kerto-S laminate properties as input yields better results, although theoretical values from one layup do not match all standard values. While theoretical values for a 8 – layered panel matches stiffness in longitudinal direction (error under 1 %), stiffness in transversal direction is overestimated by around 90 %. At the same time, theoretical values for a 11 – layered panel only match longitudinal stiffness with an error of around 9 % but transversal stiffness match the best with an error of around 45 %. Taking into consideration the deviation of errors, regardless of computation method, 11 – layered panels show theoretical values matching standard values best most consistently. Collecting theoretical values obtained for this layup with the various computing combinations is done in Table 4.5. Assuming input data as stiffness matrix constituents in combination with the A-matrix method yields best results for longitudinal and transversal laminate stiffnesses. For the longitudinal stiffness taking properties from Kerto-S as input results in a deviation from standard values of around 8 %. When taking the same method but timber material properties as input the best match in transversal stiffness is obtained with an error of 33 %. Resulting Poisson's ratios do not differ between computation methods but are instead governed by input data used. Here Kerto-S properties as input data yield best results with an underestimation of υ_{LT} of 6.2 % and an overestimation of υ_{TL} of 18.5 %. Overall, taking Kerto-S properties as input for stiffness matrix constituents and applying A-matrix method yields best results in computing Kerto-Q standard values.

Table 4.5. Properties for a 11-layered laminate for different calculation combinations.

	Kerto-S properties as input data							
	Matrix constituents				Engineering properties			
	Q-matrix		A-matrix		Q-matrix		A-matrix	
	abs	rel	abs	rel	abs	rel	abs	rel
E_L	11372	8.3%	11347	8.1%	11511	9.6%	11485	9.4%
E_T	2877	43.9%	2871	43.6%	2912	45.6%	2906	45.3%
G	600	0.0%	600	0.0%	600	0.0%	600	0.0%
υ_{LT}	0.094	-6.2%	0.094	-6.2%	0.0938	-6.2%	0.0938	-6.2%
υ_{TL}	0.024	18.5%	0.024	18.5%	0.0237	18.5%	0.0237	18.5%
stdev		18.3%		18.2%		18.8%		18.7%
	Timber material properties as input data							
	Matrix constituents				Engineering properties			
	Q-matrix		A-matrix		Q-matrix		A-matrix	
	abs	rel	abs	rel	abs	rel	abs	rel
E_L	8447	-19.6%	8359	-20.4%	8642	-17.7%	8551	-18.6%
E_T	2691	34.6%	2663	33.1%	2754	37.7%	2724	36.2%
G	600	0.0%	600	0.0%	600	0.0%	600	0.0%
υ_{LT}	0.116	15.7%	0.116	15.7%	0.116	15.7%	0.116	15.7%
υ_{TL}	0.037	84.1%	0.037	84.1%	0.037	84.1%	0.037	84.1%
stdev		37.4%		37.7%		37.0%		37.2%

Since absolute values on material properties do not yield good matches with standard values, instead the ratio between moduli can be considered. This gives a better comparison between theoretical and standard values. In Figure 4.12 the ratio between weak and strong material direction (E_2/E_1) is given for varying amount of cross layers in the layup. Numbers are computed using Kerto-S properties as constituents of the stiffness matrix and obtaining theoretical values by backtracking engineering properties from resulting A-matrices. Number of cross layers in a 9- and 11-layered sheet are varied from none to all and resulting ratios are distributed in the plot. As discussed above, 11-layered laminates yield the best match with standard values and 9-layered laminates are included since this layup is used in Modvion's production. Standard products in form of Kerto-S, Kerto-Q and plywood are included to give an understanding of how theoretical values match standard products. For Kerto-Q, 7-, 9- and 11-layered sheets are shown. According to standard values they all exhibit same material properties although differing in layup. Due to this fact, they all lay on a horizontal line with the same ratio E_2/E_1. Further, plywood with thicknesses between 12 mm and 21 mm (number of veneers ranging from 5 for thickness 12, 15 and 18 mm to 7 for thickness 21 mm) are included. Here material properties are taken from *TräGuiden*, a service provided by *Svenskt trä*, where properties are dependent on layup. In this case, sheets being 12, 15 and 18 mm thick all show similar ratios E_2/E_1, although varying in thickness and absolute values.

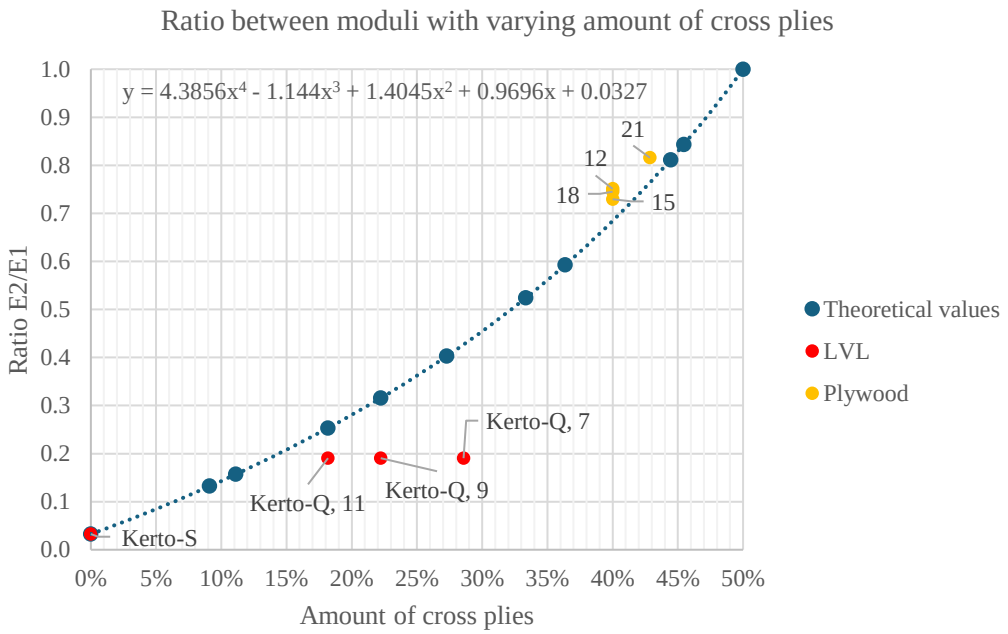

Figure 4.12. Ratio between in-plane laminate moduli for varying amount of cross plies.

With values from a Kerto-S panel taken as input data, the UD-laminate is the only configuration laying on the curve of theoretical values. Layups of Kerto-Q are all placed underneath the curve, indicating material capacity is either overestimated in strong material direction or underestimated in weak material direction. Regarding standard values being conservative, the latter must be assumed. In this case, the stiffness perpendicular to main fibre direction in a 7-layered Kerto-Q panel might be twice as high as standard values indicate according to the chosen computation approach. At the same time, ratios for different plywood layups all lay above the curve, indicating the opposite. In this case stiffness in strong material direction might be underestimated. It is however noticeable that ratios for plywood match the theoretical values better than ratios for Kerto-Q layups, although the curve is obtained by trying to relate Kerto-S to Kerto-Q material properties. The main reason for this might be the higher diversification in material properties when labelling plywood. Instead of assigning the same material properties to various plywood layups, each layup is given its own properties. The result shows the chosen

approach to determine single veneer properties is reliable and yields usable results for further analysis.

As the stiffness, Poisson's ratio is dependent on the ratio between stiffnesses in different material directions. Obtaining Poisson's ratios is done in the same way by backtracking engineering properties from the resulting A-matrices for different layups. Major (υ_{12}) and minor (υ_{21}) Poisson's ratios are linked by Equation (3.4) which is demonstrated in Figure 4.13.

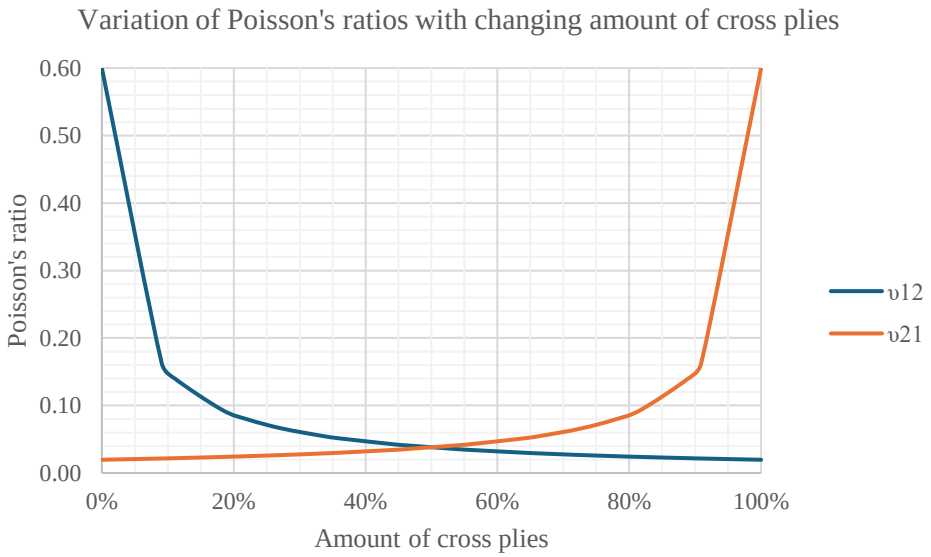

Figure 4.13. Relation between major and minor Poisson's ratio in a laminate over varying amount of cross plies.

It can be shown that a small increase in amount of cross plies to 6 % cuts major Poisson's ratio in half. With 10 % cross plies the laminate exhibits υ_{12} with a magnitude of only around one fourth of that in a UD-laminate. When the ratio between moduli is one, meaning same stiffness in both in-plane material directions and 50 % cross plies, υ_{12} and υ_{21} are the same. To obtain a curve similar to the one describing ratio between elastic moduli and cross plies, the variation of υ_{21} in the range between 0 % - 50 % is analysed. It can be shown the variation in this range can be expressed as a third order polynomic function. For further investigations, Equation (4.5) and (3.4) will be used to compute Poisson's ratios for layups with different amount of cross-plies.

$$\upsilon_{21} = 0.0528x^3 + 0.0061x^2 + 0.0201x + 0.0196, x \in [0,0.5] \quad (4.5)$$

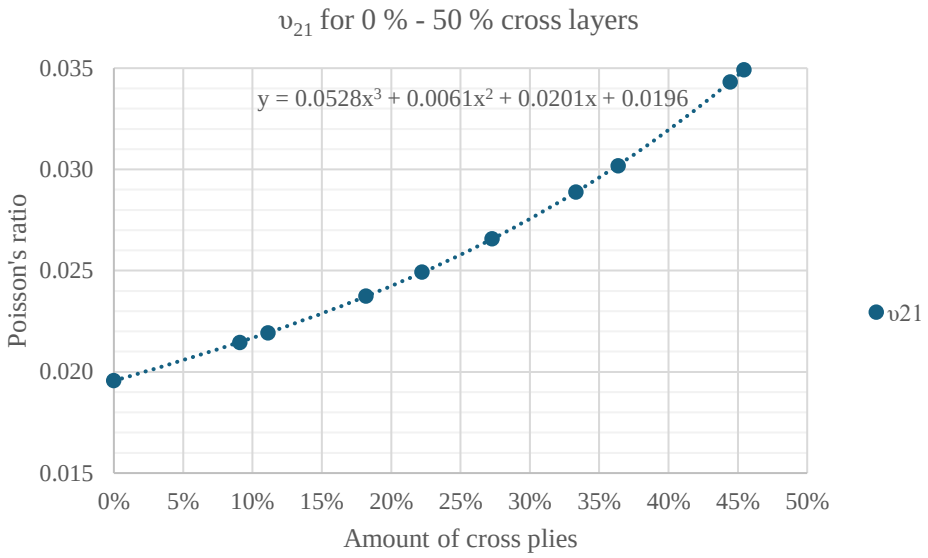

Figure 4.14. Variation of minor Poisson's ratio for amount of cross plies between 0 % - 50 %.

4.2.3 Impact on stress concentration factors

Varying panel orientation will change stress concentration factors at the opening contour. As presented in chapter 3.3.1, the angle of applied force is relevant for resulting SCF. In addition, it has been stated that the ratio between stiffnesses in main material directions affect the range between maximum and minimum SCF at any given angle. This phenomenon becomes clear when plotting variation of maximum and minimum SCF with varying panel orientation. Figure 4.15 displays max and min SCF for three standard products, Kerto-S, Kerto-Q and plywood over a range from 0° to 180° for an applied tensile load. Both the range of SCF for each angle, as well as the overall fluctuation of SCF decrease with decreased ratio E_1/E_2. While Kerto-S panels show a variation between overall max SCF of 10.7 to overall min SCF of -6.4, plywood only covers less than a third of that range, fluctuating between overall max SCF 4.5 to overall min SCF -1.2, Kerto-Q in between with overall max SCF 6.3 and overall min SCF -2.3. While the smallest range of SCF in the Kerto-S laminate occur at the orientations 0°, 90° and 180°, plywood laminate has its smallest range of SCF at 45° and 135°. The range between max and min SCF in a Kerto-Q laminate seems to be quasi-constant over all angles.

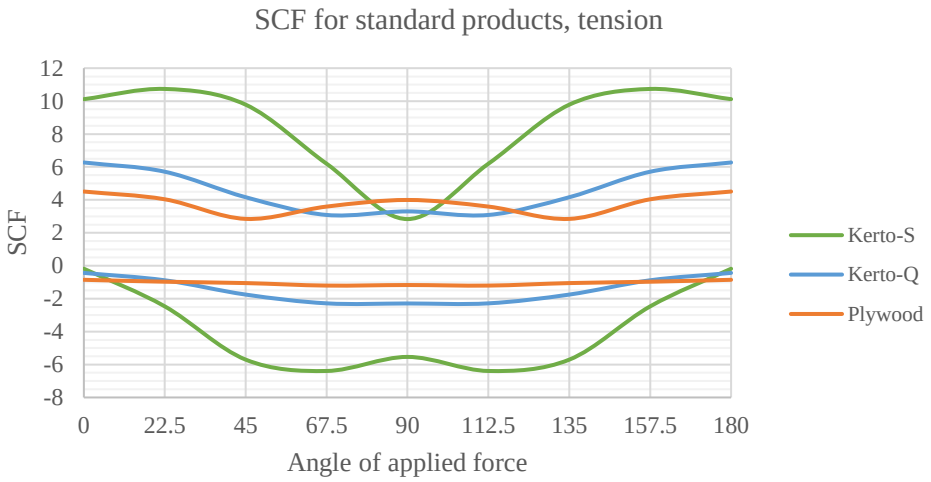

Figure 4.15. Max and min SCF for holes in standard LVL products in tension over angle of applied force.

As for the uniaxial load case, max and min SCF for the three standard products, Kerto-S, Kerto-Q and plywood over a range from 0° to 180° for applied shear load are plotted in Figure 4.16. The variation of SCF occurs with the same pattern as for tensioned plates with a 45° phase shift. The reason for this is the resulting principal stresses coming from the applied shear load resembling a loading in 45°, as stated in Chapter 3.3.1.2. Again, both the range of SCF for each angle, as well as the overall fluctuation of SCF decrease with decreased ratio E_1/E_2. While Kerto-S panels show a variation between overall max SCF 17.1 to overall min SCF -17.1, plywood again only covers less than a third of that range, fluctuating between overall max SCF 5.7 to overall min SCF -5.7, Kerto-Q in between with overall max SCF 8.6 and overall min SCF -8.6. The variation of range is similar to the previous load case, due to the phase shift the optimal orientation to reduce stresses now is at 45° and 135° for the Kerto-S laminate and 0°, 90° and 180° for the plywood laminate.

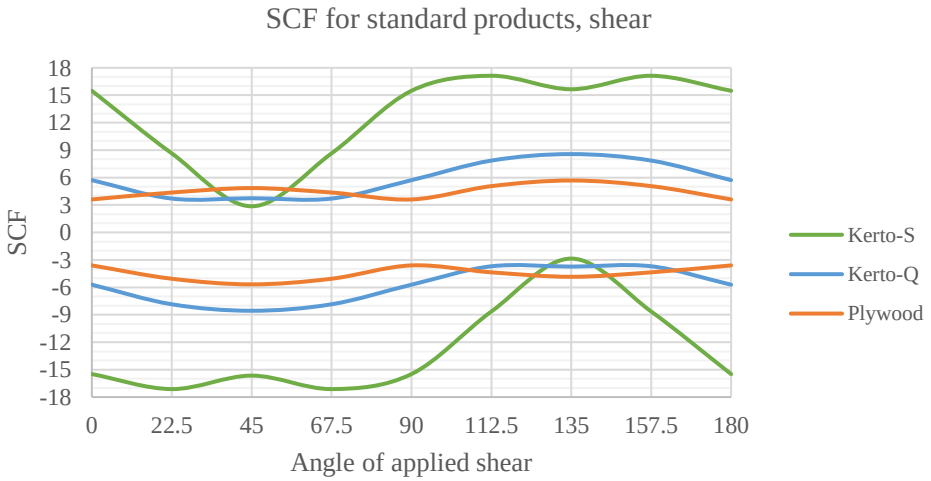

Figure 4.16. Max and min SCF for holes in standard LVL products in shear over angle of applied shear.

An interesting observation on the magnitude of SCF in the two load cases to be made is that while overall max and min show the same absolute values for an opening in a sheared plate, absolute values differ for an opening in a tensioned plate. Let δ be the midpoint between the overall maximum and minimum SCF value. δ will give an understanding on the overall formed stresses and can be obtained as:

$$\delta = max\ SCF\ - (max\ SCF\ - min\ SCF)/2 \tag{4.6}$$

Under shear loading, $\delta = 0$ for all laminates since $max\ SCF\ = |min\ SCF|$. Under tensile loading, δ is offset with varying magnitude for the different laminates. For a Kerto-S laminate, $\delta = 2.2$, Kerto-Q possesses a $\delta = 2.0$ and plywood has a $\delta = 1.7$. This implies that overall, biaxial loading challenges the material equally in tension and compression, regardless of the ratio between stiffnesses. Uniaxial loading meanwhile tends to result in stress concentrations majorly with the same orientation as the applied force, i.e. tensile forces leading to tensile stresses and compressive forces leading to compressive stresses. This shows that for laminates with a highly dominant material direction not only do the peaks reach higher altitudes, but also overall stresses are higher than in laminates with less dominant material directions or quasi-isotropic laminates.

Orienting panels other than strong material direction in vertical and weak material direction in horizontal tower direction will reduce capacity of the tower walls. While stiffness in vertical tower direction decreases when rotating main fibre direction, bending stiffness increases and complicates manufacturing of tower modules. This impact needs to be investigated further in future work for verifying viability of using rotated veneers or panels in the layup.

4.3 Variation of panel layup

Laminate stiffnesses and resulting SCF are directly dependent on the amount of cross layers in the layup. Varying amount of cross layers will change E_1 and E_2, resulting in varying SCF. Having established functions to describe variation of E_1, E_2 and υ_{21} over changing amount of cross layers, SCF in laminates with different layups but fixed orientation can be computed. Tensioned plates oriented at 0°, 45° and 90° and sheared plates oriented at -45°, 0° and 45° with the amount of cross layers ranging between 0 % - 50 % are evaluated.

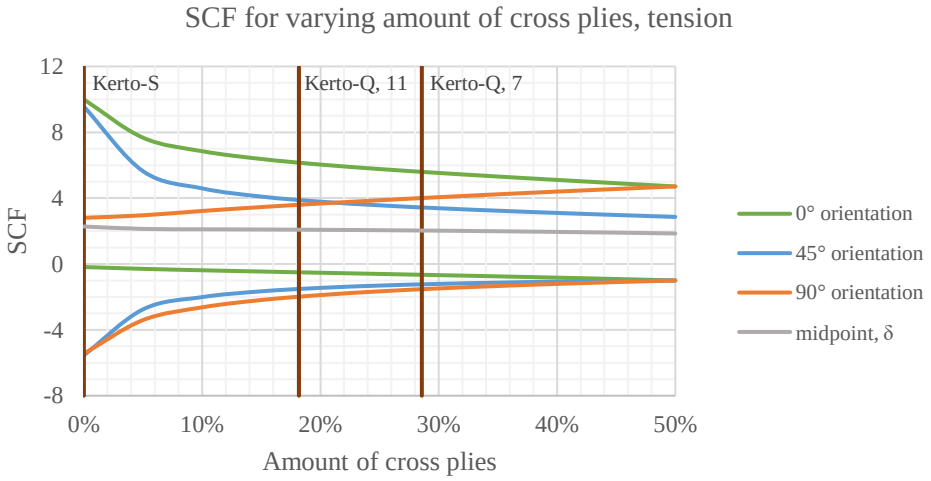

Figure 4.17. Variation of max and min SCF in tension for different amount of cross plies for different panel orientations.

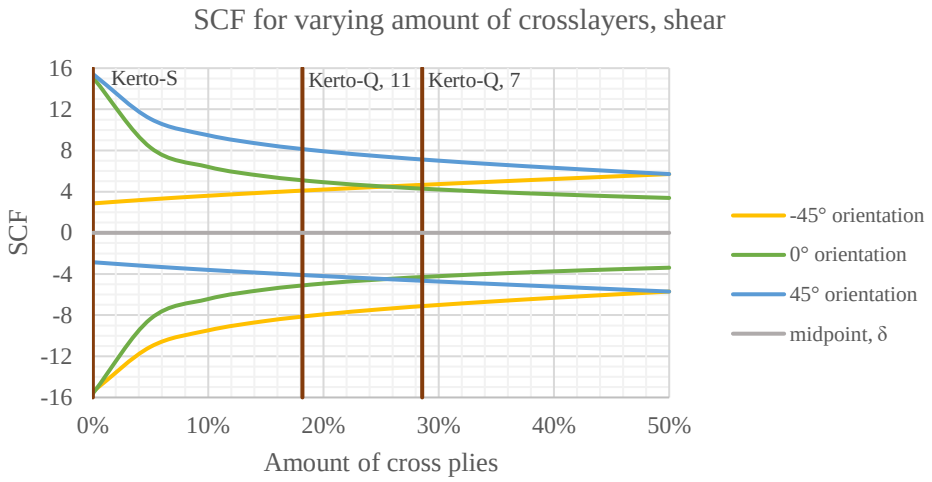

Figure 4.18. Variation of max and min SCF in shear for different amount of cross plies for different panel orientations.

Although varying in magnitude, tendencies in variation of resulting SCF for tensile and shear loading are similar. As stated in Chapter 3.3.1, SCF decrease with decreased ratio E_1/E_2. This decrease is however not linear. The biggest non-linearity occurs in tensioned panels oriented at 45° to the load or sheared panels at 0° to the load. In these cases, maximum absolute SCF drop from 10 to 5.5 in a tensioned plate and from 15 to 8 in a sheared plate for an increase in cross layer from 0 % – 5 %. For other orientations, the decrease is not as big, there is however a distinct change of slope at around 5 %. This means a 11-layered LVL panel with one cross-layer will show significantly less stress concentrations around an opening than a Kerto-S panel. For reference, standard products have been added to the plot. 7-layered Kerto-Q and 11-layered Kerto-Q form boundaries for amount of cross layers in standard products. Only 17-layered Kerto-Q with three cross plies account for an amount outside this range (17.6 %). This means that circular openings in Kerto-Q products all possess SCF between 6 and -2 for tensile loading and SCF between 8 and -8 for shear loading. In these plots, the midpoints δ, described in the previous chapter, form a horizontal line along which the highest absolute maximum and minimum value for all orientations are mirrored. Here the offset is visualised as the distance between the line of midpoints and the x-axis. In shear loading, all δ lay on the x-axis, confirming the statement from previous chapters that tensile and compressive stresses occur with the same magnitude. For tensile loading, δ vary between 2.3 and 1.9, indicating that for tensile loading of the panel, tensile stress concentrations will be greater than compressive stress concentrations. In the previous chapter it was stated that $\delta = 2.2$ for Kerto-S, $\delta = 2.0$ for Kerto-Q and $\delta = 1.7$ for plywood in tensile loading. The difference in midpoints can be explained by the fact that the investigated orientations in this chapter do not capture the overall highest and lowest SCF used in the previous investigation.

5 Finite element modelling

Modelling the wall and reinforcement concepts is done in Ansys Multiphysics. To get an understanding of how the curvature in the tower wall impacts resulting stresses a comparison between a straight and curved wall is made. To set a benchmark, stresses in a solid wall segment are evaluated. Concepts for reinforcing an opening are introduced. These can be grouped in two categories: reinforcement through added structures and reinforcement through wall layup. In this chapter, results from the finite element modelling are shown.

5.1 Stress comparison between straight and curved wall

The wall to reinforce is at the bottom of Modvion's tower *Wind of Change*. Not only is the module curved but also does the radius vary from top to bottom. To understand the impact of this radius variation and the curvature on stresses around the opening, a comparison between stresses around an opening contour in a straight wall and a curved wall will be made. In both cases, the wall segments have a height of 6 m. The radius of the curved wall midplane is 2.65 m at the bottom of the wall and 2.57 m at the top of the tower segment. This leads to a variation in width between 4.16 m to 4.03 m in the curved wall plane. The width or arc length of the curved module at the centre of the opening is 4.1 m, therefore this width is taken for the straight wall segment. The opening is created by projecting a circle on the curved module and removing the projected shape. This results in a circular opening in the straight wall, while the opening becomes slightly elliptical in the curved wall plane. The model is set up as a shell model with quadratic order elements and a mesh size of 0.05 m. Wall thickness is 35 cm and homogenous with Kerto-Q LVL properties. Investigated stresses are tensile stresses in material x-direction and shear stresses, obtained by induced vertical and horizontal displacement of 1 mm respectively at the segment top edge. Results are obtained as path results along the opening, starting at the polar 0° or global x axis and moving counterclockwise around the contour as shown in Figure 5.1.

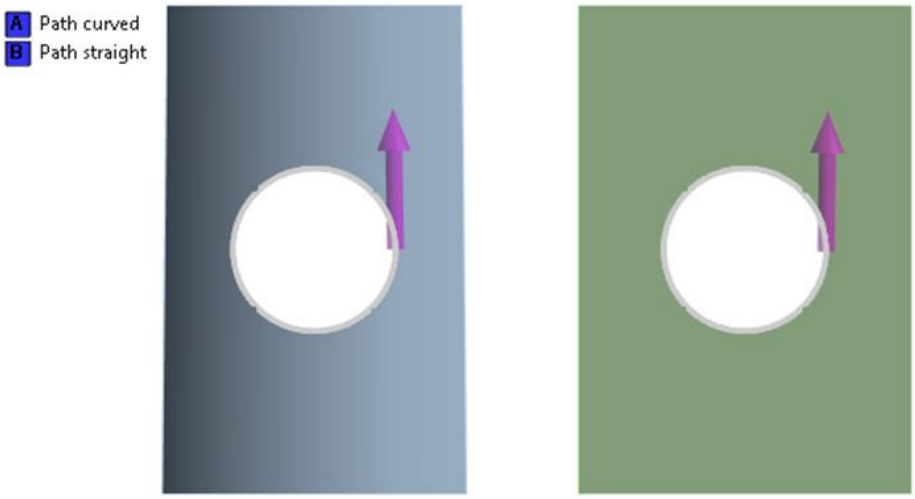

Figure 5.1. Module geometries and path orientations for investigation of differences in stresses in a curved (left) and straight wall (right).

Results for tensile and shear stresses (Figure 5.2 and Figure 5.3) show the same trend: stress peaks in the curved wall are higher than in the straight wall. While stresses at the top and bottom of the opening are very similar, stresses at the left and right edge differ. This can be explained with the in-plane shape of the opening. The opening of the straight wall has a constant radius around the opening contour, i.e. it has a circular shape while the radius of the opening in the curved wall varies, i.e. it is elliptical in the curved plane. As shown in Chapter 4.1, smaller radii

result in higher SCF, which explains the higher peaks in tensile stresses at 0° and 180° for the curved wall segment. Here the peak stress in the curved wall is around 5 % higher than in the straight wall. As presented in Chapter 4.1.2, shear stresses peak at the interference points between the optimal elliptical shape and the present opening shape. In this case the in-plane elliptical opening is oriented with its major axis along the weak material direction. Due to this the peaks tend to occur in a left-right tendency at around ± 22.5° and ± 157.5° compared to a top-bottom tendency as shown in chapter 3.3.1.2. Peaks in shear stresses are around 12 % higher in the curved wall than in the straight wall.

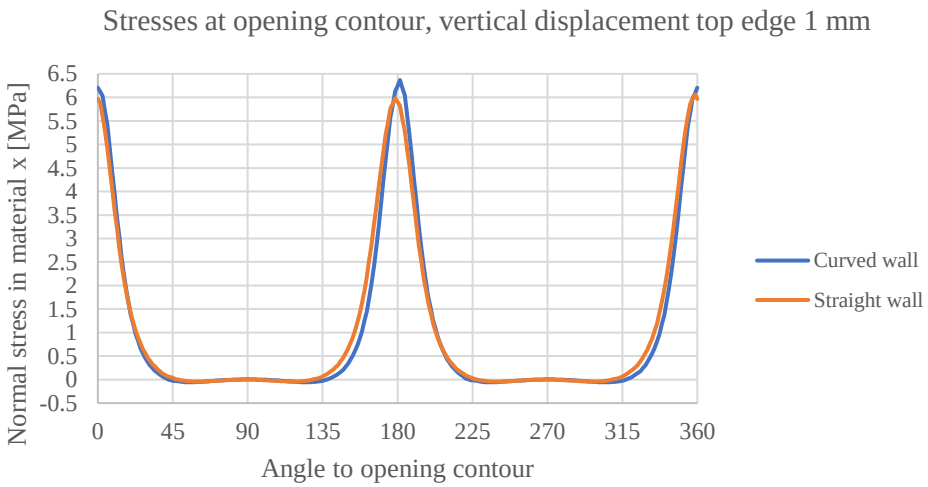

Figure 5.2. Resulting longitudinal stresses around openings in tensioned wall segments.

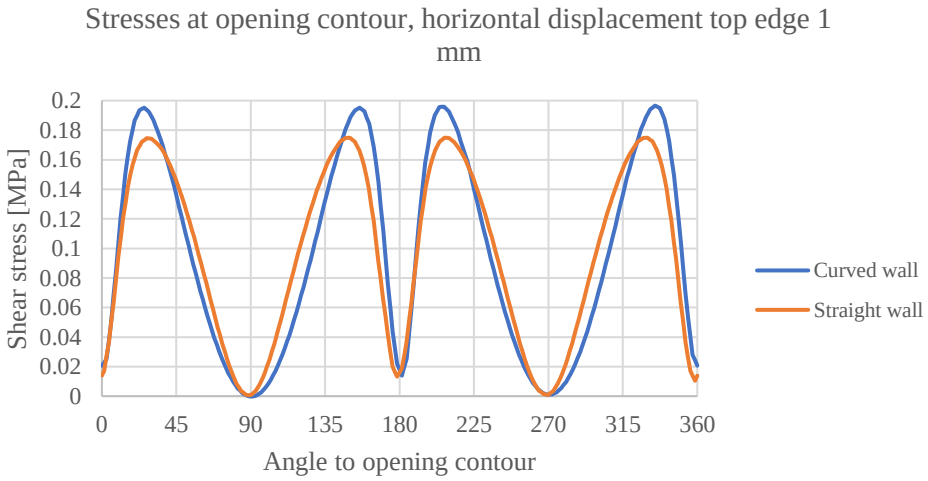

Figure 5.3. Resulting shear stresses around openings in sheared wall segments.

5.2 Stresses in a solid wall

To judge feasibility of the investigated reinforcement concepts, stress concentration factors, SCF, in the LVL module around the opening are compared. The aim is to find a concept with as low SCF as possible. Theoretically, creating a reinforcement concept with SCF = 1,0 indicates no increased stresses compared to a solid wall occur around the opening or reinforcements in the module. The opening will create stresses in directions not present in the solid wall. For instance, tensile loading in the solid wall creates only minor stresses in material

y-direction. Around an opening, stresses in y-direction will largely form. SCF will therefore be immense in this direction. For a good estimation on the performance of concepts, stress concentrations in material y should therefore be weighted according to the presence of stresses in the undisturbed wall. To gain information about the state of the solid wall, stresses in the future opening midpoint, as shown in Figure 5.4, are obtained for material x- and y-direction. In a solid wall with tensile or compressive loading, stresses perpendicular to the fibre are only around 0.1 % of stresses parallel to the fibre. Horizontal displacement leads to stresses perpendicular to the fibres around 22 % of stresses parallel to the fibres. For an adequate evaluation of concepts, SCF in y-direction must therefore be scaled to be comparable with SCF in x-direction.

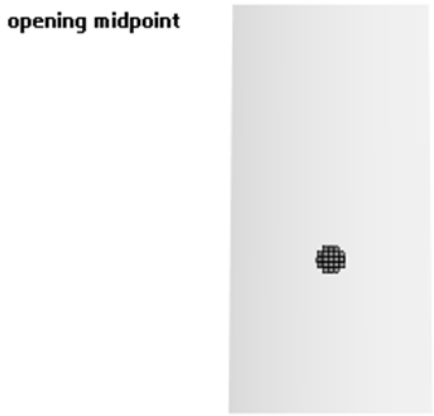

Figure 5.4. Elements in future opening midpoint.

To get a weighting factor, strengths in x- and y-direction are compared. Here the strength parallel to the fibres is at 26 MPa both in tension and compression, while strength perpendicular to the fibres depends on type of loading. Tensile strength with 6 MPa is slightly lower than compressive strength with 9 MPa. Since a first estimation of stresses does not give an indication on whether stresses perpendicular to the fibre will be tensile or compressive, a mean strength perpendicular to the fibre is formed. To get a first impression of the magnitude of reduction factor, this assumption is deemed reasonable. In a first step, allowable stress based on strength is calculated for material y direction. The assumption is that allowable stresses can reach the same utilization in the material as in x-direction. To obtain allowable stresses, stresses in x-direction are multiplied with the fraction of strength perpendicular to the fibres to strength parallel to the fibres (7.5/26). Weighting factors are thereafter created by dividing the present strength by allowable strength. Results show that SCF in material y-direction should be reduced to 0.3 % of its initial value for tensile and compressive loading to be comparable with SCF in material x-direction. The same procedure can be taken to reduce SCF in y-direction for displacement creating shear. In this case, SCF can only be reduced to 75 % of its initial value to be comparable to SCF in x-direction. A reduction factor for SCF in shear stresses cannot be obtained in the same way. Due to the lack of reference and only investigating one shear plane (xy), SCF will not be reduced.

5.3 Reinforcement concepts

Reinforcing a structure is a straightforward approach to cope with stress concentrations created by an opening. Removing material creates a weakness that can be counteracted by adding reinforcement and redistributing stresses to flow around the disturbance. For the opening in the tower wall, three different approaches will be taken: adding sheets on the tower surface around the opening to increase thickness and thereby stiffness and strength, installing a frame around the opening contour, and inserting stiffeners in the tower wall. Each reinforcement concept will be set up with different materials. The opening module is modelled as a curved, freestanding structure, fixed at the bottom and exposed to a vertical or horizontal displacement of 1 mm at

the top edge to create tensile and shear loading. The wall is modelled as homogenous, 35 cm thick Kerto-Q spruce LVL. In addition, reaction forces are evaluated to gain an understanding on how the overall stiffness of the module changes with the different concepts. When displacements are induced, different stresses and reaction forces are created. Thus, increased reaction forces compared to the solid wall indicate a stiffer module, while a decrease in reaction force indicates a weakening of the module.

5.3.1 Cover sheets

Cover sheets could be attached to the opening module externally and internally. Similar to the tested LVL beams in bending presented in Chapter 2.2.1, these sheets are intended to prevent failure anywhere around the opening. Sheets investigated in this thesis are made in spruce LVL or structural steel. Three setups are created:

- LVL cover sheet 100 mm on the external surface of the module
- LVL cover sheet 100 mm on the external and internal surface of the module
- steel cover sheet 10 mm on the external and internal surface of the module

The contact surface between the module and cover sheets is modelled as rigid. This implies the sheets are glued or fastened such that a continuous transfer of stresses throughout the contact area occurs. For the concepts with LVL cover sheets, stresses in the module, as well as in the cover sheets are evaluated. For reinforcing with steel sheets, only stresses in the timber wall are evaluated. In Figure 5.5, resulting stresses in material x-direction for tensile loading are presented. Similar figures for material y-direction and shear stresses can be found in Appendix 9.2. Note that steel plates have been removed from the result image to visualize stresses at the wall surface.

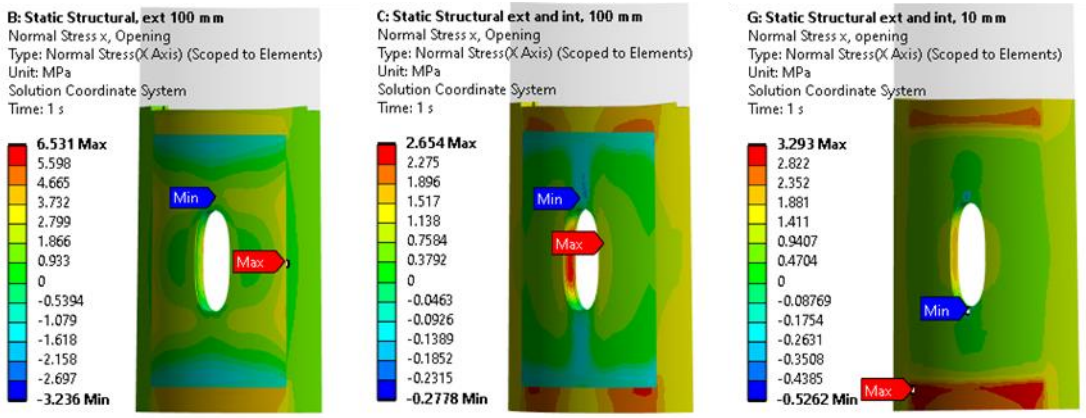

Figure 5.5. Longitudinal stresses in modules reinforced with cover sheets. Left: 100 mm spruce external. Middle: 100 mm spruce external and internal. Right: 10 mm steel external and internal.

When adding sheets made in LVL, stress peaks form at the interface between wall and cover sheet, the cover sheet itself displays only minor stresses. In the middle picture, the core of the wall shows a distinct region with high stresses, indicating no reinforcement through the wall thickness has taken place. It seems cover sheets only reinforce the outermost layers of the wall. In the right image, wall surface is visible, showing low stresses at the interface between LVL and steel. Instead, stresses peak in the area below and above the cover sheets. These areas are greatly affected by the change in stiffness induced by adding steel cover sheets. The relatively low stiffness from the LVL module meets the high stiffness of the steel sheets and creates new areas of stress concentrations compared to an unreinforced opening.

5.3.2 Frame

A frame fitted around the opening could prevent stress peaks to form at the opening contour. This method has been shown to be the most effective when designing steel wind turbine towers. Opening dimensions are constant in the different concepts and the frame is built into the surrounding wall. Depending on the stiffness and thickness of the frame, the reduction in stresses might vary. A thicker frame increases the radius of the opening contour in the LVL module but provides more reinforcement than a thin frame in the same material. A thin, stiff frame reinforces locally and absorbs stresses formed just at the opening contour. Three concepts are investigated:

- LVL frame, 100 mm thick
- LVL frame, 200 mm thick
- steel frame, 10 mm thick

Frames made of LVL are considered to be bent, meaning fibres curve around the opening, creating a continuous reinforcement. For modelling, element orientation in the frame along the opening contour is assigned in Ansys. In Figure 5.6, fibre orientation (red lines) of the frame follows the curvature of the opening, tangential direction acts through the wall thickness, out of the plane and material z- or radial direction (blue lines) act perpendicular to the inner frame surface, pointing into the opening. Contact surface between frame and module is rigid, i.e. a perfect glue line. Shown in Figure 5.7 are stresses parallel to the fibres, visualization of tangential and shear stresses can be found in Appendix 9.3. In the visualization, the steel frame has been excluded.

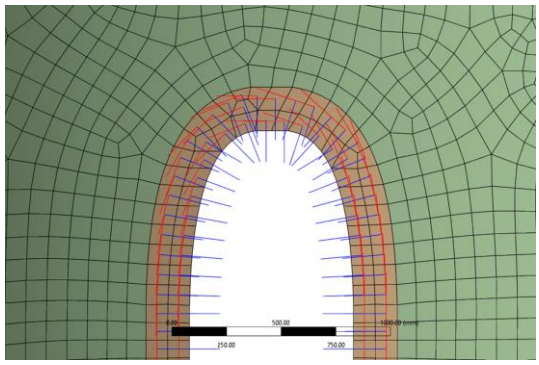

Figure 5.6. Element orientations of frame elements.

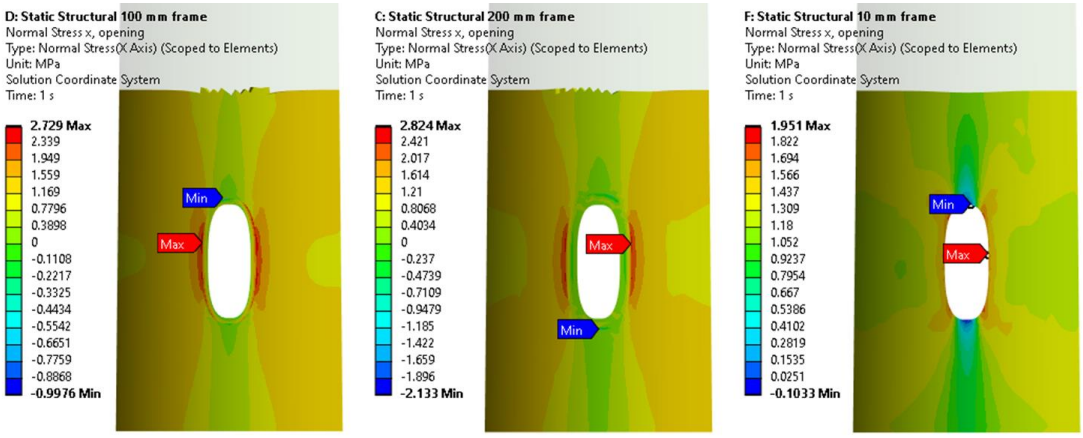

Figure 5.7. Longitudinal stresses in modules reinforced with frames.
Left: 100 mm spruce. Middle: 200 mm spruce. Right: 10 mm steel.

In general, inserting a LVL frame mainly contributes to increasing the opening and its radius in the LVL wall. For both frame thicknesses, stress peaks form in approximately the same areas as in an unreinforced wall. The frames themselves seem to exhibit stresses much lower than the adjacent wall. For a thinner LVL frame, stresses at the interface between wall and frame are lower than for a thicker frame. This could be due to the change in stiffness being smaller for a thinner, thus weaker frame. The steel frame seems to successfully reduce stresses on the opening sides. Both tensile and compressive stresses are lower than in the concepts with LVL frames. Although seeming viable when assessing stresses parallel to the fibres, shear stresses increase largely in all concepts.

5.3.3 Stiffeners

To counteract the missing material in the opening, stiff columns could be inserted to lead loads around the opening. These columns can be formed as stiffeners integrated in the wall at a distance from the opening. This concept was shown to be very effective in both steel wind turbine towers and in the study investigating improvement of load transfer around aircraft windows. For modelling, slits through the wall are created and stiffeners are inserted. Meshing is done such that finer meshes, i.e. smaller elements are created around the tips of the stiffeners and around the opening. The stiffeners are attached rigidly to the wall, implying a perfect glue line between the LVL module and the stiffeners. When not produced in the same material as the wall segment, stiffeners are excluded from the following result images. Also, images for resulting stresses in material y direction and shear are attached in Appendix 9.4.

Singularities are expected to form at the stiffener's tips. In an attempt to decrease these, material around the stiffener's tips is removed, mimicking a method used in steel structures to stop cracks from growing at crack tips, called *stop drilling*. The idea is to increase the radius of the crack tip and relieve stresses locally. Radii investigated here range from the smallest radius of 5 mm to the largest of 15 mm. A small radius forms a semicircle at the tips of the stiffeners while larger radii with 10 and 15 mm form a circular opening around the stiffener's tips, as illustrated in Figure 5.8.

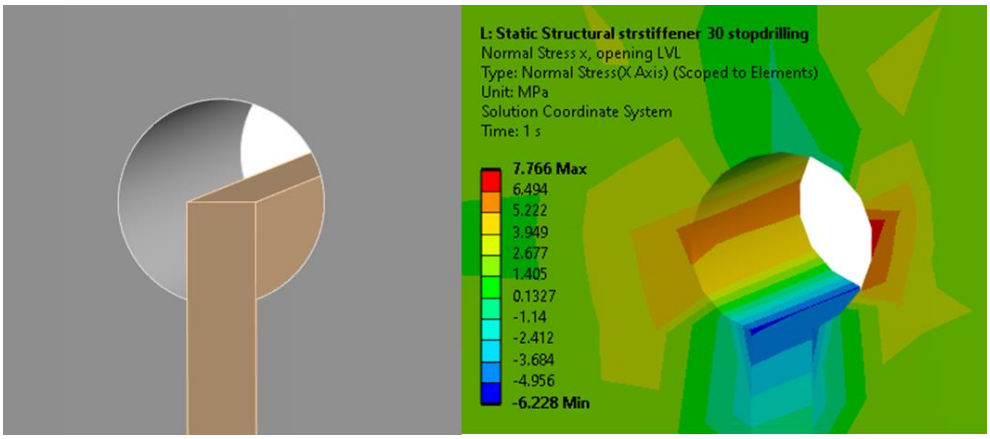

Figure 5.8. Left: Detail of stop drill. Right: Longitudinal stresses at stop drill in tensioned modules.

For all sizes of the stop drill, stresses still peak at the end of the stiffeners. Stop drilling does not remove sufficiently much material to decrease stresses at the stiffeners under a level of stresses at the opening contour. Removing too much material on the other hand might weaken the structure. Therefore, to evaluate the impact of different stiffeners on resulting stresses around the opening, only elements in a strip around the opening will be considered, excluding stiffener's tips. How to cope with stresses at the stiffeners must be subject of future work. The model, geometry and displacements remain unchanged, only for the evaluation elements assessed are handpicked. Stiffeners are placed starting from 1 m over ground and continuing to

5 m over ground, thus reaching one meter below and above the opening. The strip looked at in the evaluation of concepts includes the total width and thickness of the module but is restricted to the height 1.1 m – 4.9 m over ground, meaning 10 cm at the stiffener's ends have been neglected.

5.3.3.1 Straight stiffeners

In a first step, the impact of straight steel stiffeners, placed with different distances from the opening, is investigated. Characterizing the distance is the angle between the stiffeners, measured horizontally from the tower mid-axis. Stiffeners with a spread of 30° are close to the opening, while a spread of 45° and 60° increases the distance between stiffener and opening.

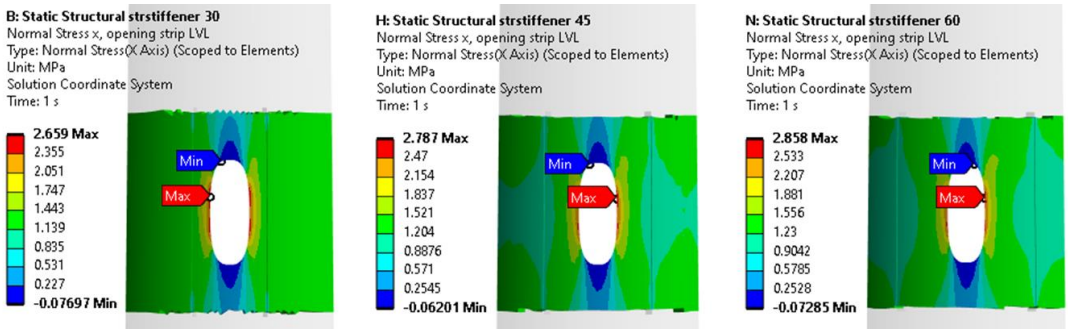

Figure 5.9. Longitudinal stresses in modules reinforced with straight steel stiffeners. Left: 30° spread. Middle: 45° spread. Right: 60° spread.

As can be seen in Figure 5.9, stress pattern around the opening is similar to an unreinforced opening. The closer the stiffeners are placed to the opening, the larger the relieve in stress peaks at the opening contour. This statement holds for stresses in both material directions and for shear stresses. However, reduction in SCF seems not to be linear with increasing spread of the stiffeners. Moving stiffeners from 45° to 30° has a greater impact on SCF than moving stiffeners from 60° to 45°. Considering continuity in results where stresses in all evaluated material directions improve with a smaller spread, i.e. narrower placement, 30° placement will be used for further concepts.

5.3.3.2 Stiffeners with varying stiffness

Although stress peaks at the stiffener's tips have been excluded for now, they still have to be considered in future design. Reducing high stresses will improve overall performance of the reinforcement and lead to a more continuous transfer of stresses from the wall into the reinforcement. Reason for stresses to peak is not only due to the change in geometry caused by the stiffener's slits, but also due to the change in stiffness caused by the change in material. Inserting steel stiffeners with a high stiffness in the relatively soft LVL wall creates an abrupt change in stiffness at the interface. Reducing this difference and allowing for a smoother transition of stiffness between wall and stiffener might improve performance and reduce forming of stress concentrations. To investigate this, stiffeners with different stiffnesses are compared. As the softest option, stiffeners made from spruce LVL with a width of 100 mm are designed. To increase stiffness, 100 mm high strength beech LVL and 10 mm aluminium is tested. In addition, stiffness can be reduced by changing geometry of the stiffener. This enables a variation of stiffness over height in the stiffener. By inserting holes as demonstrated in Figure 5.10, the stiffness can be controlled to be low at the tips and merge into a high stiffness in the middle, at the height of the opening. This option is tested both in steel and aluminium.

Figure 5.10. Geometry of holed stiffeners with varying stiffness.

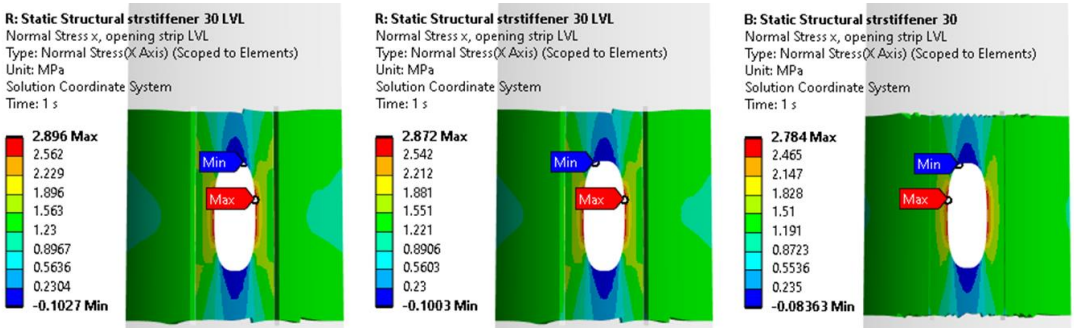

Figure 5.11. Longitudinal stresses in modules reinforced with straight, solid stiffeners. Left: 100 mm spruce LVL. Middle: 100 mm beech LVL. Right: 10 mm aluminium.

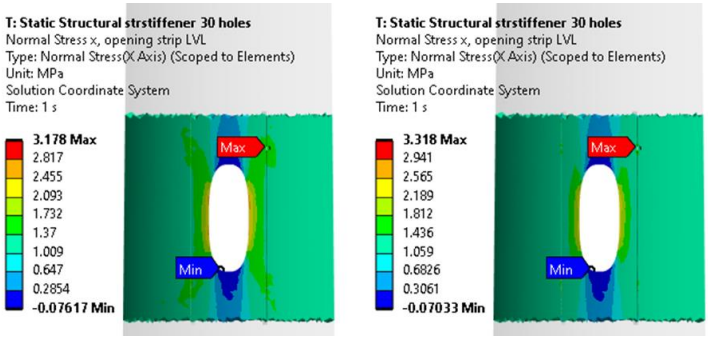

Figure 5.12. Longitudinal stresses in modules reinforced with stiffeners with varying stiffness. Left: 10 mm aluminium holed stiffeners. Right: 10 mm steel holed stiffeners.

Figure 5.11 and Figure 5.12 show stress peaks form in a similar pattern as for an unreinforced opening. When modelling solid stiffeners, peaks form around the opening contour. A decrease both in tensile and compressive stress peaks can be observed with an increase of stiffness in the stiffeners. For shear loading in concepts with LVL stiffeners, highest stresses apart from the stresses at the opening contour form at the stiffener's ends. For the holed stiffeners, peaks seem to form at a hole in the stiffener. It is unclear if this sources from a singularity or stresses at the interface between stiffener and wall exceed stresses at the opening. A holed stiffener made in aluminium seems to reduce stresses further than the same stiffener made in steel. Assessing stresses parallel to the fibres, it seems varying stiffener's stiffness by inserting holes is not beneficial. Considering stresses perpendicular to the fibres and shear stresses however show holes have an improving effect on SCF.

5.3.3.3 Streamline stiffeners

Instead of using straight stiffeners, streamline stiffeners to mimic natural stress flow can be used. The idea is to allow for a smooth redirection of stresses around the opening. Stiffeners will be formed by four equal circle segments joined together and produced in 10 mm steel. Two curvatures will be investigated, as presented in Figure 5.13. A bigger radius and smaller segment angle forms a slight turn (in this case r = 4000 mm, segment angle = 15°) and a smaller radius combined with a bigger segment angle results in a steeper turn (r = 2100 mm, segment angle = 30°). Choice of radii and angle for forming curvatures is arbitrary. The steeper turning stiffener allows for a placement closer to the opening, thus both placing at a spread of 30° and 20° will be assessed.

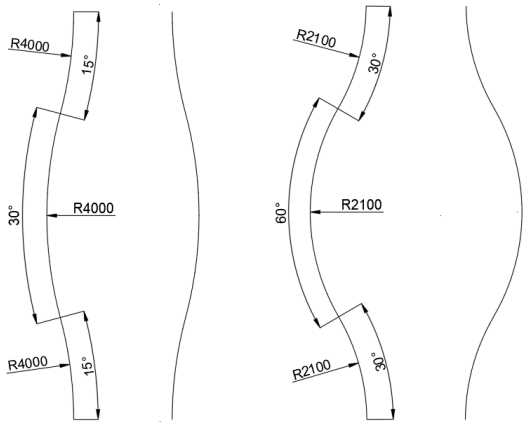

Figure 5.13. Geometry of streamline stiffeners.

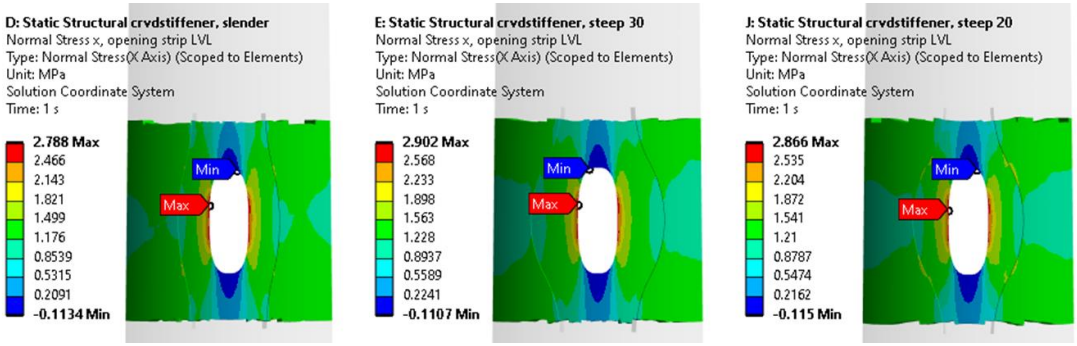

Figure 5.14. Longitudinal stresses in modules reinforced with streamline stiffeners. Left: Big radius. Middle: Small radius, 30° spread. Right: Small radius, 20° spread.

As presented in Figure 5.14, stress pattern for streamline stiffeners is the same as for straight stiffeners. It seems stiffeners with a slighter curvature outperform stiffeners with a steeper turn in reinforcing against stresses parallel to the fibres. For shear, the opposite is true. Stresses in the concepts including steeper turning stiffeners are lower, regardless of placement. Highest stresses perpendicular to the fibre form at the stiffener midpoint, although magnitude is lower than in concepts including straight stiffeners. It seems for stresses parallel to the fibres a smaller distance to the opening is beneficial while formed shear stresses depend on stiffener's curvature.

5.4 Opening module properties modification

Instead of adding reinforcing structures, the wall layup can be modified to achieve an internal stabilisation. In this way, failure can be prevented by changing properties of the tower structure, similar to dealing with layups in CF composites. The natural reinforcement provided by lignin

fibres can be used to strengthen the area around the opening by using LVL sheets to engineer with. Changing the layup and thereby stiffness of the opening module will not only influence the stresses around the opening but also the longitudinal and transversal joints between the opening module and the adherent tower modules. For analysing different module layups, a model with the whole tower was created. The opening module was modelled as a separate part while all other modules were considered to act as one unit. In Ansys Multiphysics ACP the tower was modelled with shell elements, having a thickness of 350 mm. Forces and moments at the top of the tower resulting in tensile, compressive and shear stresses in the opening module were applied. Magnitudes of these were chosen to mimic loads at the tower *Wind of Change*.

Figure 5.15. Bottom of tower with opening module.

Stress concentrations form very locally in the wall and in the laminate. Although reaching high stresses, the laminate might still be able to cope with stress concentrations due to redistribution of stresses through the laminate thickness. Rather than evaluating stress concentrations in material directions, the capacity of the laminate wall at the most critical locations is investigated. This gives an estimation of the utilization of the laminate and considers interaction of all material directions. Used failure criteria are Maximum stress and Tsai-Hill failure criteria. In ACP post processing unit, inverse reserve factors (IRF) for sample points in a laminate, indicating material utilization, can be obtained. Also, stresses, strains and failures through the laminate thickness can be illustrated and plotted. For following plots, elements with highest IRF are chosen and looked at on lamina level.

5.4.1 Wall layup

As shown in chapter 4.3, ratio between panel stiffnesses affect stresses around an opening. Orienting panels in ±45° forms a quasi-isotropic layup with properties in x- and y-direction being the same. For angles of rotation between 0° and 45°, stiffness in laminate x-direction will be greater than stiffness in laminate y-direction. Since main loads act in longitudinal tower direction, a stiffer x-direction is preferable for load carrying purposes. Presented in Figure 5.16 are stresses in laminate x-direction for a layup with alternating ±20° and ±30° panels. In this case, the opening module is under compression, thus maximum compressive stresses are negative. Two major observations can be made:

1. While maximum stresses for the ±20° layup occur at the opening, maximum stresses for the ±30° layup form at the joint between modules. Here the change in stiffness between opening module and surrounding modules creates higher stress concentrations than the irregularity induced by the opening geometry.
2. Maximum tensile stresses, formed at the back of the tower, increase with increasing angle of panel rotation. It seems the more rotation in the layup is induced, making the module weaker in longitudinal tower direction, the higher stresses on the tensioned side of the tower are created.

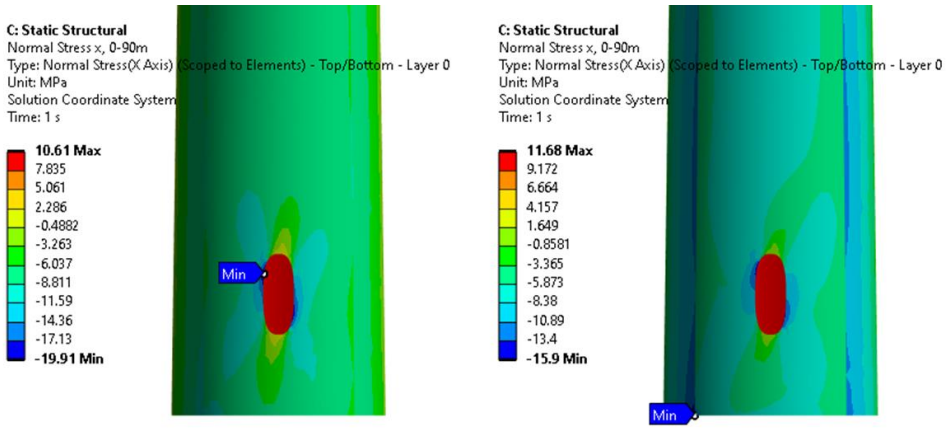

Figure 5.16. Stresses in opening module in spruce LVL with different layups. Left: ±20° rotation. Right: ±30° rotation.

Visualizing IRF reveals location where the laminate wall is most likely to fail. In the case for a layup with panels oriented alternating in ±30°, this location is at the opening, although highest stresses form at the joint between modules. Both maximum stress and Tsai-Hill criterion show maximum utilization at similar locations (see Figure 5.17). Although stresses peak at another location, the laminate as a whole is stressed the most at the opening contour. This shows evaluating layups based on laminate utilization is a more powerful method compared to looking at stress concentrations.

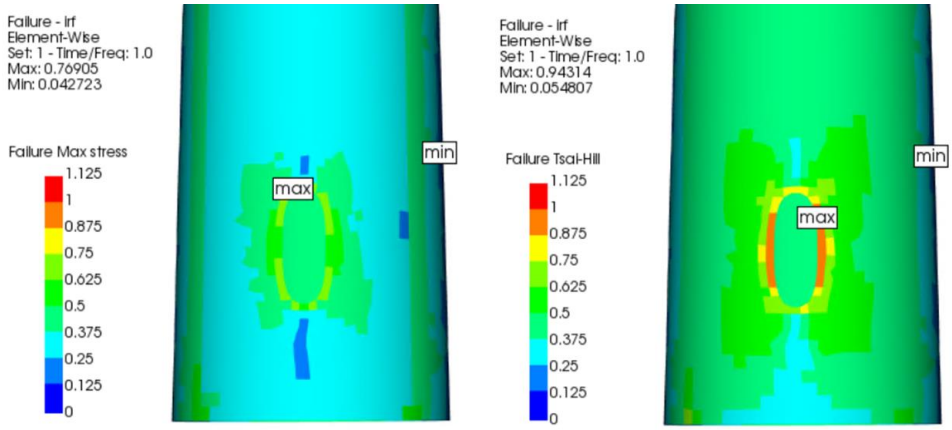

Figure 5.17. Inverse reserve factors for an opening module with ±30° spruce layup. Left: Maximum stress failure criterion. Right: Tsai-Hill failure criterion.

Instead of rotating all layers, one could also consider rotating only some of the panels. The idea behind this is to create an internal reinforcement, where some laminae take stresses formed around the opening while majority of the panels still have the load bearing function. This would combine the beneficial orientation of ±45° for reducing stress concentrations around the opening and 0° orientation providing stiffness in longitudinal tower direction. To evaluate layups, stresses through the wall thickness for the element with highest IRF are plotted. This reveals stress distribution in the different panels through the wall. In Figure 5.18, a through-thickness plot of stresses in a $[0/0/0/0/0/45/-45]_s$ layup is presented.

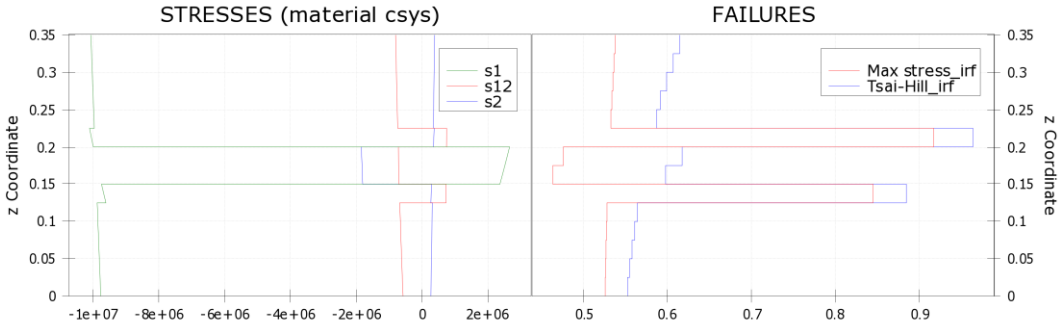

Figure 5.18. Stresses and failures through laminate thickness for a [0/0/0/0/0/45/-45]$_s$ layup in spruce.

The location of maximum IRF is in this case located at the side of the opening. Stresses in laminate x-direction, s1, are therefore governing while shear stresses, s12, are only minor at this location of the wall. The plot reveals panels oriented 45° have the highest IRF in the layup and are most likely to cause failure of the laminate. In this layup, few panels are rotated to a great extent. Choosing a layup where rotation is less but number of panels rotated is increased might reduce IRF peaks in the critical section of the wall. In Figure 5.19, stress through a layup of [0/0/0/0/25/-25/25]$_{(s)}$ is plotted. Again, stresses in longitudinal tower direction are governing. The location of the investigated element is such that panels rotated at -25° are subjected to less compressive stresses. Instead of IRF in the rotated panels being reduced, utilization of 0° panels is increased. This gives the impression that only rotating some of the panels in the layup is inferior to a uniform, alternating rotation.

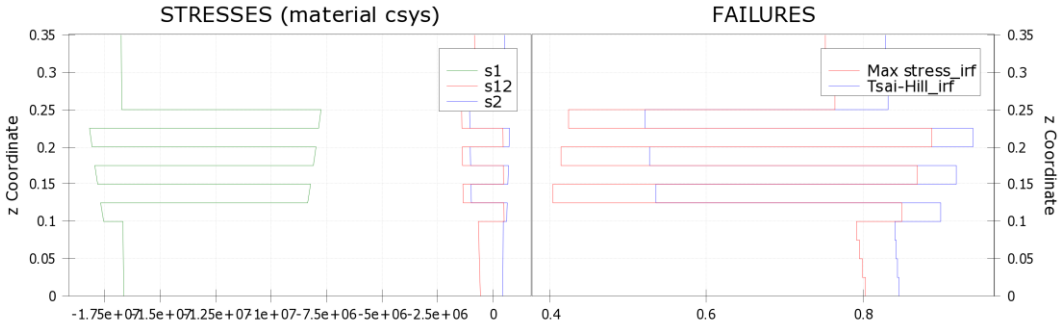

Figure 5.19. Stresses and failures through laminate thickness for a [0/0/0/0/25/-25/25]$_{(s)}$ layup in spruce.

5.4.2 Wall material

Instead of rotating several panels in the layup to create an internal reinforcement, one could also consider taking a more global approach and change the stiffness of all the panels in the module. In this way, the strong material surrounding the opening would make up for the loss of material due to the opening. High-strength beech LVL has a slightly higher stiffness than spruce LVL and significantly higher strength. Replacing spruce with beech might improve performance of the module since capacity of the surrounding material around the opening is increased, while stiffness in longitudinal tower direction is similar. In addition, as in the previous chapter, panels could be rotated to reduce stresses around the opening and create an internal reinforcement.

Taking the same two ±20° and ±30° layups, different results are obtained compared to spruce LVL, shown in Figure 5.20. Maximum stresses for both cases form at the opening contour, not

at the joint between modules. As for the spruce LVL wall, with increasing angle of rotation, tensile stresses at the opposite side of the tower increase. Comparing maximum stresses at the opening contour, peak stresses for a rotation of ±20° are higher than peak stresses in a layup with a rotation of ±30°. This is well in accordance with the theoretical approach made in chapter 4.3, showing a reduction of difference in stiffnesses between laminate directions reduces stress concentrations around the opening. In the illustration, stress peak for the ±30° seems to be misplaced and should instead be at the same location as for the ±20° layup.

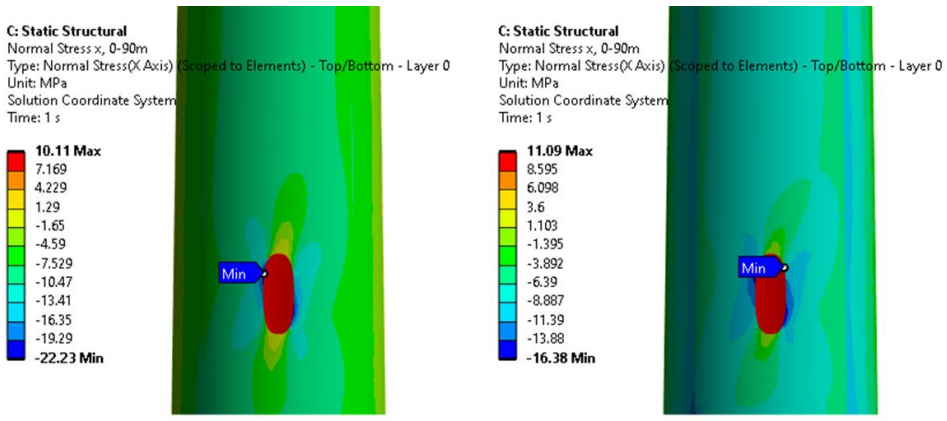

Figure 5.20. Stresses in opening module in beech LVL with different layups. Left: ±20° rotation. Right: ±30° rotation.

Although maximum stresses in this case form at the opening for both illustrated layups, looking at laminate failure in Figure 5.21 reveals differences in location of maximum IRF. For the module constructed with panels alternating in ±30°, Tsai-Hill failure criterion predicts highest IRF close to the location with maximum stress concentration. Maximum stress criterion meanwhile computes highest IRF at the joint between modules. In comparison with the module constructed in spruce, IRF for the two failure criteria differ less. One could argue this is due to the different locations of occurring max IRF. However, since change in layup of the module will affect the whole tower, elements of investigation should not be restricted to the area around the opening but instead also consider different locations of maximum laminate utilization.

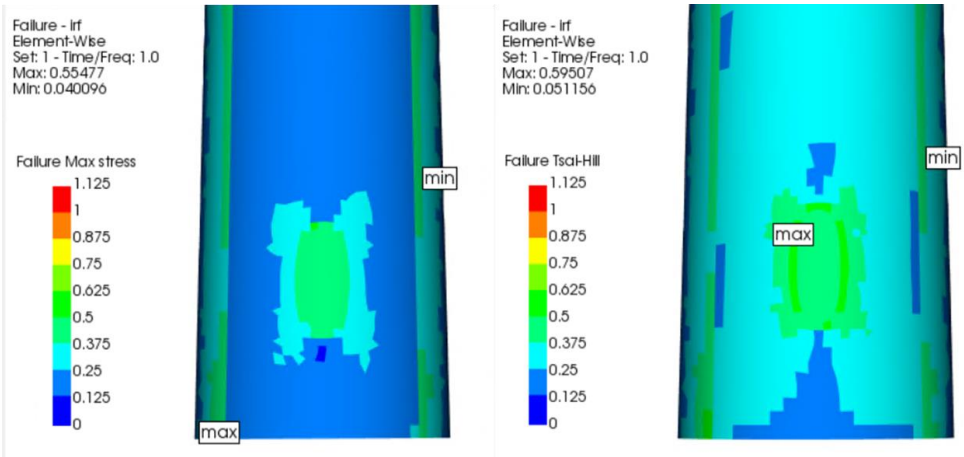

Figure 5.21. Inverse reserve factors for an opening module with ±30° beech layup. Left: Maximum stress failure criterion. Right: Tsai-Hill failure criterion.

Mixing panel orientation in the layup with the same intention as in the previous chapter, stress distribution in the $[0/0/0/0/0/45/-45]_s$ laminate is similar to the same layup in spruce. Stresses in longitudinal tower direction, s1, govern. Again, IRF in the rotated panels are highest but significantly lower than in the spruce layup.

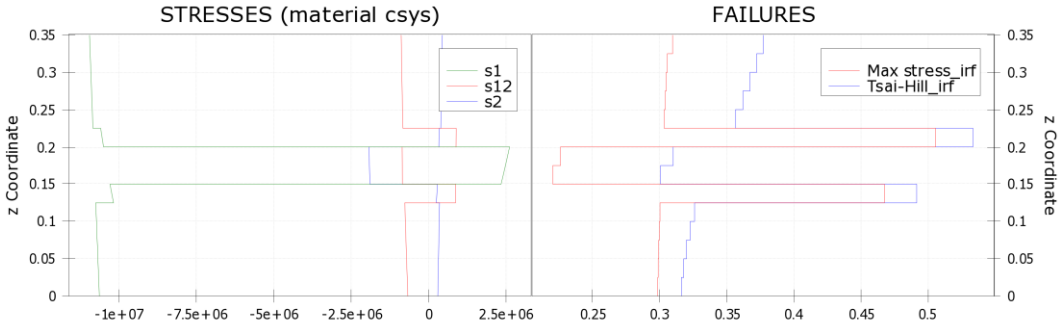

Figure 5.22. Stresses and failures through laminate thickness for a [0/0/0/0/0/45/-45]$_s$ layup in beech.

Rotating more panels less in a beech module leads to highest stresses in the 0° plies. In contrast to the plot for the same layup in spruce, the location for highest IRF is such that -25° panels don't exhibit high stresses. Panels rotated 25° show a utilization in alignment with 0° panels. The reason for this might be the location of investigated stresses. It seems maximum IRF in a beech wall with [0/0/0/0/25/-25/25]$_{(s)}$ layup form at a location where laminate x-stresses are critical.

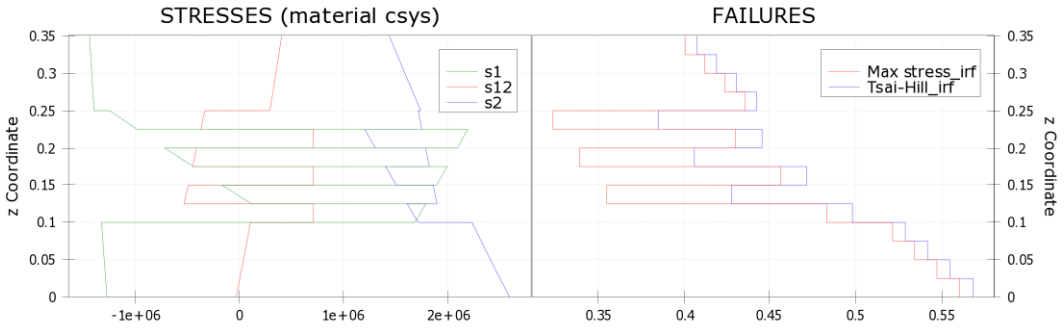

Figure 5.23. Stresses and failures through laminate thickness for a [0/0/0/0/25/-25/25]$_{(s)}$ layup in beech.

5.4.3 Change in layup and material

As seen in previous sections, rotated layers are often more prone to failure in the layup. Instead of building the whole wall in uniform material, panels with highest IRF could be changed to a higher strength class. This would decrease IRF in those panels and create a more uniform material utilization through the wall.

Looking at the layup with 0° and ±25° panels, changing rotated panels to beech creates a stiffer core in the wall that might attract higher stresses. Compared to the layup completely made in spruce, the core of the laminate shows decreased IRF. Panels remaining in spruce do not show a decrease in IRF, redistribution of stresses in the laminate seem not to be high enough to relieve stresses in 0° layers to an extent such that IRF is nearly constant through the wall. IRF of the most critical wall element is governed by the softer spruce panels.

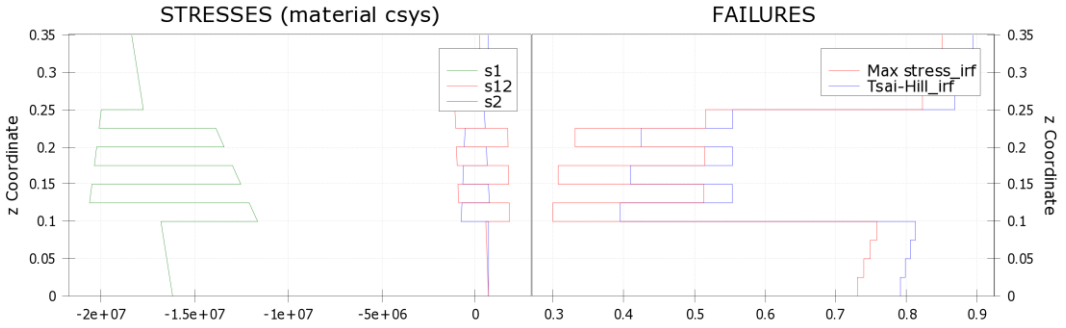

Figure 5.24. Stresses and failures through laminate thickness for a [0/0/0/0/25/-25/25]$_{(s)}$ layup with 0° layers in spruce and ±25° layers in beech.

Since a change in material of the rotated panels does not have the desired effect, instead the 0° panels could be made of beech. The idea behind this is the 0° panels taking longitudinal stresses and relaxing the rotated panels, while those reinforce the opening and reduce stress peaks around the opening contour. As seen in Figure 5.25, the stiffer, outer panels get the highest stresses in the wall section while the rotated inner panels exhibit lower stresses. The difference in stresses is however not high enough to reduce IRF in the spruce panels to a level similar to IRF in beech panels. Highest IRF occur in the panels rotated 25° and not in the outer 0° panels. It seems, regardless of which panels are made in stiffer and stronger beech, the panels in spruce LVL govern overall performance of the laminate and possess the highest IRF.

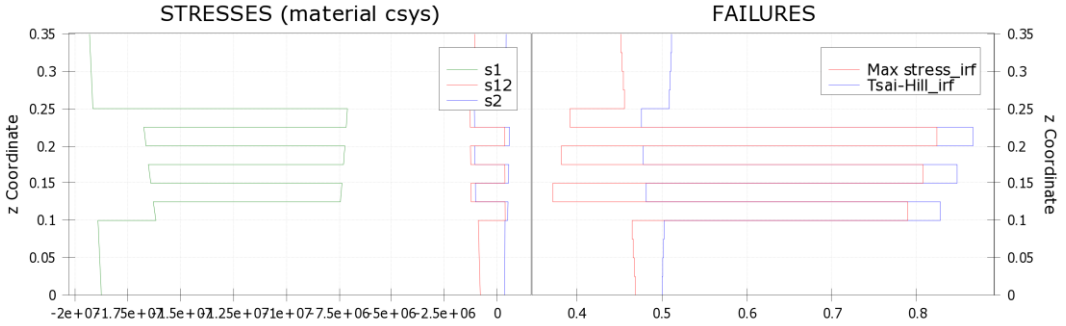

Figure 5.25. Stresses and failures through laminate thickness for a [0/0/0/0/25/-25/25]$_{(s)}$ layup with 0° layers in beech and ±25° layers in spruce.

6 Evaluation of concepts

Having given a description of resulting stresses, stress concentrations in different material directions must be evaluated. As in the previous chapter, evaluation is first done for reinforcement concepts followed by evaluation of concepts with modified module layup. With the gained knowledge, an investigation on improvement of the concepts is made. Here the best-working concepts from the two methods are combined and evaluated.

6.1 Reinforcements

To evaluate reinforcement concepts against each other, stress concentration factors for the stresses in laminate x-direction (longitudinal tower direction), laminate y-direction (tangential tower direction) and shear in the xy-plane (in the tower wall) are compared. Here the stresses in y-direction are weighted according to chapter 5.2. Only stress concentration factors forming in the LVL are considered, excluding stress concentrations in possible steel reinforcements. Comparing SCF gives an estimation on which concepts perform better and will be especially useful when comparing similar concepts within a group of concepts. An average of the three SCF is formed and used as the determining grading factor. In addition, standard deviation of the three SCF is obtained to give an indication on spread of results. Had a concept shown a high average SCF but a low deviation, it might be worth considering since it had affected all material directions equally. In Table 6.1, an overview of performance considering SCF is given, top 20% concepts are marked green.

For all concepts including cover sheets, overall stiffness of the segment is similar or increased compared to the solid wall. This implies the sheets contribute to the overall stiffness of the module. However, high values regarding stress concentrations are obtained in all material directions. SCF in longitudinal direction for the concept with LVL sheets on both sides is the lowest among concepts including cover sheets. Stresses 1.7 times higher than in a solid wall are formed. For tangential and shear stresses however LVL on both sides strangely performs worse than LVL on the outside only. Both SCF in y and xy are around 20 times higher than the concept only including a cover sheet on the outside surface of the wall. The reason for this is unclear, checking FE models no errors causing the unexpected result could be found. A singularity might have formed which would explain the unreasonably high stress concentration. For all concepts, especially shear is a problem. While steel cover sheets reduce SCF in normal material directions to still high but reasonable levels of 2.2 in x and 5.1 in y-direction, SCF in shear are too high to consider this a viable method of reinforcing the opening. As seen in the previous chapter, no reinforcement through the wall thickness is achieved. Due to the very low flatwise shear capacity of LVL, translation of stresses out of the plane needs a lot of distance. In contrast, steel can lead stresses in all directions equally due to its isotropic properties. Hence the difficulty of relieving the core of the wall from high stresses could lead to differences in stiffness on the reinforced outsides to the unreinforced inside of the wall creating new stress concentrations. The change in stiffness on the surface where cover sheets end also creates stress concentrations. Again, these are mainly caused by change in shear capacity and could explain why SCF in shear are significantly higher compared to an unreinforced opening in all concepts including cover sheets. Stresses formed in glue lines between material with different stiffnesses must also be considered. These could be especially high in regions where LVL with low out-of-plane shear stiffness meets steel with high shear stiffness.

Reinforcing the opening with frames in LVL reduces overall stiffness of the module. The thicker the frame, the greater the decrease in stiffness. This is due to additional wall material being removed beyond the opening contour to make room for the frame. The inserted frame does however not contribute to the global stiffness of the module and therefore widens the opening. Both concepts including LVL frames show reasonable stress concentrations in longitudinal and tangential direction with under 2 and around 4.5 respectively. As discussed

before, the low out-of-plane capacity of LVL hinders stresses to flow into the LVL frame. Again, great stress concentrations in shear are formed with magnitudes over 300 times higher than in a solid wall. Replacing the thick timber frame with a slender steel frame increases global stiffness of the module to 95 % of a solid wall. In this case, the frame can take vertical loads and lead them into the frame, reducing SCF to 1.3. For loads in longitudinal direction, the frame provides a reinforcement and relieves the LVL wall from stresses. Tangential stresses are similar to a thin LVL frame with SCF of 4.3. Shear capacity of the two timber frames are similar, while a steel frame shows lower but still rather high SCF in shear. Instead of 300, the steel frame shows stresses around 100 times higher than in a solid wall. This shows using a frame is good for reinforcing against stress concentrations in longitudinal direction while reinforcement in shear is not achieved. Again, the created difference in stiffness could lead to new stress concentrations forming, leading to higher SCF than around an unreinforced opening.

Table 6.1. Evaluation of reinforcement concepts.

	SCF in material direction			Average	Stdev	reaction force, rel
	x	y	xy			
unreinforced opening	1.9	5.0	38.7	15.2	16.7	0.90
cover sheets						
100 mm LVL external	4.3	26.4	2712.2	914.3	1271.3	1.08
100 mm LVL internal and external	1.7	520.7	53250.5	17924.3	24980.3	1.00
10 mm steel internal and external	2.2	5.1	655.2	220.8	307.2	1.10
frames						
100 mm LVL	1.8	4.2	334.5	113.5	156.3	0.88
200 mm LVL	1.9	4.6	394.4	133.6	184.4	0.84
10 mm steel	1.3	4.3	93.6	33.0	42.8	0.95
straight stiffeners steel						
30° spread	1.7	4.9	14.4	7.0	5.4	0.94
45° spread	1.8	5.1	19.4	8.8	7.6	0.94
60° spread	1.9	5.2	21.8	9.6	8.7	0.94
straight stiffeners, varying stiffness						
100 mm spruce LVL	1.9	4.6	16.8	7.8	6.5	0.90
100 mm beech LVL	1.9	4.6	16.1	7.5	6.1	0.91
10 mm holed plate aluminium	2.1	4.6	9.8	5.5	3.2	0.91
10 mm aluminium	1.8	5.0	15.9	7.6	6.0	0.92
10 mm holed plate steel	2.2	4.5	9.8	5.5	3.2	0.93
straight stiffeners steel with stop drill						
stop drill ø 10 mm	1.7	4.5	34.0	13.4	14.6	0.94
stop drill ø 20 mm	1.7	5.0	26.0	10.9	10.7	0.94
stop drill ø 30 mm	1.7	5.0	10.3	5.7	3.5	0.94
streamline stiffeners						
slight curve, 30° spread	1.8	4.2	26.4	10.8	11.1	0.94
steep curve, 30° spread	1.9	4.2	20.0	8.7	8.1	0.93
steep curve, 20° spread	1.9	3.9	19.2	8.3	7.7	0.93

Since the steel frame from previous concepts sits at an edge of the wall and is not embedded, stress flow is only possible from one side into the frame. Stiffeners on the other hand are

embedded in the tower wall and enable stresses from two sides to enter the reinforcement. To assess how much material next to the stiffener is needed to ensure a two-sided stress penetration, straight stiffeners are placed at different distances from the opening. As seen on the factor indicating relative stiffness of the module, placement of stiffeners has no impact on global stiffness. The chosen geometry and height lead to a stiffness of 94 % of the solid wall. SCF in the different material directions indicate a closer placement reduces stress concentrations more than a placement further away from the opening. Stresses in longitudinal direction are decreased compared to an unreinforced opening when the stiffeners are placed closer than 60° spread. Reduction takes place steadily with the lowest value at the closest placement at 30° spread and a SCF of 1.7. For stresses in y-direction only the closest placement reduces stresses slightly compared to an unreinforced opening. Moving the stiffeners away from the opening has a negative impact on stress concentrations in y-direction around the opening. Going from 4.9 in a close placement, SCF increase to 5.2 in the widest placement. Shear stresses are remarkably lower than for an unreinforced opening when stiffeners are placed close to the opening. Here SCF can be more than halved from 38.7 to 14.4 when placing at a 30° spread. Moving them further away increases SCF. This increase is however not linear. While a placing at 30° compared to 45° reduces SCF by 5, moving stiffeners the same distance from 60° to 45° only reduces SCF by around 2.5. Average SCF of 7.0 shows that a closer placement benefits performance of the reinforcement. The embedment seems to lead to a good translation of stresses from the wall into the stiffeners. Shear SCF can be reduced significantly both compared to an unreinforced opening and the previously investigated reinforcement concepts. Optimal placement of the stiffeners in relation to the opening could be investigated further in future work. Since both SCF for the frame and stiffeners placed further apart are higher than for the stiffeners at 30° spread, an optimal distance should exist. With the alternatives investigated, the placement of stiffeners with a spread of 30° is kept for further investigations.

As mentioned in previous chapters, induced change of stiffness between wall and stiffeners is part of the reason for stress concentrations to form away from the opening. In an attempt of varying the stiffness of stiffeners, the impact of reduced difference in stiffness will be investigated. The impact on module stiffness is small, the weakest stiffener made in spruce LVL does not increase stiffness of the module compared to an unreinforced module and leads to a global stiffness of 90 % of a solid wall. A holed steel plate has slightly lower stiffness than a solid steel stiffener, but still increases relative global stiffness to 93 %. Stiffeners made of 100 mm LVL provide some reinforcement, above all against shear stresses. By inserting stiffeners in the same material as the surrounding wall, SCF for shear can be decreased to under half of the magnitude in an unreinforced module to 16.8. Changing from spruce to beech has only a minor impact on performance in shear, reducing SCF to 16.1 while performance in normal material directions is unaffected and remain 1.9 in x and 4.6 in y-direction. Solid aluminium stiffeners show similar results as timber stiffeners. Stresses in x and xy can be reduced slightly to 1.8 and 15.9 but SCF in y are increased to 5.0, the same level as in an unreinforced opening. Average SCF shows no improvement compared to beech stiffeners. Weakening the ends of stiffeners has a beneficial effect on relieving stresses. Varying stiffness over height reduces SCF in shear drastically. Both for holed stiffeners made in steel and aluminium SCF drop to 9.8. SCF in x-direction increase to around 2.1, creating higher stresses compared to all solid stiffeners and an unreinforced opening. Maximum stresses do however not occur at the opening contour, instead they form at a hole in the stiffener. Applying the same reasoning as before, this location is at a place where difference in stiffness is the highest. Where the stiffener is in contact with the LVL, it offers support to the timber and increases stiffness. At the void formed by the hole of the stiffener, support is not given, thus difference in stiffness is high at this point. An option to reduce the difference could be to fill the voids in the stiffeners with a material with similar stiffness as the surrounding LVL or spread out the change in stiffness, e.g. by designing the stiffener with more but smaller holes. Investigating this topic should be done in future work. Producing the holed stiffener in steel instead of aluminium does not influence overall performance of the reinforcement. Average SCF is at 5.5 for both materials and standard

deviation indicates spread of results is equal. This indicates the improvement of the concept compared to solid stiffeners comes from the variation of stiffness in the stiffener and not from ultimate strength and stiffness of the stiffener material.

Reducing difference in stiffness at ends of stiffeners could either be done in the stiffeners as described in previous concepts, or in the adjacent wall. Removing material with peaking stresses at stiffener's tips through stop drilling affects the surrounding wall. As mentioned above, this evaluation only considers a strip around the opening and does not account for local effects from stop drills. Removed material does not have an impact on the capacity of the total module. Global stiffness is unaffected by the size of the investigated stop drills and stays at 94 % of a solid wall. The same is true for stresses in material x-direction. Regardless of the size of the stop drill, SCF stays at 1.7, the same level as for a stiffener without stop drills. For stresses in y, a small stop drill slightly improves performance to a SCF of 4.5 while stop drills with size of 20 and 30 mm roughly have the same SCF as a solid stiffener without stop drill. Shear SCF improve with increasing size of stop drill. While a size of 10 and 20 mm results in SCF higher than for a solid stiffener without stop drill (34.0 and 26.0 respectively), a hole of 30 mm has a similar effect in relieving stresses as varying stiffener stiffness. In this case, SCF in shear is reduced to 10.3, outperforming all solid stiffeners. Although local effects at the stop drill are excluded in this analysis, the method seems to relieve stresses at the opening. Effects from the stop drill affect areas in vicinity of the opening. Both this and finding a solution on how to deal with the remaining stress peaks at the stiffener's tips must be investigated in future work. Filling the stop drills with a softer material could spread out and relieve stresses further. One must also consider investigating whether this phenomenon is physically motivated or occurs due to computation methods leading to singularities in the critical areas.

Curving stiffeners to mimic natural stress flow around a knot in a tree has a slight impact on global module stiffness. Compared to straight stiffeners, stiffness is reduced to 93 % of that of a solid wall when choosing a steep curvature and more round stiffeners. Placement of the stiffeners in relation to the opening does not impact global module stiffness. The slightly curved stiffener reduces SCF in x to 1.8, while a steeper turning stiffener exhibits stresses 1.9 times higher than in a solid wall. Stresses in y are reduced compared to all other concepts. Especially a steeply turning stiffener provides good support with SCF in y at 3.9. In shear, curvature has a greater impact on reducing stress concentrations than placement. Stiffeners with small curvature perform similar regardless of placement relative to the opening and show SCF around 20. SCF in the slightly curved stiffener amount to 26.4. While being lower than in an unreinforced opening, SCF in shear are higher than in the other concepts including stiffeners. Overall, streamline stiffeners are not able to reduce stress concentrations in the same extent as straight stiffeners. With the used indicators, a stress flow mimicking natural grown trees cannot be achieved. One reason for this is that adjacent fibres in the wall are cut to make room for the stiffeners, thus interrupting natural stress flow in the wall. If the intention is to mimic natural stress flow, multiple stiffeners might be needed, relieving surrounding LVL and fibres. Also, the curvature investigated here is cylindrical. According to the findings in chapter 4.1, optimal curvature for handling shear stresses is elliptical. Considering other curvatures might improve performance of streamline stiffeners in shear.

6.2 Material modification

When changing layup and thereby stiffness of the whole module, the whole bottom of the tower is considered for evaluating layups. Inverse reserve factor based on Max stress and Tsai-Hill failure criteria are used for determining viability and IRF for a solid wall is taken as reference. Applied forces are such that tensile stresses form in the opening module. For the layups both absolute IRF and relative IRF to the solid wall are taken for evaluation. In Table 6.2, layups with alternatingly rotated panels are defined with the angle of rotation only, e.g. ±10°. When species are mixed, the first angle indicates orientation of outer panels, later number indicates

orientation of panels in the core. Information given in the parentheses consists of species (s = spruce, b = beech) and number of panels in the layup. 0° (b, 8) & 25° (s, 6) describes a layup of [0/0/0/0/25/-25/25/-25/25/-25/0/0/0/0] with 0° layers made in spruce and ±25° layers made in beech. Best performing 20 % of layups are marked in green, a difference in IRF between failure criteria over 10 % is indicated by red highlight.

Table 6.2. Evaluation of different layups in the opening module.

	Max-stress			Tsai-Hill			diff
	IRF		location	IRF		location	
	abs	rel		abs	rel		
solid wall	0.408	1.00	bottom of module	0.416	1.00	bottom of module	0.020
spruce							
alternating angle							
0°	0.857	2.10	opening	0.886	2.13	opening	0.034
± 10°	0.916	2.25	opening	0.956	2.30	opening	0.044
± 20°	0.873	2.14	opening	0.937	2.25	opening	0.073
± 30°	0.765	1.88	opening	0.905	2.18	opening	0.183
± 45°	0.728	1.78	bottom of module	0.76	1.83	opening	0.044
mix of angles							
$[0/0/0/0/0/45/-45]_s$	0.917	2.25	opening	0.952	2.29	opening	0.038
$[-45/45/0/0/0/0]_s$	0.896	2.20	opening	0.927	2.23	opening	0.035
$[0/0/0/0/25/-25/25]_{(s)}$	0.886	2.17	opening	0.925	2.22	opening	0.044
beech							
alternating angle							
0°	0.495	1.21	opening	0.533	1.28	opening	0.077
± 10°	0.526	1.29	opening	0.552	1.33	opening	0.049
± 20°	0.503	1.23	opening	0.541	1.30	opening	0.076
± 25°	0.474	1.16	bottom of module	0.548	1.32	opening	0.156
± 30°	0.555	1.36	bottom of module	0.577	1.39	bottom of module	0.040
± 45°	0.697	1.71	bottom of module	0.718	1.73	bottom of module	0.030
mix of angles							
$[0/0/0/0/0/45/-45]_s$	0.507	1.24	opening	0.523	1.26	opening	0.032
$[-45/45/0/0/0/0]_s$	0.518	1.27	opening	0.538	1.29	opening	0.039
$[0/0/0/0/25/-25/25]_{(s)}$	0.51	1.25	opening	0.526	1.26	opening	0.031
$[0/0/0/0/0/25/-25]_{(s)}$	0.522	1.28	opening	0.538	1.29	opening	0.031
spruce & beech							
0° (s, 10) & 45° (b, 4)	0.859	2.11	opening	0.888	2.13	opening	0.034
45° (b, 4) & 0° (s, 10)	0.874	2.14	opening	0.907	2.18	opening	0.038
0° (s, 8) & 25° (b, 6)	0.85	2.08	opening	0.882	2.12	opening	0.038
0° (b, 8) & 25° (s, 6)	0.824	2.02	opening	0.856	2.06	opening	0.039
0° (s, 10) & 25° (b, 4)	0.842	2.06	opening	0.865	2.08	opening	0.027

To start with, difference between failure criteria is majorly at 3 – 5 %, for some layups the difference reaches 7 %. This difference is fair, and results can be seen as reliable considering the nature of different failure criteria. Two layups show a difference over 15 %, this can be due to interaction between stresses leading to a high IRF for Tsai-Hill failure criterion, even though

stresses separately do not reach a similarly high IRF. High difference in IRF between failure criteria should be investigated further if a layup with high difference is chosen in the future tower design.

For layups in spruce and alternating angle, increasing the angle to 10° or 20° leads to an increase in IRF compared to a UD layup, peaking at around 10°, regardless of applied failure criterion. All three orientations result in an IRF around twice as high as in a solid wall. Increasing rotation further, evaluation with max stress criterion shows both 30° and 45° have lower IRF than 0° orientation, while Tsai-Hill indicates only 45° has lower IRF than 0°. Max stress criterion moreover indicates a change in location for maximum utilization of the laminate when rotating panels 45°. Instead of the opening contour being most critical, the joint between the opening module and adjacent modules becomes most critical. For Tsai-Hill, considering the change in IRF, the angle that reassembles a UD layup in IRF is probably at around 30° – 35°. IRF for 30° is slightly higher than a UD layup with an absolute IRF of 0.905 while 45° is significantly lower with 0.76. Thus, a rotation of panels of more than 35° leads to an improved IRF in Tsai-Hill failure criterion while rotations less than that show higher IRF than a UD wall. In general, keeping spruce and rotating all panels only leads to minor improvements compared to an unreinforced opening in a UD laminate. All IRF are very high compared to the solid wall. The best option, rotating all layers alternatingly in ±45°, increases IRF by 80 % to a material utilization of 0.73 – 0.76, depending on used failure criterion. Mixing angles does not outperform alternating rotation. As seen in previous chapter the rotated panels govern IRF. For the combinations investigated, mixing orientations in spruce leads to IRF higher than for alternating rotation. In general, mixing rotations in a spruce layup leads to an increase in IRF to around 2.2 – 2.3 times IRF in a solid wall, depending on failure criterion. Laminate utilization is around or over 0.90.

Changing panels in the module from spruce to beech decreases IRF significantly and outperforms all tested layups in spruce. A UD layup in beech has an IRF 21 % higher than a solid spruce wall at 0.495 for maximum stress criterion and an IRF 28 % higher at 0.533 for Tsai-Hill criterion. Both these utilizations of the laminate are within an acceptable range. Rotating panels increases IRF for both criteria but shows a dip at around 20° – 25°. Moreover, for the case with alternating angle of ±25° in beech, the most critical element is located at different places. Considering max stress criterion, the joint between modules is most critical while considering Tsai-Hill interaction an element at the opening contour gets the highest IRF. To investigate this behaviour further, a detailed plot of IRF was made for rotations between 0° and 45° (see Figure 6.1). Both failure criteria follow the same trend, increasing IRF with initiated rotation before dipping and thereafter increasing again. The lowest IRF is at different rotation angles for the different criteria. Tsai-Hill criterion has its dip at around 16° – 20° rotation of panels and does not undercut IRF from UD layup. Maximum stress criterion on the other hand shows a distinct dip at 25° with IRF lower than for a UD laminate wall. Lowest IRF with Tsai-Hill criterion occurs in a UD wall and is 28 % higher than in a solid spruce wall with a material utilization of 0.533. The lowest IRF for max stress is 16 % higher than in a solid wall with an alternating rotation of 25° and an absolute material utilization of 0.47. For rotations under 25° stresses at the opening challenge the laminate most. At 25° rotation this changes and instead stresses at the joint between opening module and adjacent modules lead to failure in the laminate. For Tsai-Hill this change in location occurs later, between 25° and 30°. Overall, curves lay close to each other with exception at angles around 25°. This gap might be caused by the missing interaction of stresses in maximum stress criterion and the changing location of maximum IRF. Both failure criteria seem to plateau at 45° but since rotating panels further doesn't improve neither longitudinal nor shear stiffness, angles bigger than 45° are not investigated. In conclusion, if a reinforcement at the opening is easier done than at the joint, rotation angle should be kept at 0° or around 20° – 25°. If the opposite is true, bigger rotation can be allowed for to relieve stresses at the opening and instead reinforcement at the longitudinal joints between modules should be added.

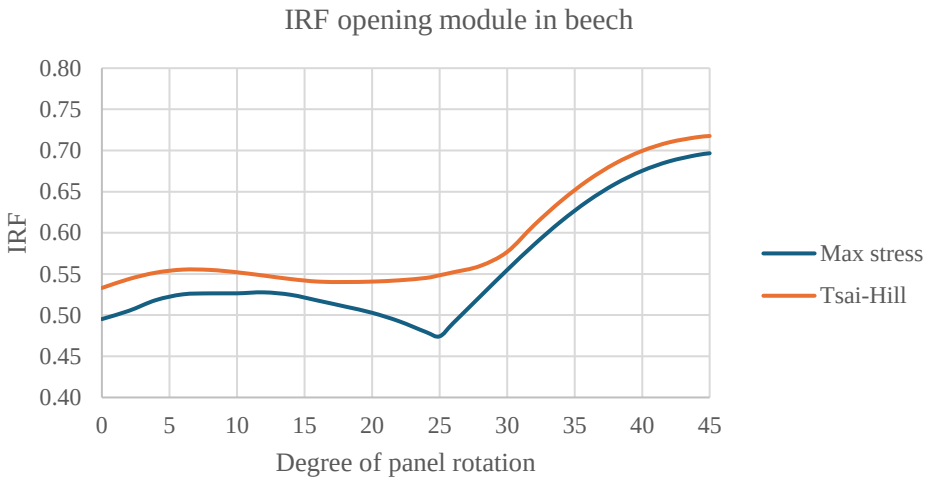

Figure 6.1. Change in IRF over panel rotation in a beech laminate.

Combining different panel orientations does not have the same negative effect as for panels in spruce. Especially when using Tsai-Hill criterion both a layup of $[0/0/0/0/0/45/-45]_s$ and $[0/0/0/0/25/-25/25]_{(s)}$ performs better than a UD wall with an IRF of 0.538, 26 % higher utilization than in a solid spruce wall. Difference in IRF between failure criteria for mixed layups in beech all lay under 4 % which can be considered a good match. Also, all investigated combinations have a low variation in laminate utilization with an IRF of around 0.51 for max stress and around 0.53 for Tsai-Hill criterion. It is noticeable that in beech, maximum stress criterion favours layups with same, alternating rotation while Tsai-Hill seems to favour a mix of angles. The reason for this could be investigated further but it seems a mix of rotation in beech enables different layers to provide strength and stiffness in different directions. Overall laminate utilization is reduced by this interaction, having a benefitting effect on Tsai-Hill failure criterion. Future work could also focus on to which extent a change from spruce to beech LVL is needed. In this model, the whole opening module was made in beech. A smaller fraction of the module in beech may be sufficient for reducing stresses around the opening.

Evaluating concepts mixing species to provide higher strength in layers with higher requirements show interesting findings. Comparing $[0/0/0/0/0/45/-45]_s$ made in spruce with the mixed layup shows the intended reinforcing effect is achieved. While absolute IRF is at around 0.92 for maximum stress and 0.95 for Tsai-Hill criterion in a single-species layup, swapping rotated panels to beech reduces absolute IRF to around 0.86 and 0.89. The same is true for a $[0/0/0/0/25/-25/25]_{(s)}$ layup where a similar improvement can be observed. However, performance is considerably lower than layups only in beech. The softer spruce panels are not relieved enough to ensure an IRF that would make the layup competitive. Mixing species and thereby strength and stiffness might also cause other unwanted effects in the laminate such as stress concentrations between differing layers. Due to above listed reasons, layups mixing species and rotation are not seen viable for further investigation.

6.3 Combining methods

A few concepts have been developed to reinforce an opening in a laminated wind turbine tower either through extra reinforcement or by modifying wall layup. Combining concepts might create synergies and improve concepts further. Concepts chosen are steel and aluminium stiffeners in combination with layups in beech in 0°, ±20° or $[0/0/0/0/0/45/-45]_s$. For modelling the composite wall, shell elements must be used with constant material properties through the wall thickness. Therefore solid, straight stiffeners will be used, although holed stiffeners showed better performance. In future work, an adjusted shell element model could be used to model a stiffener with properties and stiffness variation as in a holed stiffener. Reason for using

aluminium is to see how reduced change in stiffness between wall and stiffener affects resulting stresses. The layup with ±20° is used instead of ±25° because it ensures IRF between the two failure criteria differ less than 10 % and highest IRF for both criteria is located around the opening. Lastly, a layup with a ±45° core yielded good results with very low difference in IRF between failure criteria. The combined concepts will be evaluated in terms of IRF. Stress peaks are again expected to form around the stiffener's ends. Unlike the models for reinforcing concepts, the area of evaluation cannot be reduced to a strip around the opening due to possible effects between the opening module and adjacent modules. In this model, only elements around the stiffener's tips will be removed to ensure an assessment with stresses only peaking in vicinity to the opening. Investigation on stresses at stiffener's ends must be investigated in future work. The result is a laminate model of the whole tower with inserted stiffeners where the layup can be changed arbitrarily. Resulting stresses and IRF for a beech UD laminate wall with steel stiffeners in tension are presented in Figure 6.2.

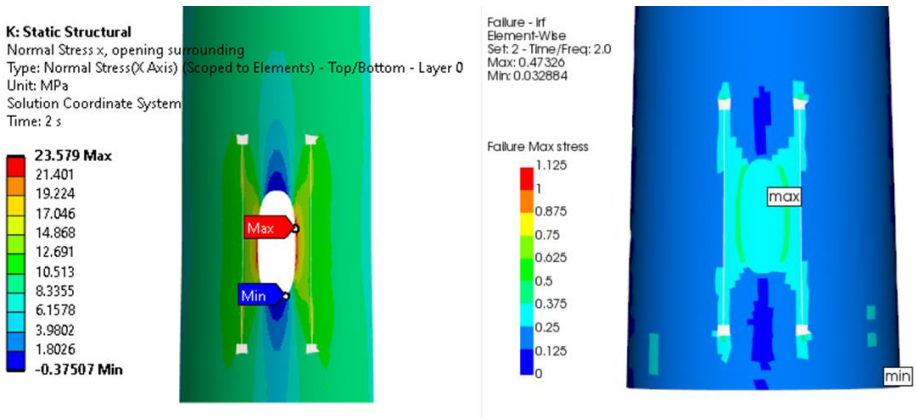

Figure 6.2. Stresses and IRF in a UD beech laminate with steel stiffeners. Left: Stresses in tensioned module. Right: Max stress IRF.

Table 6.3. Evaluation of combination of concepts.

	Max-stress			Tsai-Hill			diff
	IRF		location	IRF		location	
	abs	rel		abs	rel		
beech with stiffeners							
0°, steel stiffeners	0.473	1.16	opening	0.566	1.36	opening	0.197
0°, aluminium stiffeners	0.486	1.19	opening	0.564	1.36	opening	0.160
± 20°, steel stiffeners	0.523	1.28	opening	0.552	1.33	opening	0.055
± 20°, aluminium stiffeners	0.529	1.30	opening	0.557	1.34	opening	0.053
$[0/0/0/0/0/45/-45]_s$ with steel stiffeners	0.524	1.28	stiffener end	0.581	1.40	stiffener end	0.109
$[0/0/0/0/0/45/-45]_s$ with aluminium stiffeners	0.505	1.24	opening	0.532	1.28	opening	0.053

Inserting steel stiffeners into a UD beech laminate improves performance regarding stress concentrations considering maximum stress criterion. Absolute IRF can be reduced to 0.473, only 16 % higher than for a solid spruce wall without opening. Aluminium stiffeners also show a slight improvement compared to the wall without stiffeners, reducing IRF to 0.486. Evaluating the concept with Tsai-Hill failure criterion however indicates the opposite. Both for steel and aluminium stiffeners IRF increases to around 0.565, indicating slightly higher laminate utilization compared to an unreinforced opening in a UD beech wall. Due to the opposite effect depending on used failure criterion, the difference between failure criteria reaches a maximum value among all investigated layups. For steel stiffeners the difference is

almost 20 %, although peak stresses occur in the same area, at the opening contour. If a UD beech wall were to be reinforced, thorough assessment on resulting stresses in the laminate must be conducted to verify material utilization.

Reinforcing a layup with panels rotated alternatingly in ±20° shows a good match in IRF between failure criteria with a difference of around 5.4 %. The stiffeners do however not have the desired effect of relieving stresses in the laminate. Material used in the stiffeners does not influence IRF which is increased slightly compared to an unreinforced wall with the same layup. Applying maximum stress criterion results in an IRF of around 0.52, while Tsai-Hill yields an IRF of around 0.55. This equals an increase in laminate utilization of around 30 % compared to a solid spruce laminate wall. Reason for the increase in IRF compared to a wall in ±20° layup without stiffeners might be that inserting reinforcement not aligned with the fibres in the laminate interferes with the natural reinforcement provided by lignin fibres. In this case the loss in reinforcement due to inserting stiffeners is not gained back by the stiffeners themselves. When reinforcing the layup with a ±45° core, a similar effect can be observed. In this case steel stiffeners worsen performance while aluminium stiffeners have the same IRF for both failure criteria compared to the same layup without reinforcement. The gained stiffness from the stiffeners balances the loss of natural reinforcement by cutting fibres in the ±45° layers. When using steel stiffeners, maximum stresses occur in the vicinity of the stiffener's ends for both failure criteria. The difference between failure criteria is twice as high as for the same concept in aluminium. Location of maximum IRF indicates stresses at the stiffener's reach a magnitude such that the removed elements for evaluation are not enough to ensure peak stresses to occur at the opening contour. The question arises if the peaking stresses at this location are caused by singularities in the computation or due to the change in material and stiffness. A detailed investigation of these areas must be conducted if the concept is chosen for further applications.

7 Conclusion and outlook

Governing tensile and compressive stresses in the opening module in combination with a stretched opening in the direction parallel with major stress flow make supporting the opening in laminate x-direction most important.

Reinforcements that are placed at a surface at or around the opening, such as cover sheets and frames, do not offer sufficient reinforcement through the wall thickness. In both cases, translating and relieving shear stresses out of the wall around the opening fails. Stiffeners placed in the wall offer a better reinforcement. High strength and stiffness are needed but at the same time difference between wall and stiffener at the interface must be kept low. This is best solved through a solution where stiffness of the stiffeners is adjusted at the tips to enable a smooth transfer between stiffnesses. This can either be done in the wall by removing material and force stresses to spread out or by modifying the stiffeners to have a varying stiffness over height. Curved stiffeners investigated here do not outperform straight stiffeners, probably due to natural stress flow in the panels being disrupted or the chosen curvature not being optimal.

Changing panels in the module from spruce to beech has a major impact while spruce alone or a mix of species in the layup is not beneficial. A UD laminate in beech yields good results with an increase in laminate utilization compared to a solid spruce wall between 21 % – 28 %. If rotation of the panels is allowed for, either a layup with alternating panels in ±25° or a UD laminate with a core of ±45° or ±25°panels performs good. Regardless of material in the layup, rotation of panels between 0° – 20° is not beneficial. All viable results show an IRF slightly higher than in the solid spruce wall at around 0.50 when considering maximum stress and around 0.53 when considering Tsai-Hill failure criterion. For the layup with alternating ±25° orientation, further studies on laminate failure should be conducted to verify the reason for difference in failure criteria. Provided material data is given, Tsai-Wu, Hashin or other in-depth criteria from CF-industry could be used. For future work the question arises whether panels in the whole module have to be made in beech and rotated or if modifying panels in parts of the module around the opening is sufficient. This solution would facilitate building an opening surrounding which is later inserted into the opening module.

Combining reinforcement concepts has shown that an additional reinforcement in a laminate layup not being UD does not have a beneficial effect. Both rotating panels and reinforcing the wall takes away advantages gained by the rotated fibre orientation. Only when reinforcing in fibre direction can the stiffeners contribute to relieving stresses in the adjacent laminate. Best option considering maximum stress criterion is a UD layup in beech with steel stiffeners. This option provides a low increase in IRF compared to a solid wall from 0.408 to 0.47. The performance might improve further when adding holes in the stiffeners and inducing a stiffness variation. Second best option is using the UD beech laminate without stiffeners. Here both maximum stress and Tsai-Hill failure criterion predict similar results and IRF around 0.50 – 0.53. The same is true for layups with a reinforcing core and without stiffeners. Both $[0/0/0/0/0/45/-45]_s$ and $[0/0/0/0/25/-25/25]_{(s)}$ have a good match between failure criteria and an increase of IRF to 0.51 – 0.53. For the concepts provided here, more detailed studies must be executed on local details. Integrating stiffeners into the wall must be done in a way ensuring that they indeed reinforce the wall and do not create new stress concentrations and possible failure.

For future work, a deeper understanding of LVL and its veneers is desirable. Determining engineering properties such that arbitrary laminates can be created would make LVL a resource to engineer with. Determining veneer properties and interactions between veneers would allow for a “toolbox” design procedure like for carbon fibre composites. If the timber could be engineered with to provide properties needed for different applications, competitiveness would increase significantly and make timber laminates a game changer in timber engineering.

8 References

Agarwal, B.D., Broutman, L.J. and Chandrashekhara, K. (2017) *Analysis and Performance of Fiber Composites, 4th Edition*. John Wiley & Sons, Inc.

Alhajahmad, A. and Mittelstedt, C. (2022) 'A novel grid-stiffening concept for locally reinforcing window openings of composite fuselage panels using streamline stiffeners', *Thin-Walled Structures*, 179. Available at: https://doi.org/10.1016/j.tws.2022.109731.

Ardalany, M. *et al.* (2013) 'Experimental behavior of Laminated Veneer Lumber (LVL) joists with holes and different methods of reinforcement', *Engineering Structures*, 56, pp. 2154–2164. Available at: https://doi.org/10.1016/J.ENGSTRUCT.2013.08.034.

Hakkarainen, J. (2019) *LVL Handbook Europe*. Helsinki: Federation of the Finnish Woodworking Industries.

Hart-Smith, L.J. (1984) *Approximate analysis methods for fibrous composite laminates under combined biaxial and shear loading*.

Hashin, Z. and Rotem, A. (1973) 'A Fatigue Failure Criterion for Fiber Reinforced Materials', *Journal of Composite Materials*, 7(4), pp. 448–464. Available at: https://doi.org/10.1177/002199837300700404.

Kliger, R. *et al.* (2007) 'Strengthening glulam beams with steel and composite plates', *Proceedings of the Asia-Pacific Conference on FRP in Structures (APFIS 2007)*, pp. 291–296.

Kohlhauser, C. and Hellmich, C. (2012) 'Determination of Poisson's ratios in isotropic, transversely isotropic, and orthotropic materials by means of combined ultrasonic-mechanical testing of normal stiffnesses: Application to metals and wood', *European Journal of Mechanics, A/Solids*, 33, pp. 82–98. Available at: https://doi.org/10.1016/j.euromechsol.2011.11.009.

Lekhnitskii, S.G. (1968) *Anisotropic Plates*. New York: Gordon and Breach, Science Publishers.

Mascia, N.T. and Simoni, R.A. (2013) 'Analysis of failure criteria applied to wood', *Engineering Failure Analysis*, 35, pp. 703–712. Available at: https://doi.org/10.1016/J.ENGFAILANAL.2013.07.001.

Merhar, M. (2021) 'Application of Failure Criteria on Plywood under Bending', *Polymers*, 13(24). Available at: https://doi.org/10.3390/polym13244449.

Olsson, R. (2006) *COMPOSITE MECHANICS & LAMINATE THEORY*. London.

Pilkey, W.D. and Pilkey, D.F. (2008) *Peterson's Stress Concentration Factors*. 3rd edn. New York: John Wiley & Sons, Inc.

Schmidt, D. *et al.* (2016) 'Development of a Door Surround Structure with Integrated Structural Health Monitoring System', in P.C. Wölcken and M. Papadopoulos (eds) *Smart Intelligent Aircraft Structures (SARISTU)*. Cham: Springer International Publishing, pp. 935–945.

Shroff, S., Acar, E. and Kassapoglou, C. (2017) 'Design, analysis, fabrication, and testing of composite grid-stiffened panels for aircraft structures', *Thin-Walled Structures*, 119, pp. 235–246. Available at: https://doi.org/10.1016/J.TWS.2017.06.006.

Tomppo, L. (2013) *Novel Applications of Electrical Impedance and Ultrasound Methods for Wood Quality Assessment*.

Tsai, S.W. (1965) *Strength characteristics of composite materials*. Washington, DC: NASA.

Tsai, S.W. and Wu, E.M. (1971) 'A General Theory of Strength for Anisotropic Materials', *Journal of Composite Materials*, 5(1), pp. 58–80. Available at: https://doi.org/10.1177/002199837100500106.

Veljkovic, M. *et al.* (2012) *High-strength tower in steel for wind turbines (Histwin)*. Brussels. Available at: https://doi.org/10.2777/39656.

Wang, T. *et al.* (2022) 'In-plane mechanical properties of birch plywood', *Construction and Building Materials*, 340. Available at: https://doi.org/10.1016/j.conbuildmat.2022.127852.

9 Appendix

9.1 Evaluation table for optimized opening geometry

	b)	d)	g)
normal x			
max	4	2	1
min	4	2	1
range	4	2	1
total	4.0	2.0	1.0
normal y			
max	1	3	4
min	4	1	2
range	4	1	3
total	3.0	1.7	3.0
shear			
max	1	4	3
min	1	4	3
range	1	4	3
total	1.0	4.0	3.0
combined			
total	2.7	2.6	2.3

9.2 Stress plots for cover sheets

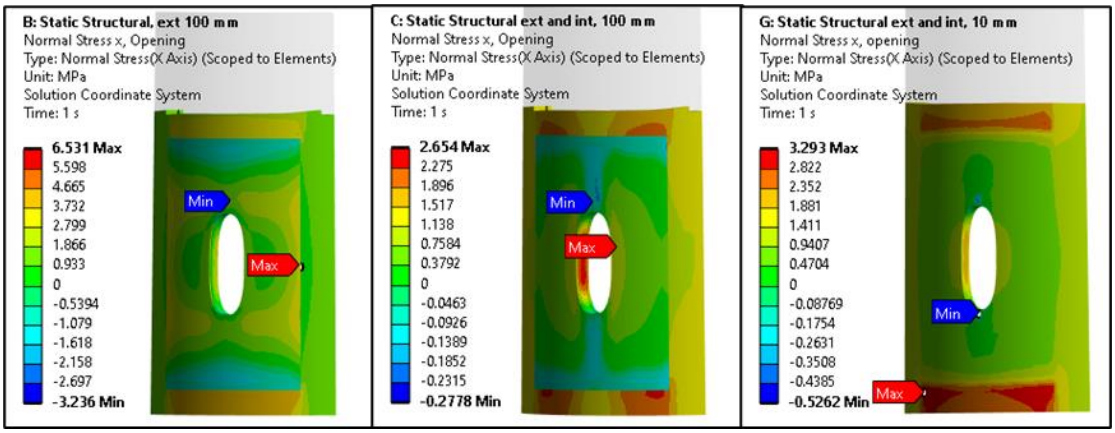

Stresses in LVL for material x-direction. Left: 100 mm spruce external. Middle: 100 mm spruce external and internal. Right: 10 mm steel external and internal.

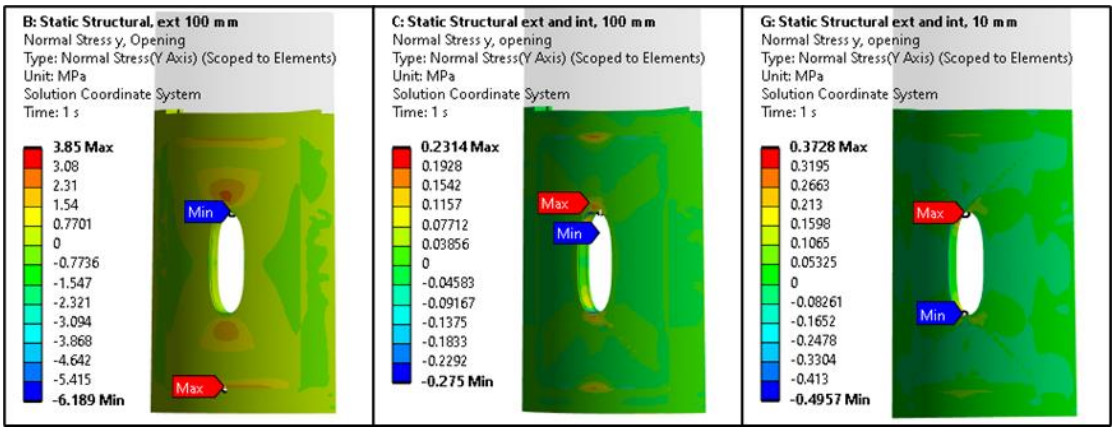

Stresses in LVL for material y-direction. Left: 100 mm spruce external. Middle: 100 mm spruce external and internal. Right: 10 mm steel external and internal.

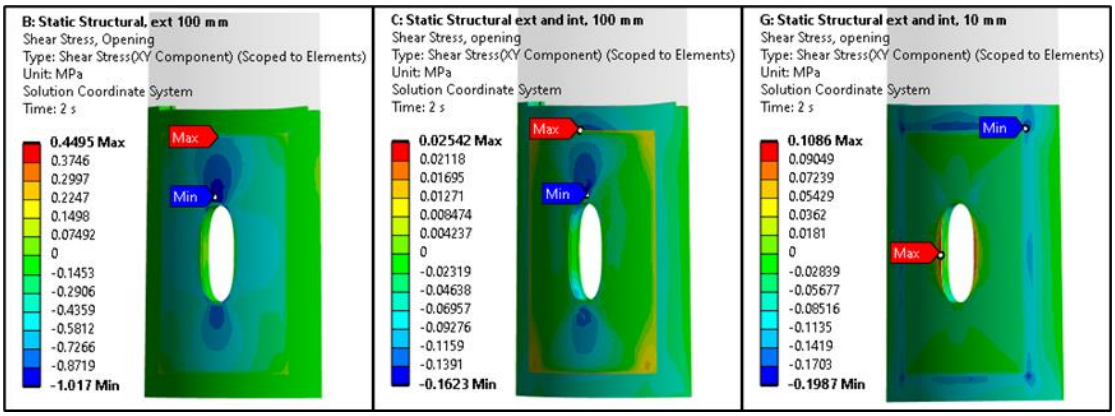

Shear stresses in LVL in xy-plane. Left: 100 mm spruce external. Middle: 100 mm spruce external and internal. Right: 10 mm steel external and internal.

9.3 Stress plots for frames

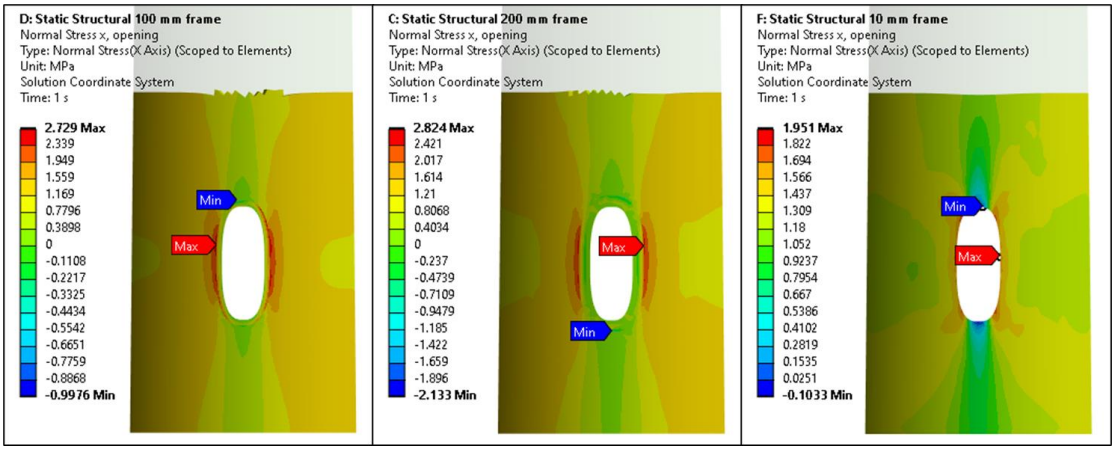

Stresses in LVL for material x-direction. Left: 100 mm spruce. Middle: 200 mm spruce. Right: 10 mm steel.

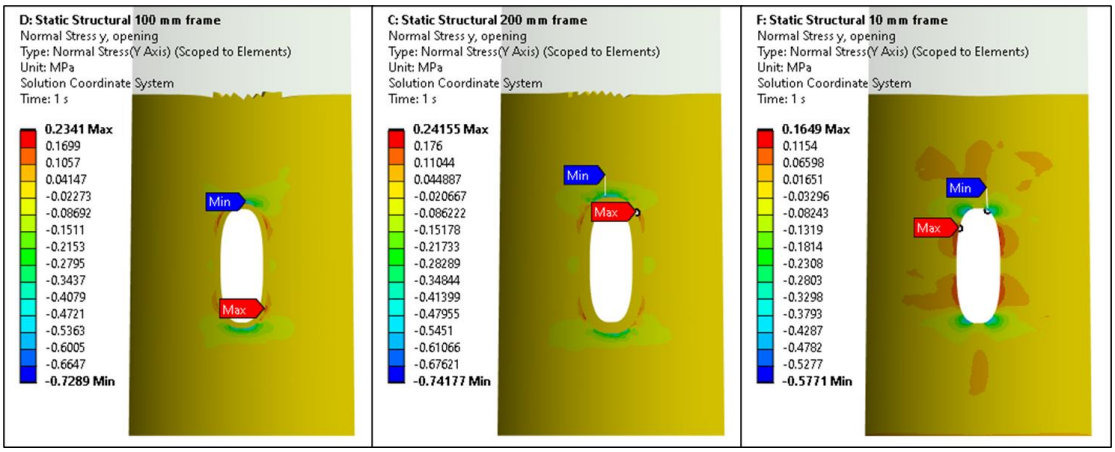

Stresses in LVL for material y-direction. Left: 100 mm spruce. Middle: 200 mm spruce. Right: 10 mm steel.

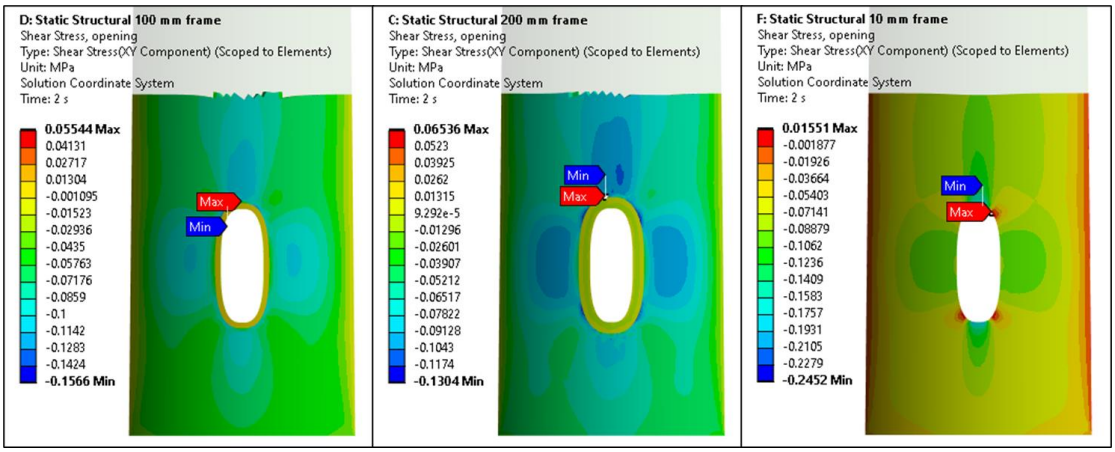

Shear stresses in LVL in xy-plane. Left: 100 mm spruce. Middle: 200 mm spruce. Right: 10 mm steel.

9.4 Stress plots for stiffeners

9.4.1 Straight stiffeners, varying distance from opening

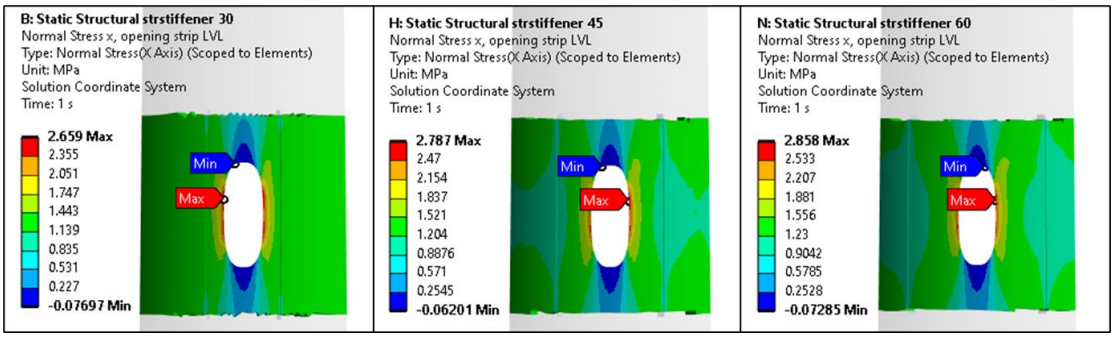

Stresses in LVL for material x-direction. Left: 30° spread. Middle: 45° spread. Right: 60° spread.

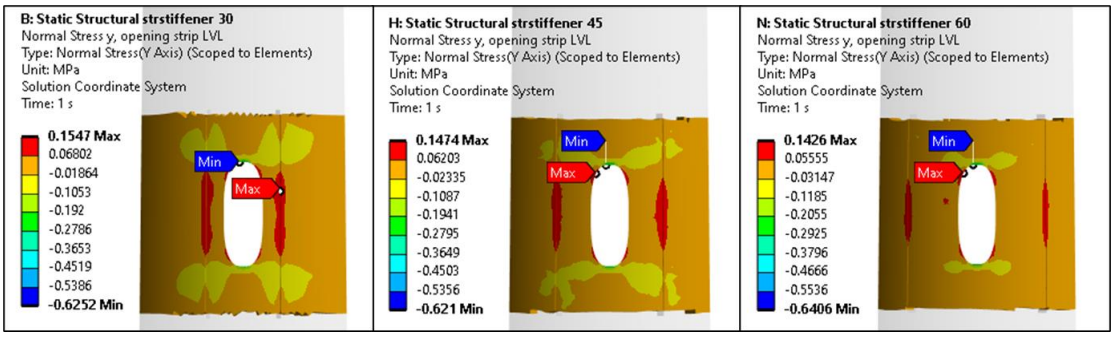

Stresses in LVL for material y-direction. Left: 30° spread. Middle: 45° spread. Right: 60° spread.

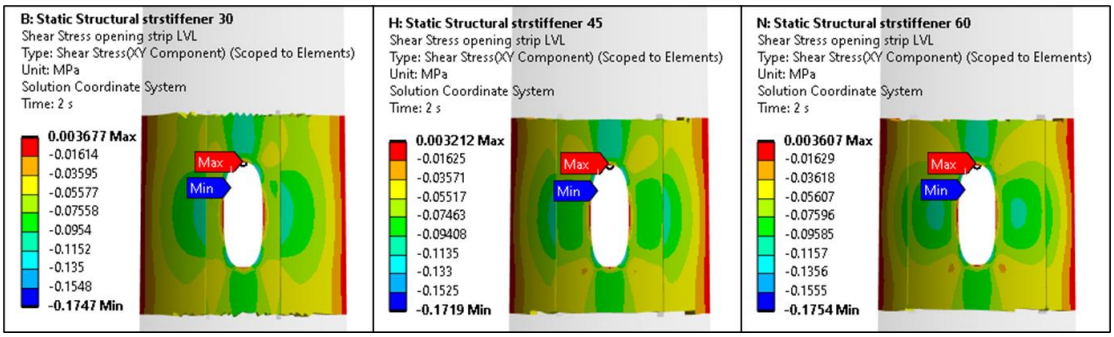

Shear stresses in LVL in xy-plane. Left: 30° spread. Middle: 45° spread. Right: 60° spread.

9.4.2 Straight stiffeners, solid, different stiffnesses

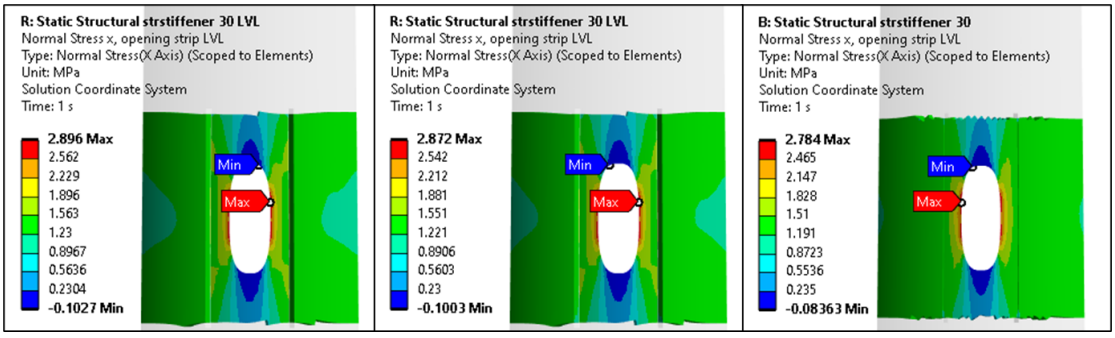

Stresses in LVL for material x-direction. Left: 100 mm spruce LVL. Middle: 100 mm beech LVL. Right: 10 mm aluminium.

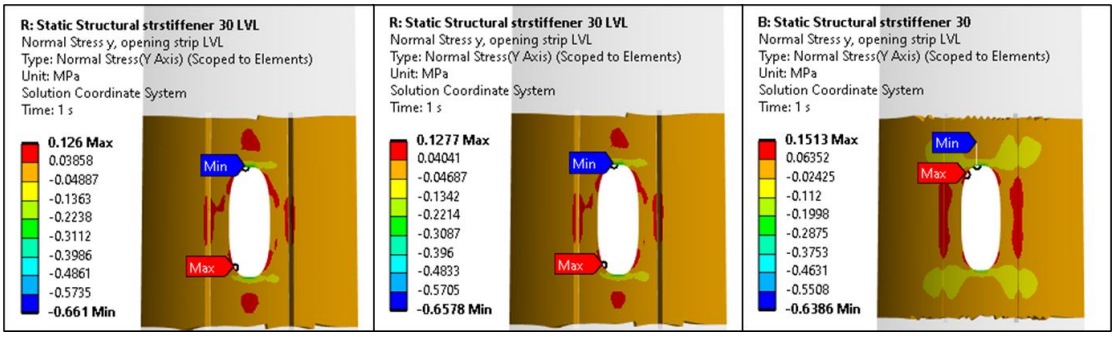

Stresses in LVL for material y-direction. Left: 100 mm spruce LVL. Middle: 100 mm beech LVL. Right: 10 mm aluminium.

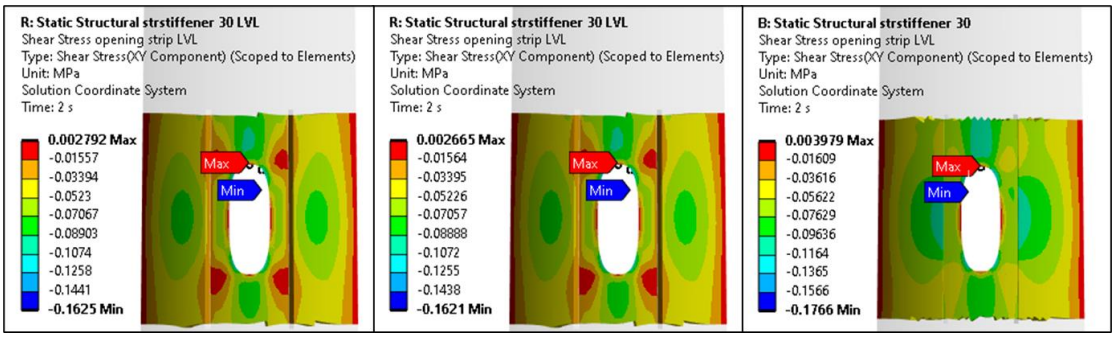

Shear stresses in LVL in xy-plane. Left: 100 mm spruce LVL. Middle: 100 mm beech LVL. Right: 10 mm aluminium.

9.4.3 Straight stiffeners, holed, varying stiffness

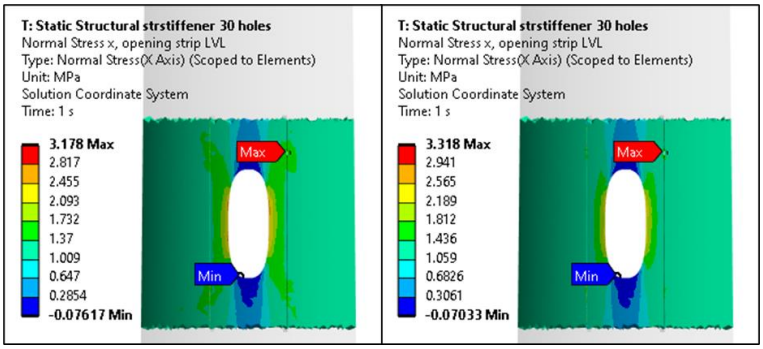

Stresses in LVL for material x-direction. Left: 10 mm aluminium holed stiffeners. Right: 10 mm steel holed stiffeners.

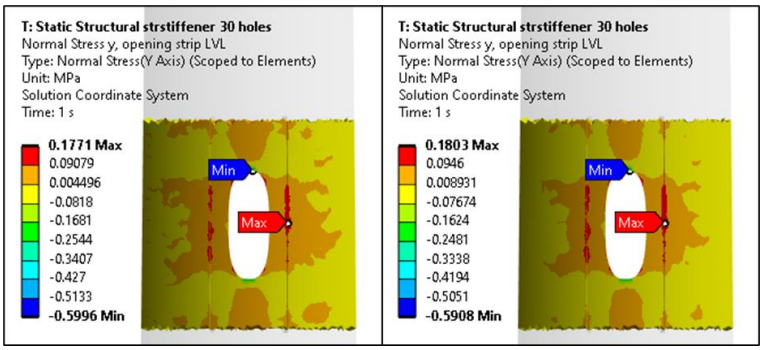

Stresses in LVL for material y-direction. Left: 10 mm aluminium holed stiffeners. Right: 10 mm steel holed stiffeners.

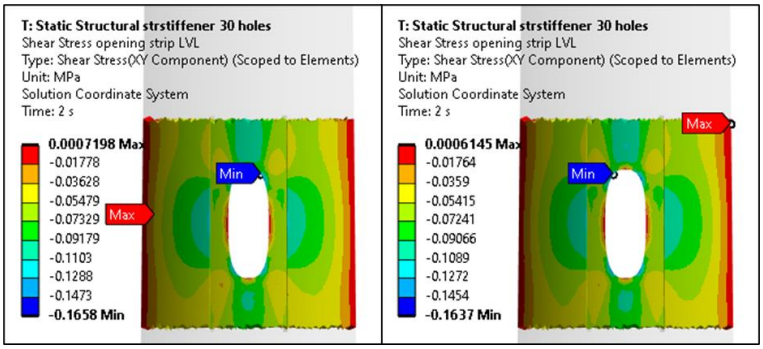

Shear stresses in LVL in xy-plane. Left: 10 mm aluminium holed stiffeners. Right: 10 mm steel holed stiffeners.

9.4.4 Stress plots for streamline stiffeners

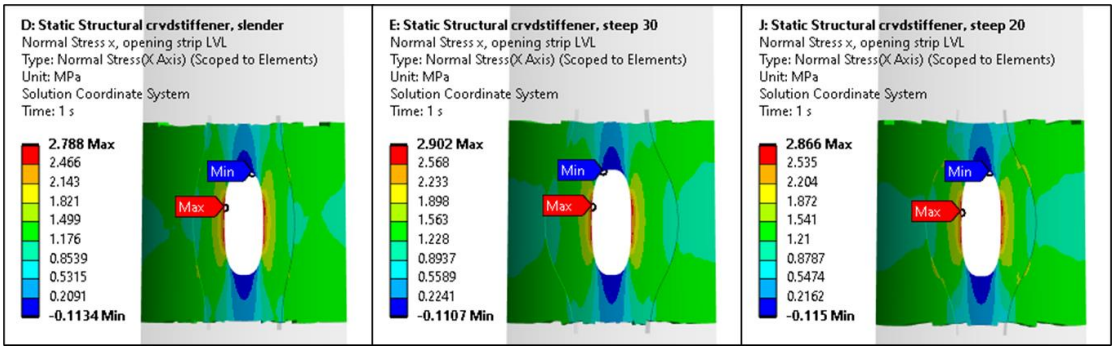

Stresses in LVL for material x-direction. Left: Big radius. Middle: Small radius, 30° spread. Right: Small radius, 20° spread.

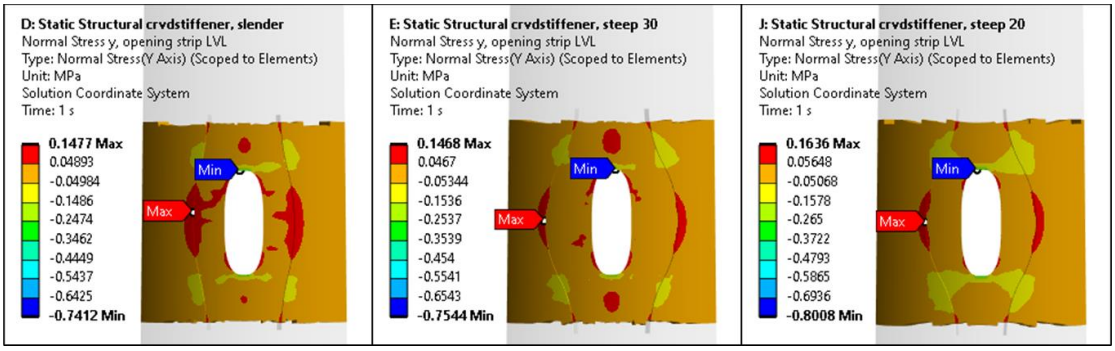

Stresses in LVL for material y-direction. Left: Big radius. Middle: Small radius, 30° spread. Right: Small radius, 20° spread.

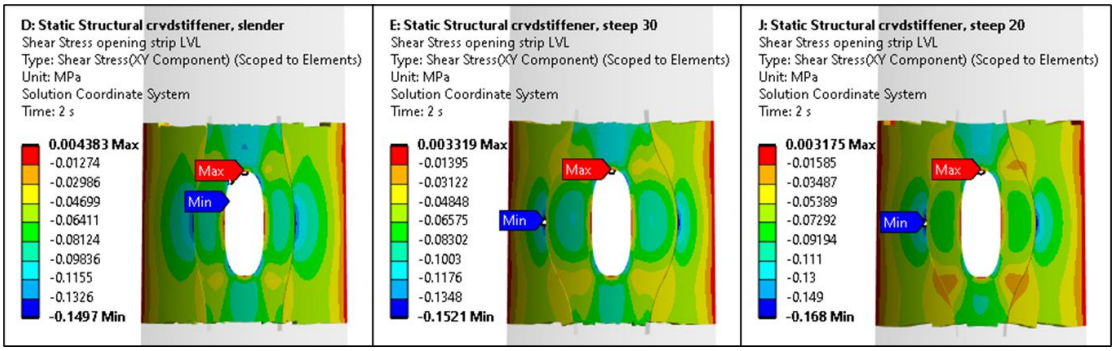

Shear stresses in LVL in xy-plane. Left: Big radius. Middle: Small radius, 30° spread. Right: Small radius, 20° spread.